

APPENDIX E

**SURFACE WATER FLOW, SEDIMENT, AND DEPLETED URANIUM
FATE AND TRANSPORT MODEL**

**Depleted Uranium Impact Area
Jefferson Proving Ground, Madison, Indiana**

THIS PAGE WAS INTENTIONALLY LEFT BLANK

TABLE OF CONTENTS

	Page
1. INTRODUCTION.....	1-1
1.1 SURFACE WATER MODELING PURPOSE AND OBJECTIVE	1-1
1.2 REPORT ORGANIZATION.....	1-2
2. SURFACE WATER FLOW AND TRANSPORT.....	2-1
2.1 CSM.....	2-1
2.1.1 CSM Area and Narrative	2-1
2.1.2 Runoff Generation	2-4
2.1.3 Surface Water Routing	2-4
2.1.4 Sediment Transport.....	2-4
2.1.5 Pollutant Transport	2-4
2.2 DATA COLLECTION AND FORMATTING	2-5
2.2.1 Surface Elevation Data	2-5
2.2.2 Site Soils.....	2-5
2.2.2.1 DU Impact Area Soils.....	2-6
2.2.3 Land Use.....	2-8
2.2.4 Meteorological Data	2-8
2.2.4.1 Onsite Data	2-8
2.2.4.2 Data From Nearby Stations.....	2-12
2.2.4.3 Creation of Time Series	2-14
2.2.5 Observed Stream Stage and Flow.....	2-14
2.2.5.1 Cave Gauges	2-16
2.2.5.2 Stream Gauges	2-16
2.2.6 Observed Suspended Sediment Transport.....	2-17
2.2.7 Observed Uranium Analytical Data.....	2-18
2.3 CODE SELECTION.....	2-25
2.3.1 HSPF (Hydrologic Simulation Program – FORTRAN).....	2-25
2.3.2 SWMM	2-26
2.3.3 SWAT.....	2-27
2.3.4 Selected Code	2-27
3. MODEL SETUP.....	3-1
3.1 BASINS 4.0.....	3-1
3.1.1 Stream Network and Watershed Delineation	3-1
3.1.2 Meteorological Data	3-6
3.1.3 Land Use.....	3-6
3.1.4 Watershed Segmentation	3-8
3.2 HSPF-JPG MODEL	3-8
3.2.1 Ftables.....	3-8
3.2.1.1 Ftables Development	3-9
3.2.2 PERLND Segment Parameters.....	3-11
3.2.2.1 PERLND Overland Flow	3-12
3.2.2.2 PERLND Overland Sediment Transport.....	3-12
3.2.3 IMPLND Segment Parameters	3-13
3.2.3.1 IMPLND Overland Flow	3-14
3.2.3.2 IMPLND Overland Sediment Transport.....	3-14
4. FLOW CALIBRATION.....	4-1
4.1 CALIBRATION TARGETS	4-1
4.2 WATER BUDGET.....	4-2

TABLE OF CONTENTS (Continued)

	Page
4.3 STAGE VERSUS FLOW AT LOW-FLOW CONDITIONS	4-3
4.4 HYDROGRAPH STAGE AND SHAPE	4-10
4.5 CALIBRATION PARAMETERS.....	4-12
4.5.1 Ftables.....	4-12
4.5.2 HSPF Parameters.....	4-12
4.6 CALIBRATION PROCESS.....	4-16
4.7 CALIBRATION RESULTS.....	4-17
4.7.1 Water Budget.....	4-17
4.7.2 Stage Versus Flow at Low-Flow Conditions.....	4-18
4.7.3 Hydrograph Stage and Shape Matching	4-22
4.8 MODELED FLOW BY SUB-BASIN.....	4-22
4.9 SENSITIVITY ANALYSIS	4-25
4.9.1 Critical Flow Parameters	4-25
5. SEDIMENT TRANSPORT CALIBRATION	5-1
5.1 OVERLAND SEDIMENT TRANSPORT.....	5-1
5.2 IN-STREAM SEDIMENT TRANSPORT	5-3
5.2.1 In-Stream Sand Fraction Transport Parameters.....	5-4
5.2.2 Silt and Clay Fraction Transport Parameters.....	5-5
5.3 SEDIMENT TRANSPORT CALIBRATION.....	5-5
5.4 MODELED SEDIMENT LOAD BY LAND USE	5-7
5.5 SENSITIVITY TO CRITICAL PARAMETERS.....	5-10
5.5.1 Overland Sediment Transport Parameters.....	5-10
5.5.2 In-Stream Transport Parameters	5-10
6. DU FATE AND TRANSPORT	6-1
6.1 SOURCE TERM EVALUATION	6-1
6.1.1 Penetrator Distribution	6-2
6.1.2 Laboratory Derived K_d Values	6-4
6.1.3 DU Corrosion and Dissolution Rates	6-4
6.1.4 Specification of DU Source	6-7
6.2 TRANSPORT CALIBRATION.....	6-8
6.3 CRITICAL PARAMETERS	6-9
6.4 CALIBRATION RESULTS.....	6-10
6.5 SENSITIVITY ANALYSIS.....	6-15
6.5.1 K_d	6-15
6.5.2 DU Dissolution Rates	6-15
7. PREDICTED FUTURE DU FATE AND TRANSPORT.....	7-1
7.1 DEVELOPING LONG-TERM BASE CASE SCENARIO	7-1
7.2 SENSITIVITY ANALYSIS (CLIMATE CHANGE SCENARIO).....	7-2
8. DISCUSSION AND ANALYSIS OF RESULTS.....	8-1
8.1 FLOW MODEL AND SEDIMENT TRANSPORT.....	8-1
8.1.1 Big Creek.....	8-1
8.1.2 Middle Fork Creek.....	8-2
8.2 DU TRANSPORT RESULTS.....	8-4
8.3 LIMITATIONS, ASSUMPTIONS, AND UNCERTAINTY	8-6
9. CONCLUSIONS	9-1
10. REFERENCES.....	10-1

LIST OF FIGURES

	Page
Figure 2-1. Surface Water Domain.....	2-2
Figure 2-2. Erosion Processes and Overland Sediment Transport (USEPA 2001b).....	2-3
Figure 2-3. Land Use and Land Cover, USDA/NRCS (2006).....	2-9
Figure 2-4. Land Use Classification from Infrared Analysis	2-10
Figure 2-5. Land Use and Land Cover	2-11
Figure 2-6. Local Weather Station Locations.....	2-13
Figure 2-7. Cross Plot of JPG and Butlerville Weather Station Precipitation Data	2-14
Figure 2-8. Weather and Gauging Stations	2-15
Figure 2-9. Suspended Sediment Concentration Versus Flow Rate at Brush Creek (1960-1968)	2-17
Figure 2-10. Suspended Sediment Concentration Versus Velocity at Vernon Fork (1977-1980).....	2-18
Figure 2-11. Surface Water and Sediment Sampling Locations.....	2-19
Figure 2-12. JPG Sediment Total Uranium (pCi/g) April 2008-February 2009	2-21
Figure 2-13. JPG Surface Water Total Uranium (pCi/g) April 2008-February 2009.....	2-22
Figure 3-1. Surface Water Model Sub-Basins.....	3-3
Figure 3-2. A Typical Stream Cross-Section (USEPA 2001c).....	3-10
Figure 3-3. A Typical Stream Cross-Section Within Middle Fork (Black: From Path Analyzer, Red: Approximated for HSPF Model).....	3-10
Figure 4-1. Correlation of Raw Transducer Data to Field Measured Depths.....	4-5
Figure 4-2. Correlation of Corrected Transducer Data to Field Measured Depths	4-5
Figure 4-3. Flow Versus Stage at BC-01 (Stage 0 to 4 Feet) With Measured Flow Data.....	4-6
Figure 4-4. Flow Versus Stage at BC-01 (Stage 0 to 16 Feet) With Measured Flow Data.....	4-6
Figure 4-5. Flow Versus Stage at BC-02 With Measured Flow Data	4-7
Figure 4-6. Flow Versus Stage at BC-03 With Measured Flow Data	4-7
Figure 4-7. Flow Versus Stage at MF-01 With Measured Flow Data.....	4-8
Figure 4-8. Flow Versus Stage at MF-02 With Measured Flow Data.....	4-8
Figure 4-9. Flow Versus Stage at MF-03 With Measured Flow Data.....	4-9
Figure 4-10. Flow Versus Stage at MF-04 With Measured Flow Data.....	4-9
Figure 4-11. Observed Stage and Precipitation Data at BC-01 November 2007 Through May 2008.....	4-11
Figure 4-12. Observed and Simulated Stage at BC-01	4-19
Figure 4-13. Observed and Simulated Stage at BC-03.....	4-20
Figure 4-14. Hourly Precipitation 2006-2011	4-21
Figure 4-15. Simulated Flow at BC-01 2006-2011	4-23
Figure 4-16. Observed and Simulated Stage Hydrographs at BC-01 November 2007 Through May 2008	4-24
Figure 4-17. Sensitivity of Stage (BC-01) to Changes in IRC and AGWRC.....	4-27
Figure 4-18. Sensitivity of Stage (BC-01) to Changes in LZSN and UZSN.....	4-27

LIST OF FIGURES (Continued)

	Page
Figure 5-1. Sediment Detachment and Overland Sediment Transport (USEPA 2001b).....	5-2
Figure 5-2. In-Stream Suspended and Bed Load Sediment Fractions (USEPA 2001b).....	5-3
Figure 5-3. Modeled Stage and Suspended Sediment on Big Creek at Gauging Station BC-01 (RCH114)	5-8
Figure 5-4. Simulated Total Suspended Sediment for Sub-Basins 21 and 114.....	5-9
Figure 6-1. Estimated Distribution of DU	6-3
Figure 6-2. Estimated DU Mass Release Into the Soil per Penetrator From Corrosion and Dissolution.....	6-6
Figure 6-3. Calibration Results for Dissolved Uranium Concentration in Big Creek at Sub-Basin 114.....	6-11
Figure 6-4. Calibration Results for Uranium Concentration in Suspended Silt, Big Creek Sub-Basin 114.....	6-12
Figure 6-5. Calibration Results for Dissolved Uranium Concentration in Middle Fork Creek Sub-Basin 5.....	6-13
Figure 6-6. Calibration Results for Uranium Concentration in Suspended Silt, Middle Fork Creek Sub-Basin 5	6-14
Figure 6-7. Dissolved Uranium Concentration K_d Sensitivity Results.....	6-16
Figure 6-8. Uranium Concentration in Suspended Silt K_d Sensitivity Results.....	6-17
Figure 6-9. Sensitivity of Dissolved Uranium Concentration to Dissolution Rate at Sub-Basin 114.....	6-18
Figure 6-10. Sensitivity of Uranium Concentration in Suspended Silt to Dissolution Rate at Sub-Basin 114.....	6-19
Figure 7-1. Predicted Dissolved Uranium Concentrations in Big Creek at Sub-Basin 114	7-3
Figure 7-2. Predicted Dissolved Uranium Concentrations in Big Creek at Sub-Basin 117	7-4
Figure 7-3. Predicted Dissolved Uranium Concentrations in Big Creek at Sub-Basin 128	7-5
Figure 7-4. Predicted Dissolved Uranium Concentrations in Middle Fork Creek at Sub-Basin 5	7-6
Figure 7-5. Predicted Dissolved Uranium Concentration in Middle Fork Creek at Sub-Basin 15	7-7
Figure 7-6. Base Case and Climate Change Scenario Evapotranspiration Rates	7-9
Figure 7-7. Base Case and Climate Change Scenario Results for Predicted Stage at Model Years 2108-2112	7-10
Figure 7-8. Base Case and Climate Change Scenario Results for Predicted Uranium Concentration at Model Years 2100-2112.....	7-11

LIST OF TABLES

	Page
Table 2-1. Summary of Soil Series at the DU Impact Area	2-7
Table 2-2. Summary of Land Use Within the CSM Area.....	2-12
Table 2-3. Monthly Precipitation and Temperature at Madison, Indiana	2-12
Table 3-1. Sub-Basins Defined for Each Drainage Basin	3-5
Table 3-2. Land Use Classification – HSPF-JPG Model	3-7

LIST OF TABLES (Continued)

	Page
Table 3-3. PERLND and IMPLND Operations in HSPF-JPG Model	3-8
Table 4-1. Water Budget Estimates HY2007 Through HY2009 (Based on SAIC 2008).....	4-3
Table 4-2. Parameters Governing Snowmelt Used in HSPF-JPG.....	4-12
Table 4-3. PERLND:PWAT-PARM2 Parameters Used in HSPF-JPG Model.....	4-13
Table 4-4. PERLND:PWAT-PARM3 Parameters Used in HSPF-JPG Model.....	4-14
Table 4-5. PERLND:PWAT-PARM4 Parameters Used in HSPF-JPG Model.....	4-15
Table 4-6. Parameters Used for Impervious Land Use Overland Flow and Retention Storage Capacity in HSPF-JPG.....	4-16
Table 4-7. Simulated Water Budget Components (Inches) for Reach 129	4-18
Table 4-8. Simulated Flow for Calendar Years 2007-2010	4-25
Table 4-9. Flow Parameters Adjusted During Sensitivity Evaluation	4-26
Table 4-10. Annual Water Budget Components (Inches) for Sensitivity Simulations – HY2007.....	4-26
Table 5-1. Pervious Overland Sediment Transport Parameters – PERLND:SED-PARM2.....	5-1
Table 5-2. Pervious Overland Sediment Transport Parameters – PERLND:SED-PARM3.....	5-2
Table 5-3. Parameters Used in Impervious Overland Sediment Transport – IMPLND:SLD-PARM1	5-3
Table 5-4. Parameters Used for In-Stream Sand Fraction Transport	5-4
Table 5-5. Silt Fraction Transport Parameters	5-6
Table 5-6. Clay Fraction Transport Parameters	5-6
Table 5-7. Annual (Calendar Year) Sediment Yield by Land Use (Tons per Acre).....	5-10
Table 5-8. Sediment Yield Sensitivity to JRER and KRER (Tons per Acre)	5-11
Table 6-1. Soil and Water Geochemical Processes Affecting Uranium Mobility and Distribution	6-2
Table 6-2. DU Mass (kg) Distribution at JPG.....	6-4
Table 6-3. Summary of Sorption Test Results	6-5
Table 6-4. Best-Estimate Values for Corrosion and Dissolution Rates	6-6
Table 6-5. Uranium K_d Values (Thibault, Sheppard, and Smith 1990) for Various Size Fractions	6-9
Table 8-1. Area Summary of Sub-Basins Having DU	8-1
Table 8-2. Annual Summary of Surface Water Flow and Sediment Transport, Big Creek 2007-2010	8-3
Table 8-3. Annual Summary of Surface Water Flow and Sediment Transport, Middle Fork Creek 2007-2010.....	8-5

LIST OF ACRONYMS AND ABBREVIATIONS

ac	Acre
ac ft	Acre Feet
ARM	Agricultural Runoff Management
BASINS	Better Assessment Science Integrating Point and Nonpoint Sources
BGS	Below Ground Surface
cfs	Cubic Feet per Second
CSM	Conceptual Site Model
DEM	Digital Elevation Model
DU	Depleted Uranium
Eh	Redox Potential
ELDAT	Elevation Difference
ERM	Environmental Radiation Monitoring
fps	Feet per Second
ft	Feet
FWS	U.S. Fish and Wildlife Service
g/cm ³	Gram per Cubic Centimeter
g/y	Gram per Year
GIS	Geographic Information System
gpm	Gallon per Minute
HSPF	Hydrological Simulation Program-Fortran
HY	Hydrologic Year
ICP-MS	Inductively Coupled Plasma-Mass Spectrometry
IMPLND	Impermeable Land Segment
in/hr	Inch per Hour
in/sec	Inch per Second
in/y	Inch per Year
IRC	Interflow Recession Parameter
JPG	Jefferson Proving Ground
K _d	Distribution Coefficient
kg	Kilogram
L/mg	Liter per Milligram
µg/L	Microgram per Liter
MCL	Maximum Contaminant Level
mg/kg	Milligram per Kilogram
mg/L	Milligram per Liter
mi ²	Square Miles
mL/g	Milliliter per Gram
MRCC	Midwest Regional Climate Center
MUSLE	Modified Universal Soil Loss Equation
NHD	National Hydrography Dataset
NPS	Nonpoint Source
NRCS	Natural Resources Conservation Service
pCi/g	Picocurie per Gram
pCi/L	Picocurie per Liter
PERLND	Pervious Land Segment
RCHRES	River Reach or Reservoir
RESRAD	Residual Radiation
SAIC	Science Applications International Corporation
SDWA	Safe Drinking Water Act

LIST OF ACRONYMS AND ABBREVIATIONS (Continued)

SWAT	Soil and Water Assessment Total
SWMM	Storm Water Management Model
T0	Time Zero
TSS	Total Suspended Sediment
U-234	Uranium-234
U-238	Uranium-238
USDA	U.S. Department of Agriculture
USEPA	U.S. Environmental Protection Agency
USGS	U.S. Geological Survey
USLE	Universal Soil Loss Equation
WDM	Watershed Data Management

THIS PAGE WAS INTENTIONALLY LEFT BLANK

1. INTRODUCTION

The fate and transport of depleted uranium (DU) via the surface water pathway (overland flow and runoff to streams draining the DU Impact Area and the former Jefferson Proving Ground [JPG]) was evaluated through modeling to provide an understanding of the key processes affecting this pathway into the future. DU penetrators were fired at soft targets from 1984 to 1994 with periodic recovery of penetrators. A review of similar investigations indicates limited fragmentation of penetrators when fired at soft targets (Parkhurst et al. 2012) and, therefore, the majority of DU mass remaining onsite occurs as full or large pieces of penetrators. The penetrators occur within an area referred to as the DU Impact Area, which is almost entirely forested and is drained by Big Creek and Middle Fork Creek and their tributaries. Sampling results indicate elevated concentrations in soils near penetrators and some limited elevated concentrations within surface water within the DU Impact Area. No or very limited migration in surface water immediately downgradient from the DU Impact Area or to groundwater has been observed.

Surface water and sediment transport modeling were conducted to quantify the volume of surface water and sediment runoff from the watersheds draining the DU Impact Area as well as upstream and downstream contributions important to understanding the potential for transport via the surface water pathway. The area model encompasses the upgradient extent of Big Creek and Middle Fork Creeks downstream to their confluence south and west of JPG. The surface water and sediment transport model was calibrated to observed conditions (primarily flow and stage) and formed the basis for DU transport.

The distribution of penetrators remaining at JPG was estimated from historical documentation. DU mass available for transport was determined from studies on the weathering (corrosion and subsequent dissolution of corrosion products) of penetrators. DU transport calibration was performed by adjusting the mass released from penetrator weathering until model predictions matched observed conditions (surface water and sediment sampling data).

Initially, modeling over a 1,000-year period was planned. However, during model development, calibration, and predictive simulations, a period of 500 years was sufficient to predict the peak concentrations of DU in surface water and sediments within Big Creek and Middle Fork Creek. Code selection, model development, flow and transport calibration, predictive simulations, and uncertainty/sensitivity analyses are presented in support of both current and predicted future DU fate and transport at the former JPG.

1.1 SURFACE WATER MODELING PURPOSE AND OBJECTIVE

The purpose of the surface water modeling effort consisted of:

- Incorporating pertinent site features, characteristics, and operational history and match (calibrate) observed flow conditions in Big Creek and Middle Fork Creek drainage areas
- Calibrating to DU surface water and sediment sampling levels using the calculated DU mass in each drainage area and information on the corrosion and dissolution of the penetrators
- Predicting the fate of DU via the surface water pathway over time at the former JPG.

The surface water modeling objective consisted of:

- Utilizing the model to predict future DU concentrations over time within Big Creek and Middle Fork Creek within and downgradient from the DU Impact Area
- Supporting residual radiation (RESRAD) dose-based calculations and serving as a check on those portions of the RESRAD calculations that pertain to the surface water pathway.

1.2 REPORT ORGANIZATION

The remainder of the report is organized as follows:

- Section 2 presents the conceptual site model (CSM), data and code selection
- Section 3 presents model setup
- Section 4 presents the flow model calibration, including calibration targets, process, results, and sensitivity analysis
- Section 5 presents sediment transport calibration
- Section 6 presents DU fate and transport, including source term, calibration process and results, and sensitivity analysis
- Section 7 presents predicted future DU fate and transport
- Section 8 presents a discussion and analysis of results
- Section 9 presents the conclusions
- Section 10 provides a listing of references cited.

2. SURFACE WATER FLOW AND TRANSPORT

Transport of DU via surface water runoff represents a significant potential pathway for the migration of DU from the DU impact and adjacent areas. Development of the numerical model for JPG began with a CSM describing the area and key components of the surface water pathway, identification of data sources, and code selection.

2.1 CSM

DU penetrators were test fired at JPG from 1984 through 1994 along three firing lines at targets placed at 1,000-meter (m) intervals from gun positions extending up to 4,000 m down range. The area where penetrators impacted the ground is referred to as the DU Impact Area. Most penetrators (89 percent) were fired along 500 Center, resulting in the formation of a trench roughly 1,900 m long, 20 to 30 m wide, and 1 m deep. Twice per year during this period, penetrators were recovered by JPG personnel to ensure the facility remained within permit requirements. Of the 100,000 kilograms (kg) of penetrators fired, approximately 26,500 kg were recovered, leaving 73,500 kg in the DU Impact Area and vicinity.

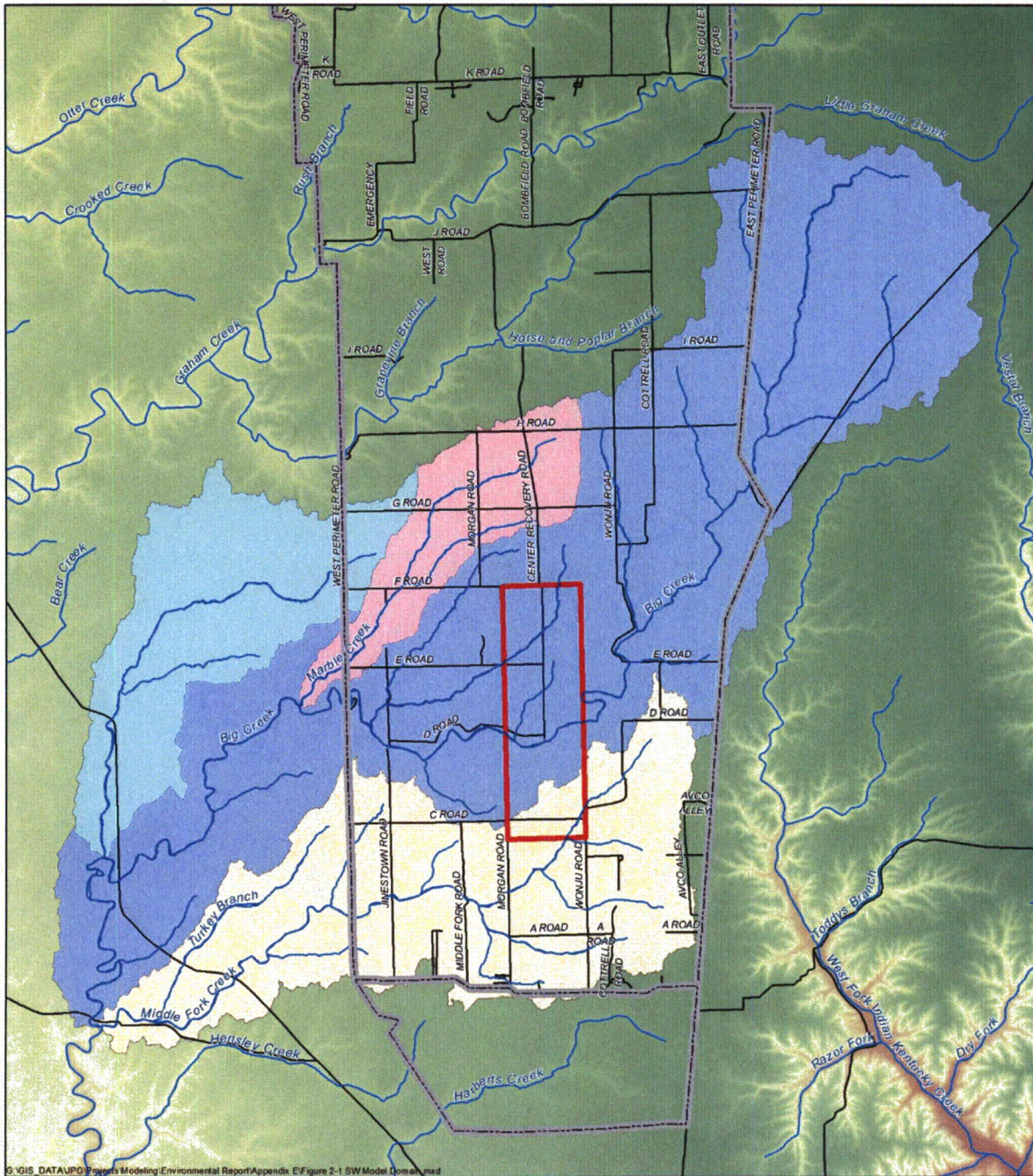
The DU Impact Area is within the Muscatatuck Plateau physiographic region and is characterized by broad uplands covered by glacial till with entrenched valleys (Gray 2001). The glacial deposits overlie Paleozoic bedrock consisting of interbedded limestone, dolomite, and shale, and overburden thicknesses based on previously installed monitoring wells range from 10 to greater than 65 feet (ft) thick (SAIC 2002). According to Franzmeier et al. (2004), the glacial till is Pre-Wisconsinan age and thought to be Illinoian age or older and is covered with a thick (>6 ft thick) mantle of Wisconsinan age loess (wind deposited silt). The soil region that encompasses the DU Impact Area is described as “moderately thick loess over weathered loamy glacial till” (USDA NRCS 1999).

The DU Impact Area is incised by two streams (i.e., Middle Fork Creek and Big Creek and associated tributaries). The surface relief generally is a result of erosion and down cutting associated with the streams and surface water flow to the streams. The surface water drainage is characterized as exhibiting a dendritic pattern that discharges to the streams. The vegetative cover consists of wooded areas containing deciduous trees and open spaces populated with grasses, sedges, and other herbaceous plants. The U.S. Fish and Wildlife Service (FWS) uses controlled burns (management of vegetation by fire) to manage some of the grassland areas. A wide variety of wildlife inhabits the area, including terrestrial crayfish and other burrowing animals that may cause localized bioturbation of the soil.

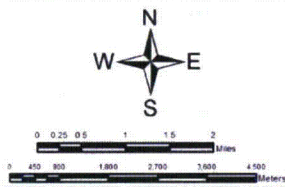
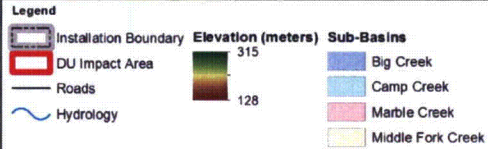
The entire DU Impact Area has undergone anthropogenic disturbance of various types and magnitude. Prior to the establishment of JPG, the majority of the land was agricultural and the soils were disturbed in the act of tilling the lands. Following the establishment of JPG, disturbances ranged from installation and maintenance of the infrastructure (e.g., utility trenching, construction of buildings/structures, and road building) to testing operations in impact fields (i.e., disturbance by detonation) for a great number and variety of ordnance between 1941 and 1994.

2.1.1 CSM Area and Narrative

The CSM area (including the DU Impact Area) falls within the U.S. Geological Survey (USGS) hydrologic unit (0512020701) of the Muscatatuck River and is drained by Big Creek and Middle Fork Creek. Big Creek includes two smaller tributaries: Marble Creek and Camp Creek. The total area included for the surface water model extends to the confluence of Middle Fork Creek with Big Creek, covering a total area of roughly 44,949 acres (ac) (Figure 2-1). The majority of this area consists of Big Creek with 34,060 ac; Marble Creek (3,053 ac) and Camp Creek (5,843 ac) occur downstream from the DU Impact Area. The Middle Fork Creek drainage area consists of 10,889 ac.



G:\GIS\DATA\UPO\Projects\Modeling\Environmental Report\Appendix E\Figure 2-1 SW Model Domain.mxd



Surface Water Domain

Figure 2-1

Date: 8/6/2013

The area is characterized by limited aquifer recharge and exhibits relatively low and decreasing permeability with depth (SAIC 2010). An analysis of hydrologic components suggests that surface water may be the most significant potential migration pathway from the DU Impact Area. The hydrographs from nearby USGS stream gauges and results from onsite stream gauges indicate that surface runoff after a precipitation event spikes rapidly and dissipates quickly, resulting in sharp rising and falling limbs. When stream flow rates are high, DU migration may include either sediment with DU attached and/or the disintegrated DU particles moving with the flow and followed by deposition downstream when flow velocities dissipate.

The land use patterns in the JPG watershed are fairly diverse. Erosion processes that can mobilize and transport soil from the DU Impact Area to streams such as Big Creek or Middle Fork Creek are illustrated in Figure 2-2. Rain falling on the land surface can detach soil particles, making them available to wash off in overland flow. Scouring of soils also can occur during precipitation runoff events. Land cover influences the amount of soil (or sediment) eroded. Farm land typically has greater erosion rates than forested or grass lands. Precipitation falling in upland areas of the watershed that were either uncultivated/bare or under active agriculture are expected to generate a large amount of sediment relative to the forested and grassy areas comprising the DU Impact Area.

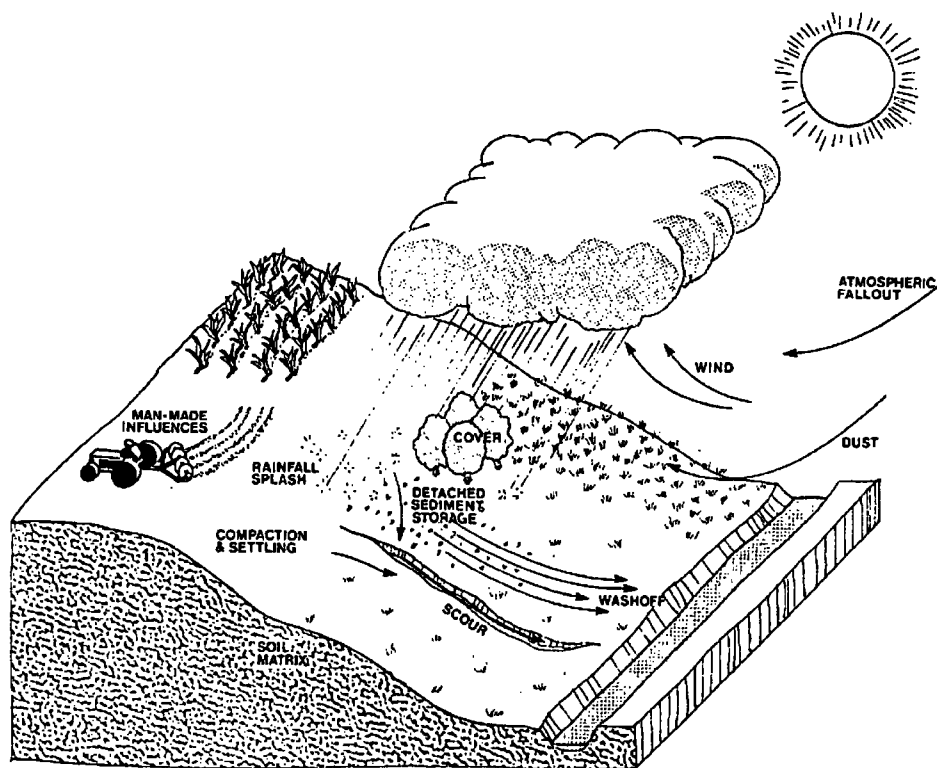


Figure 2-2. Erosion Processes and Overland Sediment Transport (USEPA 2001b)

This sediment and runoff will be transported by Big Creek and Middle Fork Creek through the DU Impact Area, where nonimpacted sediment and runoff from upstream will mix with the impacted sediment generated by erosion within the DU Impact Area. As this flow moves downstream from the DU Impact Area, additional mixing with nonimpacted sediment and runoff occurs. The cumulative output of sediment from the DU Impact Area is assessed at points downstream from the area to the confluence of Middle Fork Creek with Big Creek (approximately 2 miles from the site boundary).

2.1.2 Runoff Generation

Surface runoff (or simply runoff) is the portion of total precipitation that flows over the ground surface to a receiving surface water stream and is the primary transport mechanism for eroded soils. Interflow represents the portion of precipitation that migrates above the water table and can be a component of runoff if the interflow reaches a surface water discharge point before reaching the water table. Runoff at JPG is highly correlated to precipitation (rainfall or snowmelt). Peak flows are flashy and generally occur immediately following a precipitation or melting event. Conceptually, the site can be divided into several sub-watersheds (sub-basins), with each sub-basin described by its land use, vegetative cover, topography, and other physical characteristics to assess the timing and percentage of precipitation that will return into stream segments as runoff.

In addition to runoff, the soil type, nature and spatial extent of vegetation, and topographic characteristics of sub-basins will determine the amount and type of sediment (size fractions) that will be carried (by the runoff) into the stream network.

2.1.3 Surface Water Routing

Most precipitation events generate surface and/or subsurface runoff from sub-basins into associated streams (also referred to as channels or reaches). At JPG, a significant part of the subsurface runoff (interflow and base flow) and the direct surface runoff eventually enter a network of streams. The total runoff and the dissolved and entrained constituents are routed through this stream network. Spatial and temporal variations in stream flow, stage and concentration of sediments, and associated quality components (DU) can be estimated.

The connectivity of the various stream channels was determined by the surface topography and reflects the overland flow system under prevailing site conditions. The National Hydrography Dataset, in conjunction with the digital elevation model for the area, was used to establish the stream drainage network. The width, depth, side slopes (curvature), bed slope, and surface roughness of the streams determine their transport capacity, stage versus specific flow rate relationship (rating curve), and the characteristics of the runoff hydrograph (the timings of low and peak flows in the watershed).

2.1.4 Sediment Transport

Precipitation intensity, duration and spatial distribution, land slopes, soil characteristics, and land use patterns determine the erosion potential and the composition of sediment (size fractions) entering the stream network. Once within the stream network, surface water flow velocity (channel velocity) is one of the most critical flow characteristics governing the fate and transport of sediments and the associated DU. Flow rates are determined by the bed slope, surface roughness, stream stage, and cross-section configuration (slopes and floodplain extents) of the flow channels.

In sections with rapid flow, sediments in suspension are likely to stay in suspension and part of the bed load may scour and re-suspend into the overlying column of water and be transported downstream. In stream segments associated with low and mild flow velocities such as in areas associated with larger cross-sections and/or low flows (due to seepage and evaporation losses and flow diversions upstream), sediments in suspension have the tendency to settle out and become part of the bed load. This process normally starts with heavier particles (sand) followed by lighter (silt, clay) fractions. In general, lighter particles are more likely to remain in suspension and transport downstream.

2.1.5 Pollutant Transport

One of the primary mechanisms for pollutant (DU) transport in the surface water was likely to be the DU fraction adsorbed to the sediments. The laboratory estimated distribution coefficient (K_d) of DU suggests a potential for preferential transport of DU adsorbed to the sediments, particularly to the clay and

silt size fractions. Other pathways include DU dissolved in the overland flow, interflow, and the base-flow. A small fraction may include the larger DU particles disintegrating from the penetrators and transporting under high flow conditions away from the DU penetrators and depositing downstream either within the sub-basin or the stream. Transport of DU fragments is believed unlikely except in extraordinary circumstances (such as flash flood like conditions), due to the high density and size of the fragments and is supported by a literature review of field studies pertaining to DU oxidation and environmental fate (Parkhurst et al. 2012). Transport of smaller fragments from corrosion products may occur, as these particles are smaller and less dense. However, uranyl species dominate in oxidizing environments (such as surface water [note quarterly surface water samples collected from 20 locations for a total of 80 samples on Big Creek, Middle Fork Creek, and tributaries all had positive redox potential results, averaging 244 millivolts and averaged dissolved oxygen of 9.4 milligrams per liter {mg/L}], sediment, and near surface soils) and, as such, the corrosion products are more susceptible to dissolution and are likely to break down further and transport in solution or be adsorbed to sediments (Kaiser-Hill 2002, Parkhurst et al. 2012). Analysis of groundwater, surface water, and sediments shows little to no physical DU transport outside the DU Impact Area over the past 25 years. Land use within the DU Impact Area is primarily forested, which also will limit the amount of sediment (including DU fragments or fragments of corrosion products) runoff following precipitation events.

The most critical physical characteristics controlling pollutant transport are the K_d s; penetrator corrosion and dissolution rates of corrosion products; and the diameter, length, and density of the penetrators. DU will partition between solid phase (primary and weathered), dissolved phases, and adsorbed fractions. The kinetics (rate) is largely governed by the mass transfer rates between these phases. The dissolved fraction will mix into the stream flow and transport downstream with some sorption or partitioning to sand, silt, and clay sediments in the channel. DU adsorbed to sand, silts, and clay in suspension or as bed sediment may undergo desorption (this is likely to be a very small fraction as reverse reactions are generally slow).

2.2 DATA COLLECTION AND FORMATTING

In order to construct a useful surface water flow and transport model, a large amount of reliable data is required. Data are typically used both in construction of the model (to define input parameters), as well as in the calibration and verification of the model.

2.2.1 Surface Elevation Data

The most easily accessible data for mapping and determining stream networks are digital elevation models (DEMs). Several DEMs of various degrees of resolution are available with the higher resolutions requiring increasingly more memory for storage and use in computer modeling. Surface topography is a key component of surface water flow and sediment transport and requires an accurate depiction of the elevations encountered across the modeling domain. DEM resolution (higher-resolution DEMs are much larger in file size than lower-resolution DEMs for the same area) was balanced against the project objectives and code capabilities. The Better Assessment Science Integrating Point and Nonpoint Sources (BASINS) 4.0 data library includes 30-m resolution DEM files. Initial model setup and testing used these 30-m resolution DEMs. The final calibrated model utilized a 6-m resolution DEM (Indianamap.org 2005). The horizontal accuracy is 2.5 ft at 95 percent confidence level; the vertical accuracy is 6 ft (sufficient to generate 10-ft contours) at 95 percent confidence level.

2.2.2 Site Soils

Soil type data within the BASINS 4.0 database in conjunction with information on soil types within the DU Impact Area (Section 2.2.2.1) were used to define the soils for the surface water modeling efforts. Soil type influences infiltration characteristics and surface water storage, sediment detachment, and overland flow (runoff) and transport. The soil moisture holding capacities and adsorption characteristics

are also soil texture dependent. Several soil samples were collected from various sub-basins and from the stream bed deposits across the site. Particle size analysis was performed for 32 soil samples collected from various sub-basins. The average sand, silt, and clay mass fractions determined were 0.205 ± 0.118 , 0.490 ± 0.075 , and 0.305 ± 0.105 , respectively. Particle size analysis performed for eight sediment samples collected from stream bed deposits contained average sand, silt, and clay mass fractions of 0.627 ± 0.161 , 0.254 ± 0.094 , and 0.119 ± 0.061 , respectively. Compared to the soil sampling results, silt- and clay-sized fractions of sediment are substantially less in the stream beds, while the sand-sized fractions are more than three times on average the sand-sized mass fraction in site soils.

2.2.2.1 DU Impact Area Soils

Seven soil series are mapped in the DU Impact Area (USDA NRCS 2005): Avonburg, Cincinnati, Cobbsfork, Grayford, Holton, Rossmoyne, and Ryker. A soil verification study (SAIC 2007) was conducted to confirm the soil series as mapped by the U.S. Department of Agriculture (USDA). All seven soil series have similar texture, consisting of silt loam derived from different parent materials and occurring on slightly different slopes at the land surface. Table 2-1 summarizes the soil series. Six soil series are derived from parent material consisting of loess, underlying till-derived paleosols, and limestone residuum, and one soil series is derived from alluvium on floodplains:

- **Avonburg Series**—Very deep, somewhat poorly drained soils formed in loess and underlying paleosol in till
- **Cincinnati Series**—Deep, well-drained soils formed on mantle of loess
- **Cobbsfork Series**—Poorly drained soils on broad summits of till plains; formed in loess and underlying till-derived paleosols
- **Grayford Series**—Deep, well-drained soils formed in loess, till of Illinoian age, and residuum from limestone on dissected till plains and sink holes
- **Holton Series**—Deep, poorly drained soils formed in loaming alluvium on floodplains
- **Rossmoyne Series**—Very deep, moderately well-drained soils formed on mantle of loess and underlying till of Illinoian age
- **Ryker Series**—Very deep, well-drained soils formed in loess, underlying drift, and residuum from limestone on till plains.

Results from the field observations indicate the soil mapping units delineated on the Natural Resources Conservation Service (NRCS) map are reasonably accurate. From the soil borings observed, the site soil conditions may be wetter than indicated by the NRCS soil survey map. The field data indicate that the somewhat poorly drained Avonburg series may be grouped together with the poorly drained Cobbsfork series for the purpose of interpretation. Combined, these two soil series would comprise approximately 55 percent of the DU Impact Area. The well-drained Cincinnati and Rossmoyne series also may be grouped together, since both have a fragipan subsurface diagnostic horizon, which tends to perch water during parts of the year, and this combination would account for another 32 percent of the DU Impact Area. The well-drained Grayford, Ryker, and somewhat poorly drained Holton series all have somewhat unique soil conditions.

The portion of the DU Impact Area (>55 percent) with somewhat poorly and poorly drained soil exhibits redoximorphic features (soil mottling) that indicate a reducing environment exists in the shallow (<3 ft) subsurface for some period of time during the growing season. Redoximorphic features or soil drainage mottling are color patterns in the soil formed by the oxidation and reduction of iron and/or manganese caused by saturated or near saturated conditions within the soil. Seasonally high perched water is noted at or near (within 6 inches [in]) land surface for the soils present within the DU Impact

**Table 2-1. Summary of Soil Series at the DU Impact Area
Jefferson Proving Ground, Madison, Indiana**

Soil Series ^a	Map Symbol ^a	Slope ^a	Depth ^a	Drainage Class	Taxonomic Classification ^a	Total Acreage as Mapped ^a	Percent of Total Acres ^a	Saturated Hydraulic Conductivity (m/s) ^b
Avonburg	Av	0-6%	Very Deep	Somewhat Poorly Drained	Fine-silty, mixed, active, mesic Aeric Fragic Glossaqualf	311.97	14.8	Upper solum moderately high to high 4.23E-2 to 1.41E-1 Lower solum low to moderate 7.0E-4 to 1.41E-2
Cincinnati	Cn	1-18%	Very Deep	Well Drained	Fine-silty, mixed, active, mesic Oxyaquic Fragiudalf	409.12	19.4	Moderate permeability
Cobbsfork	Co	0-1%	Very Deep	Poorly Drained	Fine-silty, mixed, active, mesic Fragic Glossaqualf	861.47	40.7	Upper solum 1.41E-2 to 1.41E-1 Lower solum 7.0E-4 to 1.41E-2
Grayford	Gr	2-35%	Deep	Well Drained	Fine-silty, mixed, active, mesic Ultic Hapludalf	144.81	6.8	Moderately high to high 4.23E-2 to 1.41E-1
Holton	Ho	0-2%	Very Deep	Somewhat Poorly Drained	Coarse-loamy, mixed, active, nonacidic, mesic, Aeric Endoaquept	36.22	1.7	Moderately high to high
Rossmoyne	Ro	0-25%	Very Deep	Moderately Well Drained	Fine-silty, mixed, superactive, mesic Aquic Fragiudalf	259.85	12.3	Moderate above fragipan, moderately slow below fragipan
Ryker	Ry	0-18%	Very Deep	Well Drained	Fine-silty, mixed, active, mesic Typic Paleudalf	90.8	4.3	NA

^aFrom Tables 2-1 through 2-3 of the Final Well Location Selection Report (SAIC 2007).

^bFrom Appendix A of the Final Well Location Selection Report – official soil series descriptions (SAIC 2007).

Area. This seasonally high perched water and degrading organic matter produce periodic reducing conditions.

This reducing environment is sufficient to reduce the ferric iron to ferrous iron. The presence of ferrous or ferric iron is an indicator of the oxidative state. No direct measurements of redox potential (Eh) were obtained during this investigation. Corrosion of metals and therefore DU penetrators can be greatly affected by the environment in which it is located. DU penetrator corrosion rates and processes are much lower under reducing conditions than those present under oxidation (Parkhurst et al. 2012)

2.2.3 Land Use

Land use characteristics have a significant influence on runoff, sediment, and DU transport. Land use patterns affect plant water uptake (evapotranspiration), infiltration (such as preferential flow within root channels), water holding capacities (due to soil organic matter), and canopy interception. Land use data were collected from the National Land Cover dataset (USDA NRCS 2006), as shown in Figure 2-3.

Land use also was classified from infrared analysis of air photos. Infrared coverage consisted of 4-channel (visual spectrum + infrared) data from 2008 to produce a detailed 6-m resolution land use classification (versus the 30-m grid from the National Land Cover dataset). A supervised classification was performed on the same infrared image using all four bands. In this process, areas of known land uses or physical features were defined (as separate classes) on the image as training data. The processing software then can use the spectral properties of the different classes of training data to classify the rest of the image (as illustrated in Figure 2-4). One problem with the classification is that the shadow area and water are very alike spectrally with available bands. As a result, some shadows may be classified as water, and vice versa. Figure 2-5 depicts the land uses determined from this process.

The land use percentages are similar in both data sources (Table 2-2). Both show forested and farm lands cover the majority of the CSM area. The infrared analysis attributes a larger percentage of land use as grass land, both on and off of the JPG property. Both datasets also show the marked difference in land use on JPG property (predominantly forest and grass land) versus off JPG property (predominantly farm land).

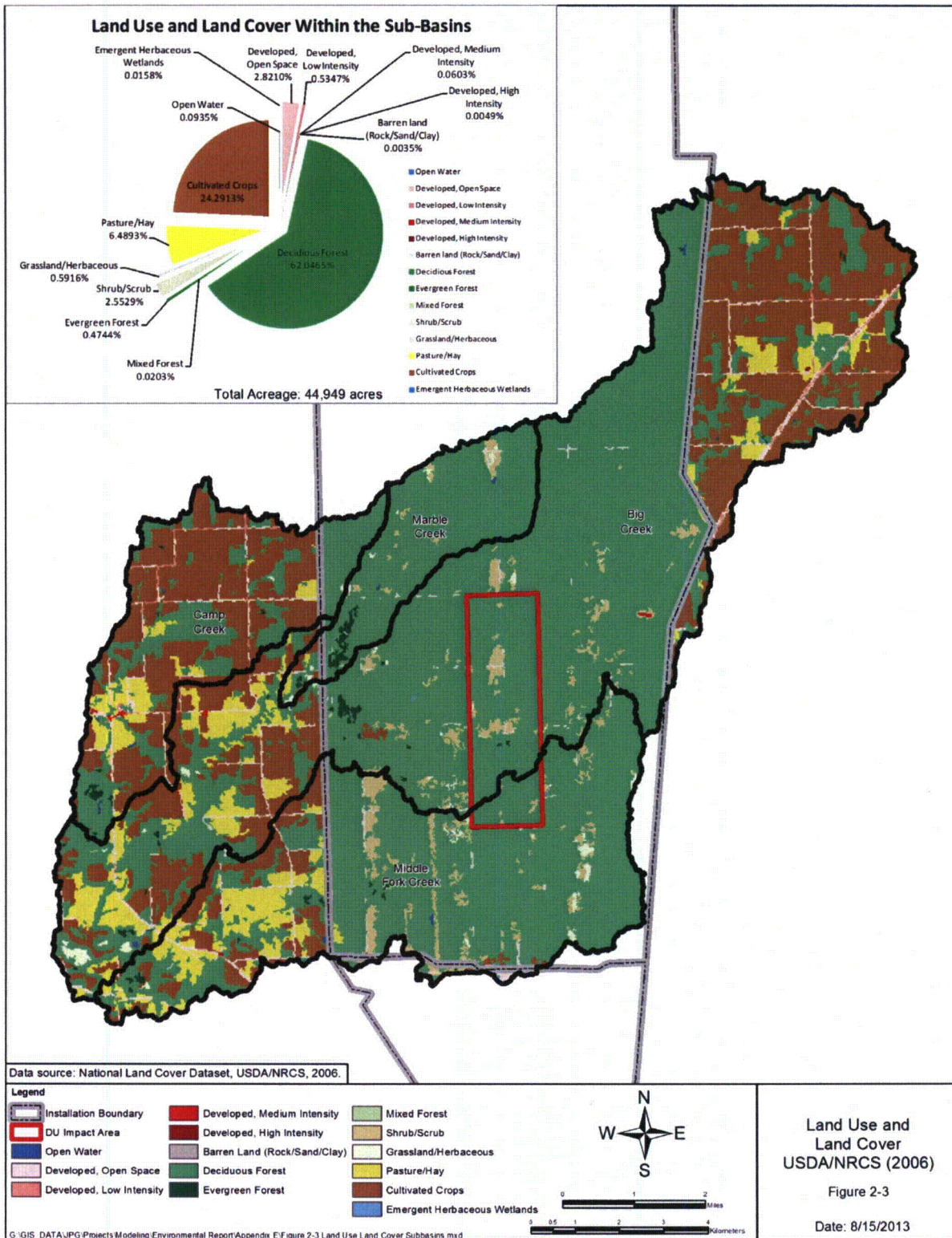
2.2.4 Meteorological Data

JPG lies within a temperate climate zone. Average annual precipitation is 47 inches per year (in/y) for the period 1976 through 2007 at Madison, Indiana (SAIC 2008). Data from this period were used to develop the water budget for JPG. During this same period, annual precipitation extremes ranged from a low of 33.2 inches in 1987 to a high of 60.9 inches in 1990. Average monthly precipitation ranges from a high of 5.08 inches in May to a low of 2.8 inches in February (Table 2-3). For comparison, the average annual precipitation from nearby Versailles, Indiana, weather station for 57 years (1949 through 2005) is 43.1 in/y, ranging from a low of 26.9 inches in 1953 to a high of 60.2 inches in 1990.

Table 2-3 lists monthly temperatures and record extremes at Madison, Indiana. On average, July and August are the warmest months, and January is the coldest month.

2.2.4.1 Onsite Data

A weather station exists onsite, northeast of the DU Impact Area. This weather station served as the basis for meteorological data for the 2003 through 2011 period. Some gaps were found in the time series when data were not recorded at this station. Meteorological data recorded at the nearby Butlerville Weather Station were used to fill these gaps and to extend the time series duration through January 2011.



- Infrared Coverage
 - 4-channel (visual spectrum + infrared) data from 2008 was processed to produce a detailed 6 meter Land Use Classification

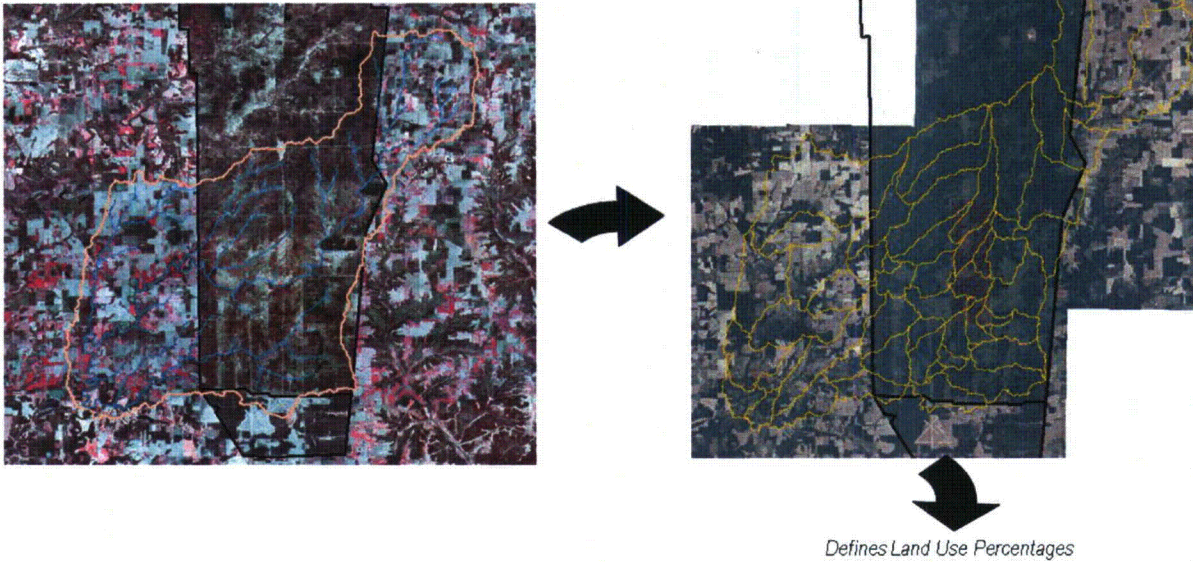
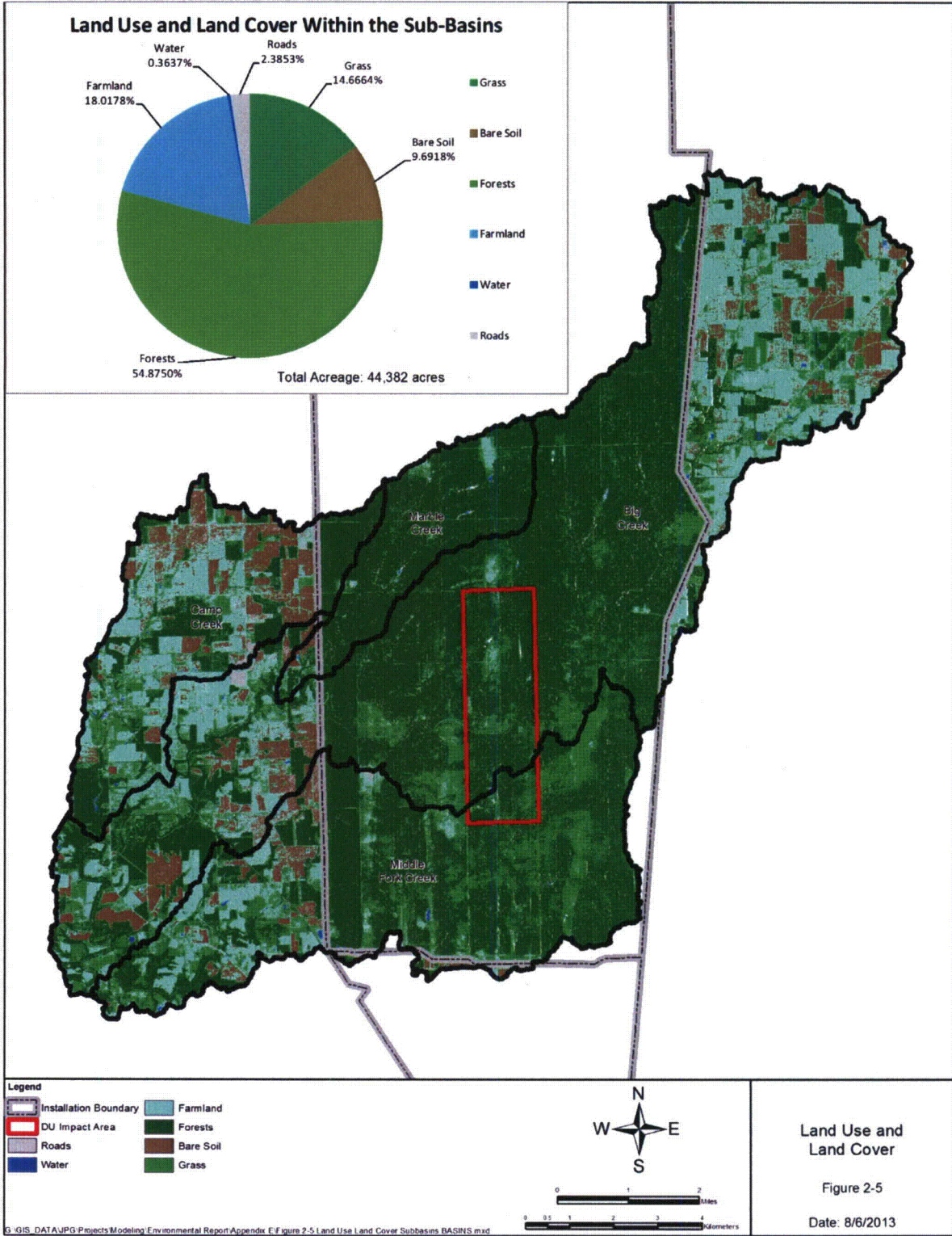


Figure 2-4. Land Use Classification from Infrared Analysis



**Table 2-2. Summary of Land Use Within the CSM Area
Jefferson Proving Ground, Madison, Indiana**

National Land Cover Dataset		Infrared Analysis	
Description	Model Area (%)	Description	Model Area (%)
Developed	3.4	Roads	2.4
Forest (deciduous, evergreen, mixed)	62.5	Forests	54.9
Farm land (pasture, hay, cultivated)	30.8	Farm land and bare soil	27.6
Grass (grass land, shrub/scrub)	3.1	Grass	14.7
Water (water, emergent wetland)	0.1	Water	0.4

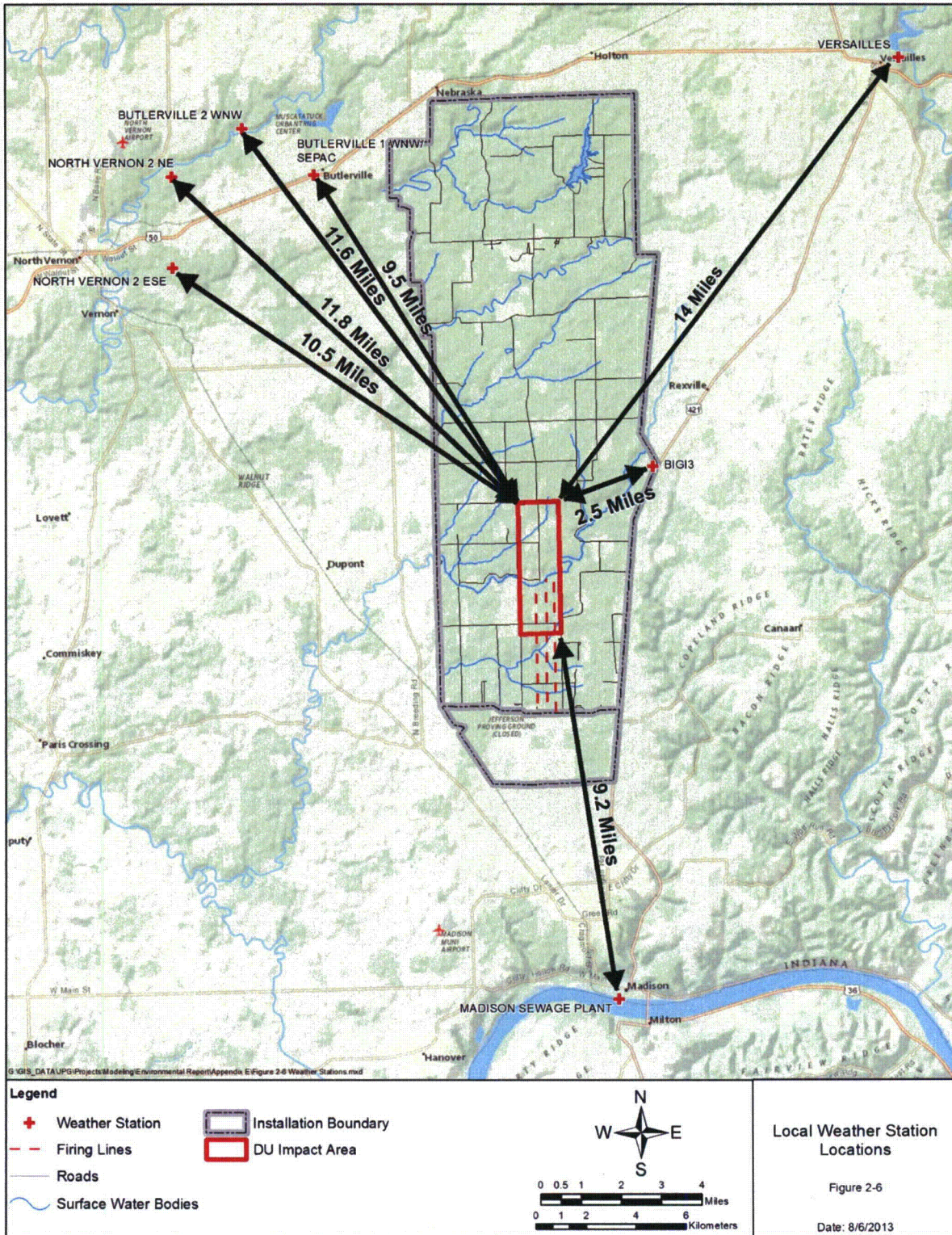
**Table 2-3. Monthly Precipitation and Temperature at Madison, Indiana
Jefferson Proving Ground, Madison, Indiana**

	Jan	Feb	Mar	Apr	May	Jun	Jul	Aug	Sep	Oct	Nov	Dec
Monthly Precipitation (in) for Madison, IN (1976-2007)												
Average	3.41	2.80	3.87	4.18	5.08	4.18	4.61	4.36	3.08	3.67	3.93	3.81
Min	0.52	0.22	1.04	0.88	1.31	0.34	0.94	1.16	0.24	0.83	0.94	0.50
Max	8.21	7.82	7.80	8.22	11.63	9.00	9.36	8.90	8.22	12.30	7.39	7.93
Monthly Temperature (°F) source: http://www.weather.com/weather/wxclimatology/monthly/USIN0386												
Average High	42	47	57	68	76	85	88	88	81	70	58	46
Average Low	23	25	32	42	53	62	66	65	57	45	35	27
Mean	33	36	45	55	65	74	77	77	69	58	47	37
Record High	75 (1950)	76 (2000)	84 (1981)	93 (1957)	97 (1953)	103 (1988)	108 (1954)	104 (1988)	108 (1953)	96 (1953)	88 (1950)	77 (1982)
Record Low	-17 (1994)	-12 (1951)	-2 (1980)	10 (2007)	27 (1963)	37 (1966)	48 (1972)	43 (1986)	33 (1995)	23 (1981)	0 (1950)	-18 (1989)

2.2.4.2 Data From Nearby Stations

To address data gaps within the onsite weather data, a second hourly dataset was obtained from the Midwest Regional Climate Center (MRCC) website. The closest MRCC weather station is the Butlerville Weather Station (Indiana), located approximately 2 miles west of the northern portion of JPG (Figure 2-6).

The onsite data were compared with data collected from the Butlerville station. A cross plot was generated by plotting the Butlerville daily precipitation data against the JPG daily precipitation data (created by summing the hourly data for each day). The cross plot (Figure 2-7) was evaluated to determine the correlation between the two datasets, taking into account the slope and R-squared value of the best fit line. As illustrated in Figure 2-7, the R-squared and the best fit line slope were 0.49 and 0.95, respectively, indicating a correlation between the two datasets. Comparing the two populations (null hypothesis data are not related) results in a p value of <0.05, indicating the two datasets are related. Based on this evaluation, Butlerville data were substituted into the JPG dataset where gaps were present in the onsite precipitation data. Temperature and evapotranspiration data from Butlerville also were incorporated into the JPG onsite weather station time series.



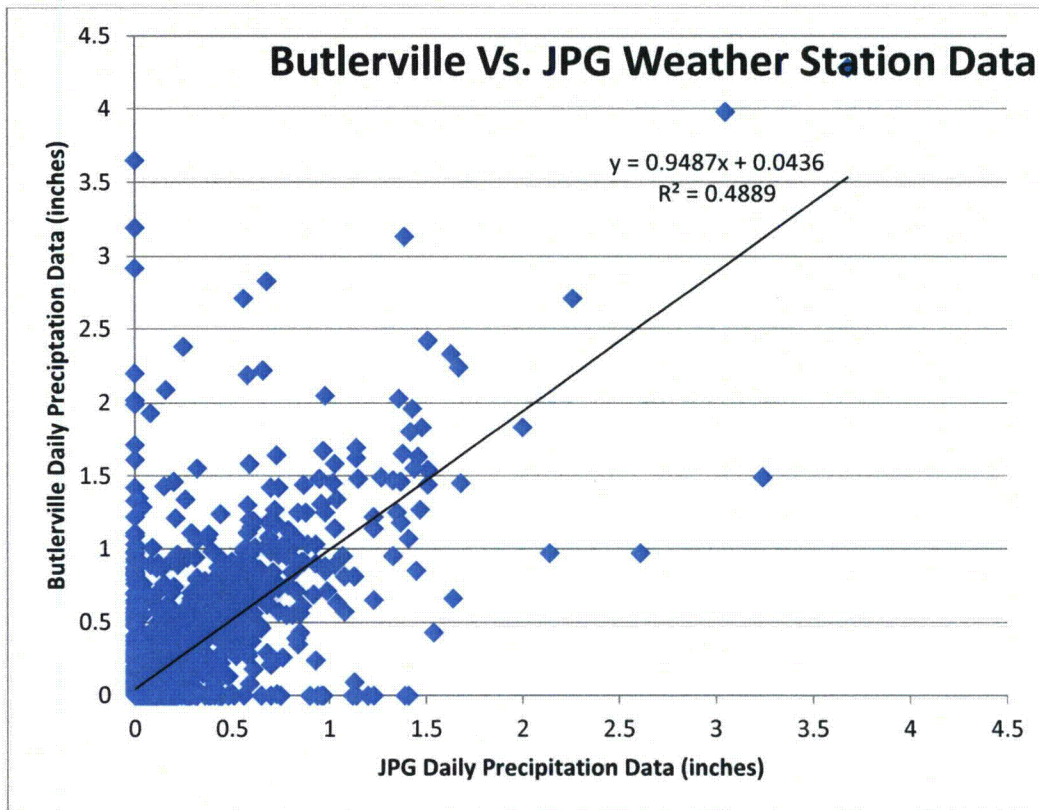


Figure 2-7. Cross Plot of JPG and Butlerville Weather Station Precipitation Data

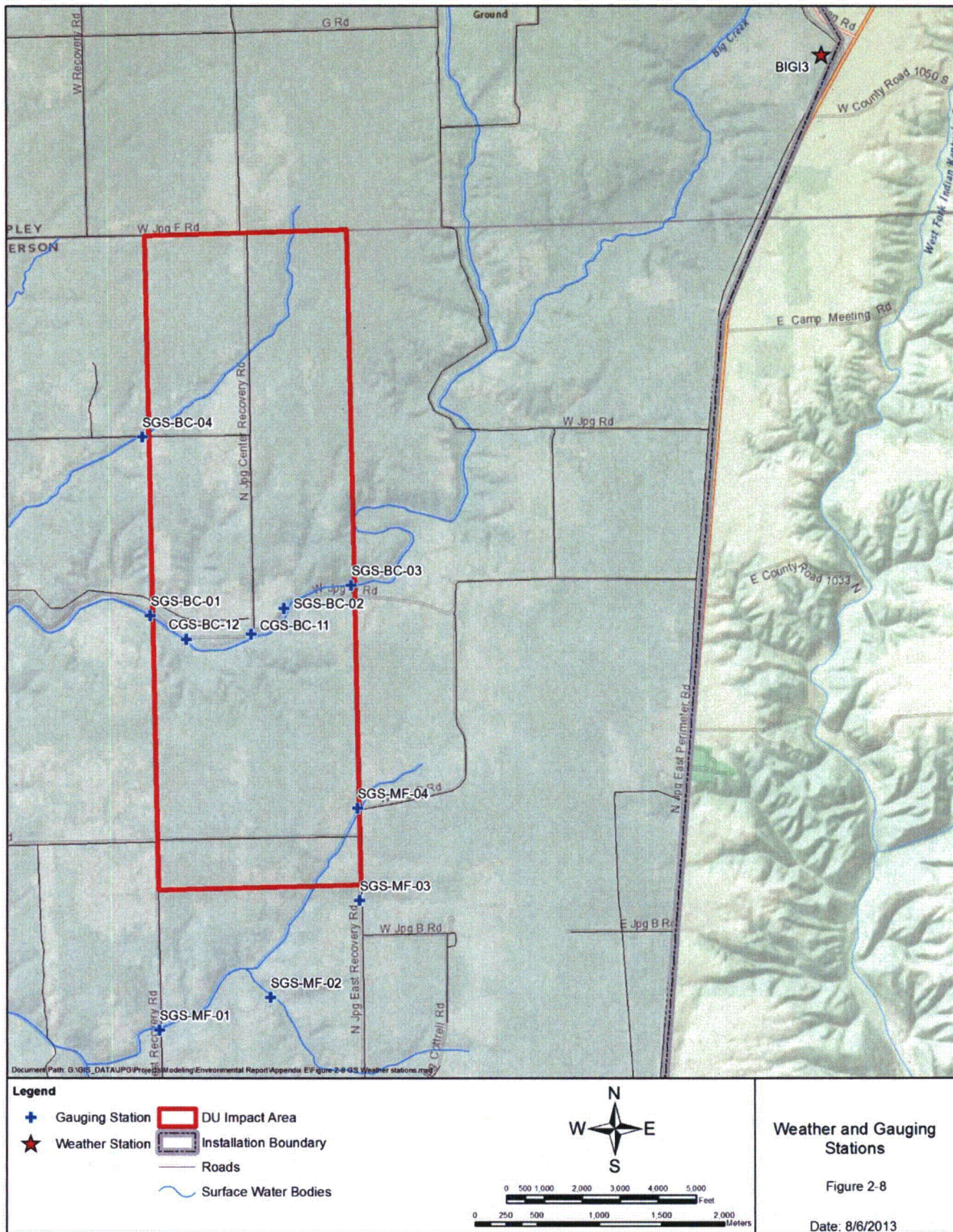
2.2.4.3 Creation of Time Series

Using data collected from JPG and Butlerville, a complete hourly time series for precipitation, potential evapotranspiration, and temperature was successfully created. The data required minor manipulation in order to work correctly with WDMUtil, a program that generates, calculates, manages, displays, and exports meteorological data to or from a Watershed Data Management (WDM) file. Precipitation and temperature data were collected from the field, while potential evapotranspiration data were generated from the daily minimum and maximum temperatures.

2.2.5 Observed Stream Stage and Flow

Surface water gauging stations were installed in September 2006 (from the SAIC 2008 Final Well Construction and Surface Water Data Report). They include automatic, continuous, recording stream gauging stations on Big Creek (three locations) and Middle Fork (four locations), selected cave springs along Big Creek (two locations) inside the DU Impact Area, and one visual staff gauge along an unnamed tributary of Big Creek. These locations are shown in Figure 2-8.

The surface water gauging stations collect stream stage data at each location. Generally, the gauge stations consist of a stilling well and a pressure transducer/electronic data logger. Manual flow measurement locations were selected close to the stilling well locations in areas that had stream bank and bottom flow conditions conducive to collecting manual flows (e.g., flat bottom, clear of obstructions, [SAIC 2007]). Stage data and the corresponding manually measured flow rates were used to develop a rating curve for each station that was used to construct surface flow hydrographs for the streams at each gauge station. These hydrographs were compared to existing USGS gauge stations near the site.



2.2.5.1 Cave Gauges

Excluding the periods of time where flow exceeded the capacity of the weirs, flows from the cave springs ranged from 0 to 646 gallons per minute (gpm) (1.4 cubic feet per second [cfs]) in BC-11 and 0 to 355 gpm (0.8 cfs) in BC-12. Cave stream hydrographs show that the flow is extremely flashy, meaning that after precipitation events, the flow increases and decreases rapidly, causing the spiky nature of the hydrographs. The hydrographs showed periods of no-flow in all months except February through April, interrupted by sharp rises in flow as a result of precipitation events. These observations suggest that the cave stream networks feeding Big Creek and Middle Fork Creek are above the groundwater table most of the year. The cave streams appear to serve as storm water conduits, capturing surface water runoff, presumably through sink holes and well-drained depressions.

2.2.5.2 Stream Gauges

At each stage recorder location, the flow in the stream was measured manually using an in-stream flow meter. The methodology used to measure the streams is in accordance with the U.S. Environmental Protection Agency's (USEPA's) Wadeable Stream Assessment Field Operations Manual (USEPA 2004).

Ten measurements were collected on most stations in the year after installation to collect a range of flow data at different stages, as the streams reacted to seasonal runoff flows. A comparison of the manual flow measurements and the corresponding stage indicates uncertainty in the measurements. Some measurements were impacted by log jams observed by field staff, and it was reasonable to exclude the data while developing the rating curve. The calculated discharge using the rating curve formula compared to the measured discharge shows a large degree of uncertainty in the measurements.

The poor correlation between recorded stage and measured flow is likely due to changing stream channel configuration caused by frequent storm flows, log and ice jams, and the numerous and changing beaver dams/pools, or field measurement error, especially at lower flow conditions where accurate measurement of flows using the flow meter methodology is difficult.

Observations of the character of the stream stage hydrographs are useful. The following observations from these hydrographs about the stream flow characteristics are offered:

- The streams are extremely flashy, meaning that after precipitation events, the flow increases and decreases rapidly, causing the spiky nature of the hydrograph
- The hydrographs showed a period of low- to no-flow for 4 to 6 weeks of the year, during June and July.
- The median discharge for the period of record ranges from 0.04 to 0.49 cfs per square mile. Onsite stream hydrographs were compared to hydrographs from USGS gauging stations for the same time period.
- Station 03368000 is located 11.3 miles northwest of the JPG DU Impact Area boundary near Nebraska, Indiana. The gauge is on Brush Creek, with a drainage area of 11.40 square miles. From a review of topographic maps and aerial photographs, the drainage basin topography and land use/cover appear to be very similar to Big Creek, with mostly agricultural and wooded land use. The geology in both basins is nearly identical (Indiana Geological Survey 2002). The station has continuously recorded discharge from 1 June 1955 through the present day. The geology and topography of the basin are very comparable to the Big Creek and Middle Fork Creek basins onsite. The basin had a median flow of 2.1 cfs (0.18 cubic feet per second per square mile [cfs/mi²]) for the period of interest, nearly identical on a unit area basis to the median flow measured in the three Big Creek gauges in the DU Impact Area (0.14 to 0.22 cfs/mi²). The median flow for the entire period of record is 2.3 cfs (0.20 cfs/mi²). Periods of low- to no-flow were common in late June through November. The hydrograph of this stream shows the same flashy nature as the hydrographs on Big Creek in the DU Impact Area.

- Station 03366500 is located 14 miles southwest of the JPG DU Impact Area, on the Muscatatuck River near Deputy, Indiana. This station is downstream from and includes the JPG area and Brush Creek, and has been continuously recording discharge from 1 April 1948 through the present day. From a review of topographic maps and aerial photographs, the drainage basin topography and land use/cover appear to be very similar to Big Creek, with mostly agricultural and wooded land use. The geology of this basin compared to the Big Creek basin in and upgradient of the DU Impact Area appears to be very similar. The larger basin is underlain by bedrock units somewhat above and below the units exposed in the Big Creek Basin, but the rock types are very similar and should have similar hydrogeologic properties. The 296-square-mile basin had a median flow of 83 cfs (0.28 cfs/mi²) for the period of interest, slightly higher than measured in the three Big Creek gauges in the DU Impact Area (0.14 to 0.22 cfs/mi²). Periods of no-flow were observed from July through November. The hydrograph of this stream shows the same flashy nature as the hydrographs on Big Creek in the DU Impact Area.

2.2.6 Observed Suspended Sediment Transport

No suspended sediment data have been collected and reported for Big Creek or Middle Fork Creek. Two streams located near JPG, Vernon Fork and Brush Creek, have suspended sediment data. The streams are similar to those at JPG, and suspended sediment data are used as a proxy for the JPG site. Stream flow velocities at the Vernon Fork were estimated from the reported flow rates and the cross-sectional characteristics. For Brush Creek, the cross-sectional characteristics were not readily available in the reviewed reports. Both streams (Brush and Vernon) have point measurements of suspended sediment and corresponding flow rates measured and reported for a few events since 1964. More than half total suspended sediment (TSS) values reported for Brush and Vernon streams are <100 mg/L. Figure 2-9 shows a relationship between TSS and stream flow rate for Brush Creek. Figure 2-10 shows the relationship between TSS and stream velocity for the Vernon Fork (Muscatatuck River) stream.

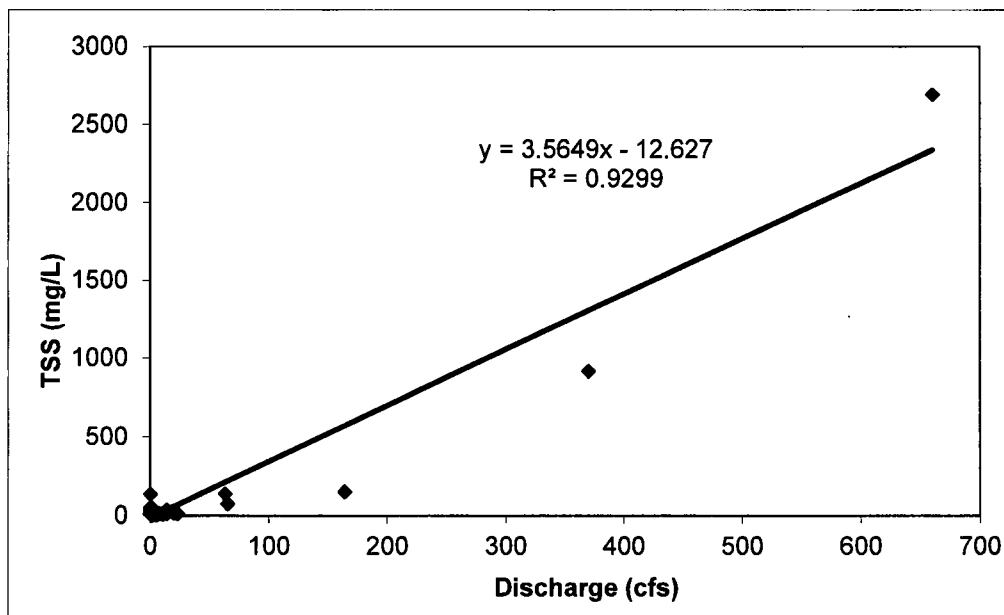


Figure 2-9. Suspended Sediment Concentration Versus Flow Rate at Brush Creek (1960-1968)

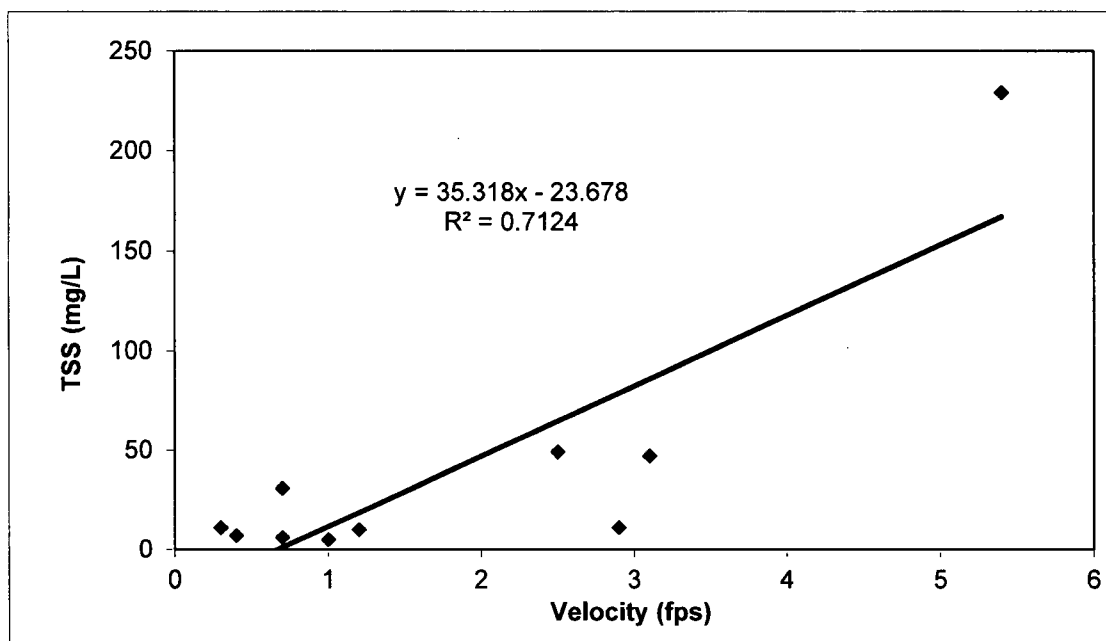
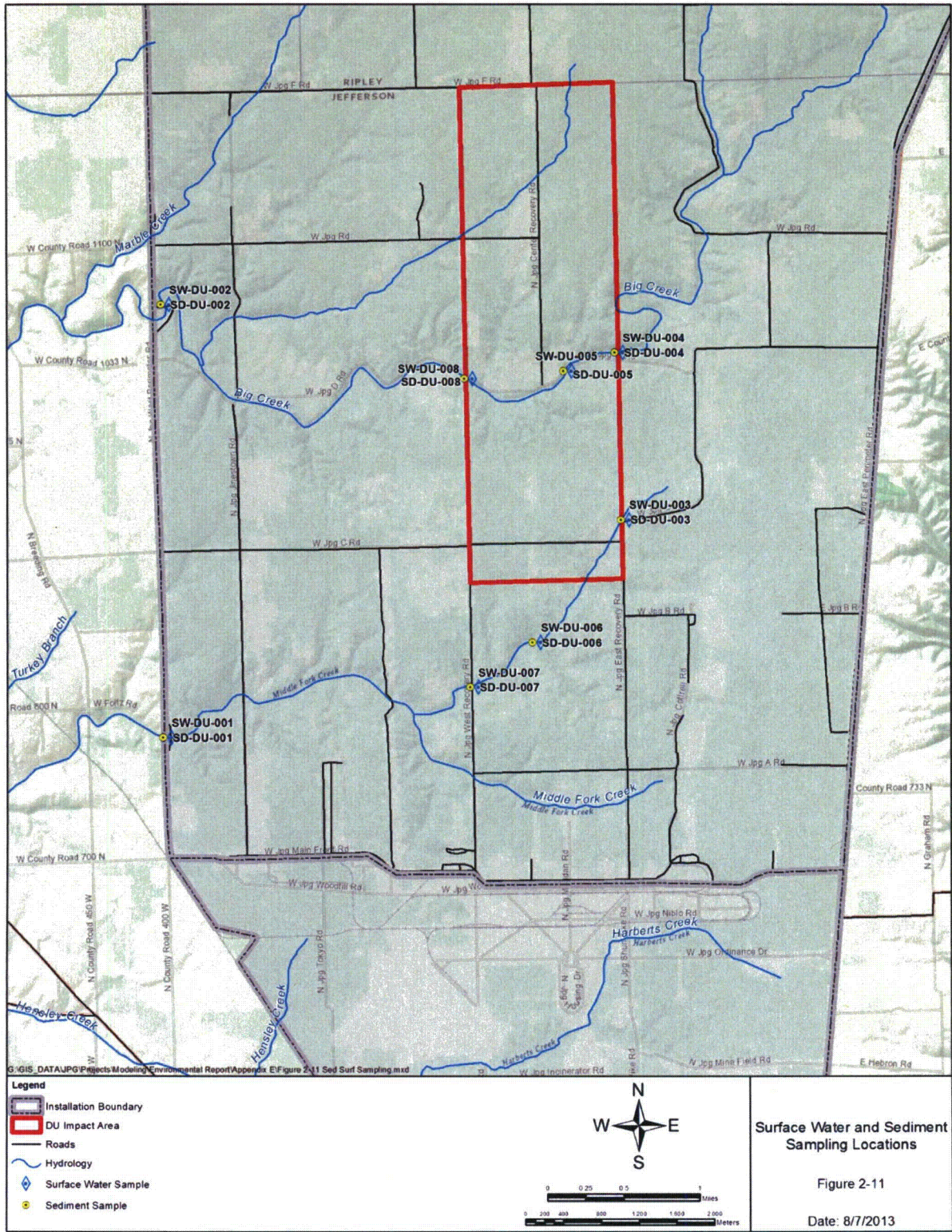


Figure 2-10. Suspended Sediment Concentration Versus Velocity at Vernon Fork (1977-1980)

2.2.7 Observed Uranium Analytical Data

Environmental media (groundwater, surface water, sediment, and soils [Figure 2-11]) are regularly monitored to ensure DU remaining within the DU Impact Area does not pose a risk to human health or the environment (SAIC 2013). Surface water and sediment samples are co-located to the extent possible. Results by media indicate low levels of total uranium activity at JPG and are not indicative of significant trends or migration in any media. October 2012 Environmental Radiation Monitoring (ERM) Program (SAIC 2013) fall sampling event and historical data are summarized below:

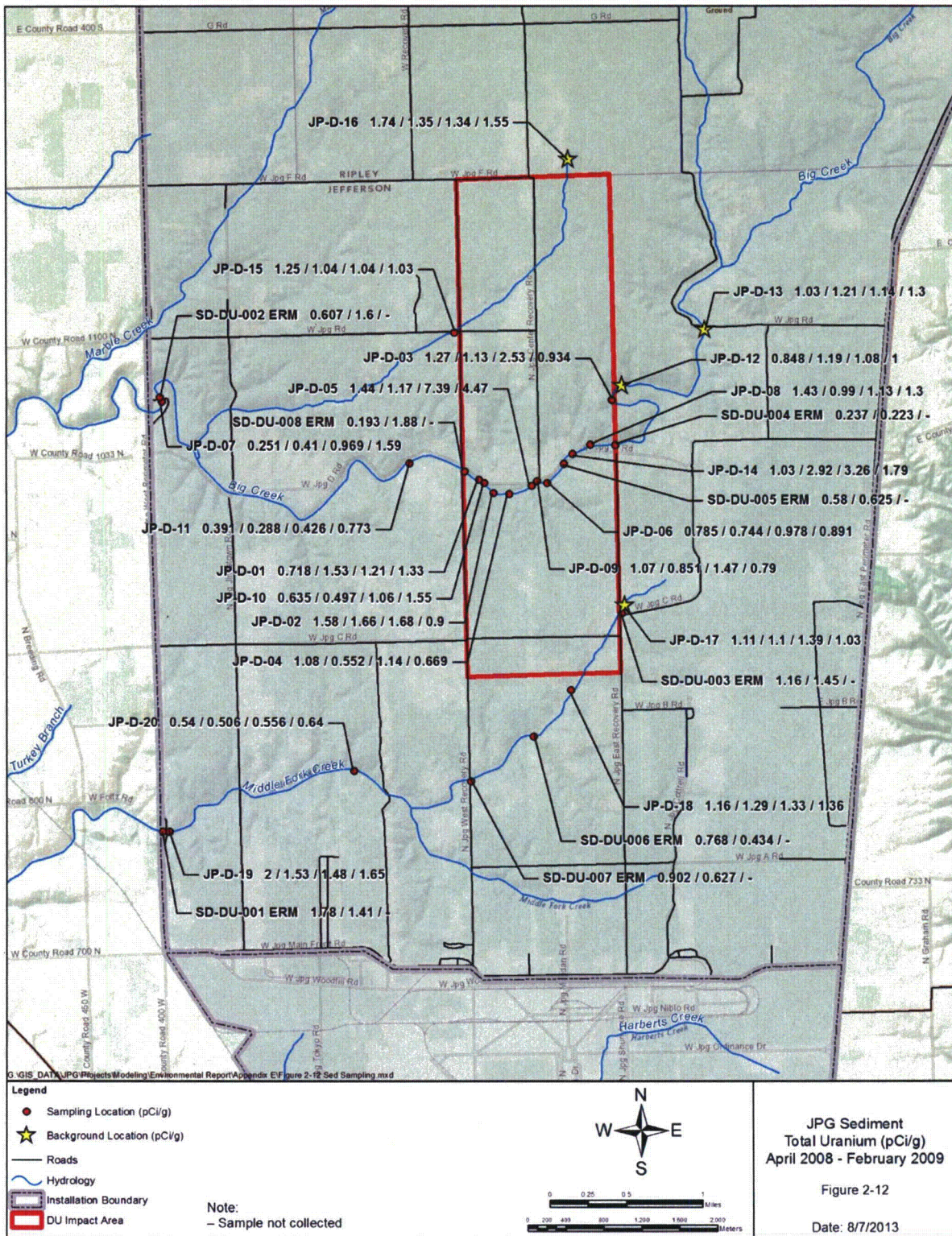
- Groundwater quality (11 monitoring wells; filtered sample results)
 - October 2012 total uranium ranged from 0.19 ± 0.09 picocuries per liter (pCi/L) with an average concentration of 1.4 ± 1.0 pCi/L.
 - Historical assessment from 202 discrete samples collected from 2004 through October 2012 showed average total uranium concentration of 1.4 pCi/L (3.9 μ g/L), the standard deviation is 1.2 pCi/L (3.3 μ g/L), and the maximum detected concentration is 5.7 ± 0.6 pCi/L (16 μ g/L).
- Surface water quality (eight locations; filtered sample results)
 - October 2012 total uranium ranged from 0.24 ± 0.09 pCi/L to 1.8 ± 0.3 pCi/L with an average concentration of 0.65 ± 0.46 pCi/L.
 - Historical assessment from 145 discrete samples collected from 2004 through October 2012 showed average total uranium concentration of 0.88 pCi/L (2.5 μ g/L), the standard deviation is 2.4 pCi/L (6.9 μ g/L), and the maximum detected concentration is 19 ± 2 pCi/L (53 μ g/L).

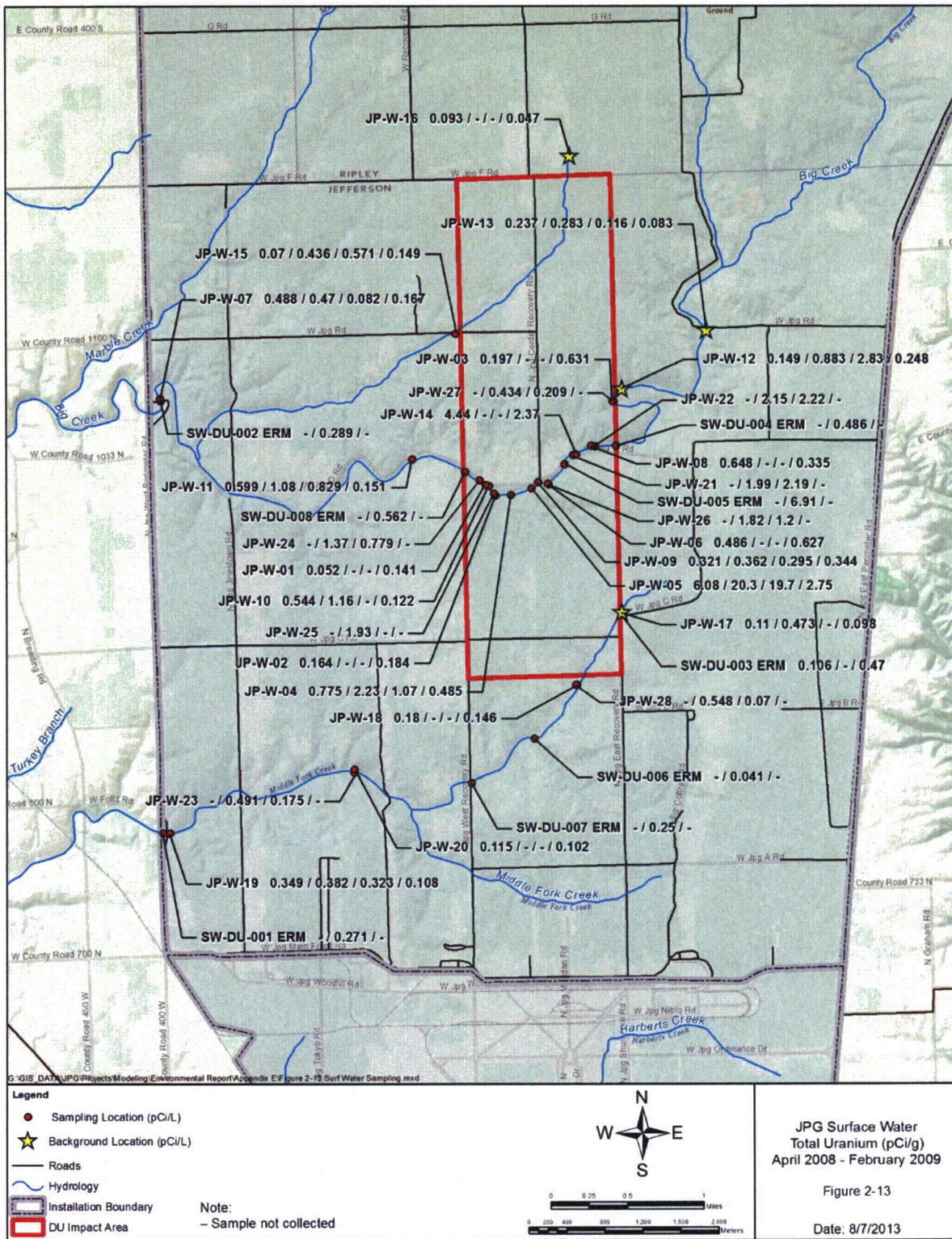


- Sediment (eight locations)
 - October 2012 total uranium ranged from 0.38 ± 0.08 to 1.0 ± 0.1 picocuries per gram (pCi/g) (1.1 to 2.8 mg/kg) with an average concentration of 0.77 ± 0.36 pCi/g (1 milligram per kilogram [mg/kg]). One sediment sample result from Big Creek within the DU Impact Area slightly exceeded a uranium-238:uranium-234 (U-238:U-234) activity ratio of 3.0, indicating the possible presence of DU in the sample.
 - Historical assessment from 151 discrete samples collected from 2004 through October 2012 showed average total uranium concentration of 0.97 pCi/g (2.7 mg/kg), the standard deviation is 0.49 pCi/g (1.4 mg/kg), and the maximum detected concentration is 2.4 ± 0.4 pCi/g (6.7 mg/kg).
- Soils (four locations)
 - October 2012 total uranium ranged from 0.8 ± 0.12 to 1.4 ± 0.2 pCi/g (0.8 to 3.9 mg/kg) with an average concentration of 1.2 ± 0.4 pCi/g (3.3 mg/kg).
 - Historical assessment from 86 discrete samples collected from 2004 through October 2012 showed average total uranium concentration of 1.5 pCi/g (4.2 mg/kg), the standard deviation is 0.3 pCi/g (0.83 mg/kg), and the maximum detected concentration is 2.2 ± 0.5 pCi/g (6.1 mg/kg).

In addition to regular ERM monitoring, site investigation data have been collected to further define the nature and extent of DU in the environmental media within and adjacent to the DU Impact Area. Groundwater, surface water, and sediment samples were collected quarterly (April 2008, July 2008, October 2008, and February 2009). Surface water and sediment sampling locations were co-located to the extent possible; samples were collected from locations along Big Creek and Middle Fork Creek and are most pertinent to the surface water modeling effort. Figures 2-12 and 2-13 show the locations and results of surface water and sediment sampling, respectively, along Big Creek and Middle Fork Creek. Key findings from these data include:

- Groundwater (42 wells sampled quarterly; April 2008, July 2008, October 2008, and February 2009)
 - 189 total samples, 44 background, and 145 site wells; some wells were periodically dry and could not be sampled
 - 14 overburden wells, 20 shallow bedrock wells, and 8 deep bedrock wells
 - Ten samples collected from overburden wells in background/upgradient locations were analyzed for total and isotopic uranium and ten additional samples were collected, filtered in the field, and analyzed for total and isotopic uranium. Total uranium concentrations in unfiltered samples ranged from 0.81 ± 0.21 to 6.4 ± 1.1 pCi/L (2.2 to 18 $\mu\text{g/L}$) in filtered samples and from 0.98 ± 0.25 to 4.8 ± 0.88 pCi/L (2.7 to 13 $\mu\text{g/L}$) in unfiltered samples with mean concentrations of 2.5 (unfiltered) and 2.2 (filtered) pCi/L (6.9 and 6.1 $\mu\text{g/L}$, respectively).
 - 60 samples collected from overburden wells within and downgradient from the site were analyzed for total and isotopic uranium and 59 additional samples were collected, filtered in the field, and analyzed for total and isotopic uranium. Total uranium concentrations in unfiltered samples ranged from 0.076 ± 0.15 to 40 ± 6.6 pCi/L (0.21 to 112 $\mu\text{g/L}$) in filtered samples and from 0.027 ± 0.14 to 47 ± 7.7 pCi/L (0.075 to 131 $\mu\text{g/L}$) in unfiltered samples with mean concentrations of 2.6 (unfiltered) and 2.9 (filtered) pCi/L (7.2 and 8.1 $\mu\text{g/L}$, respectively).





- 36 samples collected from shallow bedrock wells in background/upgradient locations were analyzed for total and isotopic uranium and 35 additional samples were collected, filtered in the field, and analyzed for total and isotopic uranium. Total uranium concentrations in unfiltered samples ranged from 0.14 ± 0.16 to 2.6 ± 0.58 pCi/L (0.39 to 7.2 $\mu\text{g/L}$) in filtered samples and from 0.18 ± 0.13 to 2.2 ± 0.49 pCi/L (0.5 to 6.0 $\mu\text{g/L}$) in unfiltered samples with mean concentrations of 0.88 (unfiltered) and 0.79 (filtered) pCi/L (2.4 and 2.2 $\mu\text{g/L}$, respectively).
- 56 samples collected from shallow bedrock wells within and downgradient from the site were analyzed for total and isotopic uranium and 54 additional samples were collected, filtered in the field, and analyzed for total and isotopic uranium. Total uranium concentrations in unfiltered samples ranged from 0.065 ± 0.065 to 5.0 ± 0.98 pCi/L (0.18 to 14 $\mu\text{g/L}$) in filtered samples and from 0.085 ± 0.071 to 4.7 ± 0.92 pCi/L (0.24 to 13 $\mu\text{g/L}$) in unfiltered samples with mean concentrations of 1.4 (unfiltered and filtered) pCi/L (3.9 $\mu\text{g/L}$).
- Three samples collected from deep bedrock wells in background/upgradient locations were analyzed for total and isotopic uranium and one additional sample was collected, filtered in the field, and analyzed for total and isotopic uranium. Total uranium concentrations in unfiltered samples ranged from 0.060 ± 0.058 to 0.10 ± 0.065 pCi/L (0.17 to 0.28 $\mu\text{g/L}$) in filtered samples with a mean concentration of 0.080 pCi/L (0.22 $\mu\text{g/L}$). Total uranium was detected in the single filtered sample at 0.11 pCi/L (0.31 $\mu\text{g/L}$).
- 31 samples collected from deep bedrock wells within and downgradient from the site were analyzed for total and isotopic uranium and 27 additional samples were collected, filtered in the field, and analyzed for total and isotopic uranium. Total uranium concentrations in unfiltered samples ranged from 0.066 ± 0.059 to 21 ± 3.5 pCi/L (0.18 to 57 $\mu\text{g/L}$) in filtered samples and from 0.042 ± 0.17 to 17 ± 2.8 pCi/L (0.12 to 47 $\mu\text{g/L}$) in unfiltered samples with mean concentrations of 3.9 (unfiltered) and 3.0 (filtered) pCi/L (10.8 and 8.3 $\mu\text{g/L}$, respectively).
- Surface water (20 locations sampled quarterly; April 2008, July 2008, October 2008, and February 2009; plus 4 background locations; locations are on Big Creek and Middle Fork Creek)
 - 90 total samples, 13 background, and 77 site locations; some locations were dry and could not be sampled
 - Total uranium concentrations in 59 unfiltered samples collected from Big Creek ranged from 0.082 ± 0.14 to 20 ± 4.1 pCi/L (0.23 to 56 $\mu\text{g/L}$) and from 0.059 ± 0.14 to 22 ± 4.4 pCi/L (0.16 to 61 $\mu\text{g/L}$) in 59 filtered samples with average concentrations of 1.6 pCi/L (4.4 $\mu\text{g/L}$) for both filtered and unfiltered samples; highest observed concentration where runoff is expected to enter Big Creek from DU impact trench
 - Total uranium concentrations in 19 unfiltered samples collected from Middle Fork Creek ranged from 0.070 ± 0.15 to 0.55 ± 0.21 pCi/L (0.19 to 1.5 $\mu\text{g/L}$) and from 0.32 ± 0.14 to 0.65 ± 0.23 pCi/L (0.089 to 1.8 $\mu\text{g/L}$) in 16 filtered samples with average concentrations of 0.24 and 0.30 pCi/L (0.67 and 0.83 $\mu\text{g/L}$) for filtered and unfiltered samples, respectively
 - Total uranium concentrations in 11 unfiltered samples collected from North Tributary ranged from 0.047 ± 0.14 to 0.64 ± 0.24 pCi/L (0.13 to 1.8 $\mu\text{g/L}$) and from 0.057 ± 0.068 to 0.56 ± 0.17 pCi/L (0.16 to 1.6 $\mu\text{g/L}$) in 10 filtered samples with average concentrations of 0.26 and 0.23 pCi/L (0.72 and 0.64 $\mu\text{g/L}$) for filtered and unfiltered samples, respectively

- Results from four samples exceeded USEPA's 30 µg/L (9 pCi/L) Safe Drinking Water Act (SDWA) maximum contaminant level (MCL). Results for the following four samples collected from JP-W-05 exceeded the MCL: July 2008 at 22 ± 4.4 (filtered) and 20 ± 4.1 (filtered) pCi/L and October 2008 at 18 ± 3.5 (filtered) and 20 ± 3.8 (filtered) pCi/L. Samples collected from location JP-W-05 were collected from a point in the vicinity where overland flow from 500 Center trench intersects with Big Creek. These samples were collected from standing pools of water (i.e., limited or no water flow).
- Sediment (20 locations sampled quarterly; April 2008, July 2008, October 2008, and February 2009; plus 4 background locations; locations are on Big Creek and Middle Fork Creek)
 - 96 total samples, 16 background, and 80 site locations
 - Most samples indicate total uranium concentrations were detected at less than 2 pCi/g.
 - Total uranium concentrations ranged from 0.25 ± 0.13 to 7.4 ± 1.6 pCi/g (0.70 to 21 mg/kg) for Big Creek sediment samples, 0.51 ± 0.20 to 2.0 ± 0.55 pCi/g (1.4 to 5.6 mg/kg) for Middle Fork Creek sediment samples, and 0.96 ± 0.16 to 1.7 ± 0.38 pCi/g (0.97 to 4.7 mg/kg) for North Tributary sediment samples, with overall mean concentrations of 1.3, 1.2, and 1.3 pCi/g (3.6, 3.4, and 3.6 mg/kg) for Big Creek, Middle Fork Creek, and North Tributary, respectively.
 - All concentrations are low with respect to potential radiological dose (35 pCi/g).
 - The highest concentrations were observed where runoff is expected to enter Big Creek from the 500 Center trench.
 - Evidence of DU was observed in eight sediment samples collected from five locations based on elevated U-238/U-234 ratios (i.e., exceeding 3.0) during one or more of the quarterly site characterization sampling events or semiannual ERM sampling events. Isotopic ratios (U-238/U-234) exceeded 3.0 in the following samples: JP-D-05 (4.7 ± 2.9 in April 2008, 4.4 ± 2.9 in July 2008, 5.1 ± 1.7 in October 2008, and 4.5 ± 1.5 in February 2009) and JP-D-14 (4.2 ± 2.7 in April 2008, 5.2 ± 2.5 in July 2008, 5.2 ± 1.8 in October 2008, and 1.7 ± 0.6 in February 2009). All sediment samples with elevated isotopic ratios were collected from Big Creek in close proximity to the trench associated with the 500 Center line of fire.
- Soil (140 locations)
 - 647 soil samples (127 background and 520 characterization samples)
 - Sampling results from within impact trenches and above/below penetrators elevated compared to background
 - Background results ranged from 0.15 (0.43 mg/kg, measured with inductively coupled plasma-mass spectrometry [ICP-MS]) to 3.8 ± 0.81 pCi/g, (0.43 to 10.6 mg/kg) with means 1.3 (Avonburg/Cobbsfork), 1.4 (Cincinnati/Rossmoyne), and 1.7 (Grayford/Ryker) pCi/g (3.6, 3.9, and 4.7 mg/kg, respectively)
 - Total uranium concentrations in soil samples collected away from the trench and penetrators ranged from 0.71 ± 0.18 to 19 ± 5.4 pCi/g (2.0 to 53 mg/kg)
 - Samples from the glacial till ranged from 0.16 (0.43 mg/kg, measured with ICP-MS) to 2.2 ± 0.24 pCi/g (0.43 to 6.1 mg/kg)
 - Samples collected from within the trench area (Category 6) and samples collected from over or under penetrators ranged from -1.8 ± 2.7 to 142 ± 16 pCi/g (0 to 394 mg/kg)

- Above/below penetrators ranged from 22 ± 4.7 to $40,694 \pm 16$ pCi/g (61 to 113,000 mg/kg), with means of 6,831 (Avonburg/Cobbsfork), 3,960 (Cincinnati/Rossmoyne), and 3,814 (Grayford/Ryker) pCi/g (18,975, 11,000, and 10,594 mg/kg, respectively).
- Soil sampling results indicate elevated uranium detected up to 4.5 ft below ground surface (BGS). The mean concentration for samples from over/under penetrators falls from 13,729 pCi/g (0 to 0.75 ft BGS) to 1,926 pCi/g (0.5 to 1.25 ft BGS) to 547 pCi/g (1 to 2.5 ft BGS) to 208 pCi/g (2 to 4.5 ft BGS). However, the deepest samples, on average, are well above background levels for total uranium with means from 1.3 to 1.7 pCi/g. In addition, the number of samples exceeding U-238/U-234 ratios of 3.0 change with depth from 34 (0 to 0.75 ft BGS) to 26 pCi/g (0.5 to 1.25 ft BGS) to 27 pCi/g (1 to 2.5 ft BGS) to 18 pCi/g (2 to 4.5 ft BGS).

2.3 CODE SELECTION

Watershed computer models have been extensively used to simulate interaction between various hydrologic processes and management practices, and to investigate their impact on the agricultural productivity, quality of natural resources, and the environment health. The technical capabilities, robustness, and data needs of some leading surface water models were compared (in a broad sense) to guide model selection for simulation of runoff, transport of sediment, and DU corrosion products. The important processes involved in water quality and quantity simulations included estimation of surface runoff; sediment and contaminant fate and transport; and routing of surface runoff, sediments, and DU in a network of open channels and/or conduits.

The models investigated were Hydrological Simulation Program-Fortran (HSPF) USEPA (2001b), Storm Water Management Model (SWMM) USEPA (2013), and Neitsch et al. (2011) Soil and Water Assessment Total (SWAT); each is a comprehensive watershed model that can be used for event based or continuous simulations. Each model has modules to simulate critical processes such as runoff, transport, and routing, but the key factors in model selection were data availability, robustness, and accuracy of computational procedures to simulate runoff, transport, and routing to permit attainment of modeling objectives. The following sections provide a brief discussion for each model and the important factors that were considered in the model selection process.

2.3.1 HSPF (*Hydrologic Simulation Program – FORTRAN*)

HSPF is a USEPA code and is considered to be one of the most comprehensive watershed management and planning models available. The data needs of the HSPF models are generally extensive, and when suitable data are either not available or unreliable, suitable assumptions are invoked to simplify the problem and assume and/or generate the missing data.

HSPF has modules to estimate surface runoff from snow and/or rainfall. Runoff from snow was estimated using one of the two approaches: 1) energy balance method and 2) temperature index (degree-day) method. The energy balance approach needs precipitation, air temperature, solar radiation, dew-point, wind velocity, and cloud cover (optional) time series. The temperature index approach needs precipitation, air temperature, and dew-point (optional) time series.

Surface runoff resulting from rainfall is an important component of the water budget and plays an important role in soil erosion and transport of sediments and chemicals. Runoff estimation algorithms in HSPF account for interception (by vegetation and surface cover), surface storage, lateral inflow/outflows, infiltration, interflow, and deep percolation to groundwater. Depending on the options invoked, user needs to supply hourly precipitation, evaporation, temperature, wind speed, solar radiation, dew point, and cloud cover time series. However, the potential evapotranspiration, precipitation, and average temperature time series are always required.

The user may supply several input parameters such as interception capacity, varying each month or input as fixed value for the duration of the simulation. Subsurface is considered, consisting of an upper, lower, and underlying groundwater zones. The user needs to input nominal storage capacities (water holding capacity) for the upper and lower zones. Transient infiltration rate as a function of soil moisture is based on the work of Philips (1957). Simplified empirical relationships are used to estimate various components of the water budget.

The soil erosion and sediment transport modules are based on the predecessor ARM (Agricultural Runoff Management) and NPS (Nonpoint Source) models; HSPF offers options to select a method for simulating sediment transport from pervious land segments (PERLND). HSPF includes a module to simulate detachment of soil particle by rain impact, but requires the user to specify a detachment coefficient and exponents (dependent on soil properties). The soil detachment by rainfall equation has been improved based on the management practices "P" factor in the Universal Soil Loss Equation (USLE). The equation to estimate scouring of the matrix soil was derived from Negev's method for simulating gully erosion.

HSPF simulates removal of contaminants adsorbed to the sediment and assumes that the mass of the particular constituent is directly proportional to the mass of sediment removed – the relationship is specified by user-input through potency factors – defined separately for the suspended and scoured sediments. HSPF offers several options to specified spatial and temporal application of source(s) of contamination and they include adsorbed to soil matrix and/or in dissolved form and/or as external deposition (such as from atmosphere) directly to the sub-basins and/or to the streams. The user needs to specify these sources as hourly time series.

HSPF divides the sediment load into three soil fractions (sand, silt, and clay) and a potency factor (~ adsorption parameter) of each component of concern to the three soil fractions as specified by the user. Therefore, the user must divide the total sediment into sand, silt, and clay fractions to route through the channel system. Values for settling velocities, erodibility coefficient, critical shear stress for scour, and critical shear stress for deposition must be provided for cohesive fractions (clay, silt). The user also inputs a coefficient and an exponent for the sand-load transport within streams (channels).

The SCHEMATIC and MASS-LINK modules allow the user to specify the watershed network links of land segments to stream reaches and reach-reach connections. The MASS-LINK block defines the specific time series data to be transferred from one operation to another.

2.3.2 SWMM

SWMM is a USEPA code and is one of the most extensively used watershed management models. SWMM has modules applicable to conditions most common in urban and rural watersheds. SWMM is rigorous; however, the data requirements for various modules involved with runoff, transport, and routing estimations are relatively less extensive compared with those in HSPF and SWAT models.

SWMM estimates snowmelt at each time step using a degree-day (temperature index method) approach during dry weather and Anderson NWS equation (1973) – basically the temperature index method during the wet (rainfall) periods. The simple snowmelt techniques such as Anderson NWS method (1973) implemented in SWMM should work at the JPG facility; however, the probability of snowmelt causing extreme runoff and flooding events are likely to be low. The significant runoff and flooding events are likely caused by high-intensity rainfall.

SWMM users can opt for one of two infiltration models – the Horton model or the modified Green-Ampt model. Horton's model (like Philip's model used in HSPF) was one of the best known empirical infiltration equations used to model transient infiltration in the unsaturated soils.

Soil erosion/sedimentation from catchment areas in SWMM is estimated using USLE. Soil erosions (time series) from various sub-basins can be linked to a network of conveyance elements (channels, pipes) and sediment can be transported to common outlet(s). SWMM incorporates sediment transport, scouring, and deposition along the conveyance system length based on user-defined particle size distribution and sediment specific gravity of the eroded material. Scour and deposition are simulated using Shields criterion to determine the critical diameter for particle motion and deposition.

Like HSPF, SWMM can simulate transport of contaminants adsorbed to the sediment assuming that the mass of the component was directly proportional to the mass of sediment removed; the relationship is specified by user-input through assignment of a potency factor.

2.3.3 SWAT

SWAT is a code from Grassland, Soil & Water Research Laboratory, Temple, Texas, and Blackland Research and Extension Center, Temple, Texas. In SWAT, watersheds are divided in sub-basins. Each sub-basin is divided in hydrologic response units (areas with unique land use, soil, and management attributes) allowing accurate representation of the agricultural characteristics. SWAT includes capabilities for tributaries, channels, ponds, reservoirs, external sources, and permits routing of flow and sediment to/from such features. These capabilities make SWAT one of the most advanced watershed models for simulating various cultural and crop management practices (such as crop rotation, planting and harvesting dates, irrigation/drainage, and fertilizer and pesticide application amount and timing). SWAT also includes features that can be used to simulate urban areas. SWAT uses a time step of one day and is more suited as a long-term management/planning model; therefore, SWAT is not efficient for detailed single event flood routing applications.

SWAT offers two options to estimate surface runoff: 1) SCS Curve Number, and 2) Green-Ampt Infiltration model. SWAT estimates erosion due to rainfall and runoff using the Modified Universal Soil Loss Equation (MUSLE). MUSLE uses a runoff factor (represents energy needed in the detachment and transport) instead of the rainfall factor (representing energy needed in the detachment, as in USLE) and sediment delivery ratio (needed in USLE). User-defined Channel Erodibility Factor and Channel Cover Factor are also needed in the sediment transport simulations. SWAT estimates maximum sediment transport from a reach segment as a function of peak channel velocity and a power function (expressed in terms of a user-defined coefficient and an exponent). User-defined peak rate flow adjustment factor and peak rate sediment transport routing adjustment factor are used to estimate sediment transport, since it is a function of the sub-daily hydrograph (SWAT operates only on a daily time step size).

Due to inherent difficulties in modeling metals, SWAT only allows point source addition of metals to the channel/stream network and does not simulate various in-stream processes. A simple mass balance equation with user-defined potency factors or adsorption coefficients could be used to route metals through the river network.

2.3.4 Selected Code

After careful review of the watershed models available, HSPF (WinHSPF 3.0) was selected for investigating DU fate and transport in surface water as dissolved and adsorbed phases at the JPG site. The following were the key factors leading to this decision.

HSPF allows an accurate representation of precipitation, evaporation, and other meteorological data in form of hourly time series, and this feature is critical. Rainfall intensity and duration are important parameters to accurately simulate surface runoff and hydrograph characteristics; they are critical to estimate transport of sediment fractions (sand, silt, and clay) and the fate and transport of dissolved and adsorbed contaminants (such as DU species). For species (such as DU) strongly adsorbed to sediments, HSPF has options to specify distribution coefficients for sand, silt, and clay fractions, allowing flexibility

to accurately simulate the fate and transport of contaminants in dissolved, and as adsorbed to, various sediment fractions in suspension (within surface water stream) and in the bed load.

BASINS and WDMUtil are the companion utilities and significantly facilitate the creation of comprehensive HSPF watershed projects allowing input of geographic information system (GIS) shape files and hydrologic parameters, and creation of input time series for the model. HSPF interface is user friendly and allows input of data along with guidance on default and the range of values for various hydrologic parameters. WDMUtil and GenScn are valuable utilities for post-processing and analysis of results, and presentation in tabular and graphical forms.

3. MODEL SETUP

The surface water model was set up using BASINS to collect, organize, and format data for input to HSPF. Using HSPF (USEPA 2001b) as the platform, a surface water flow and sediment and DU model (HSPF-JPG) was developed. HSPF-JPG was used to simulate and investigate the long-term on/offsite migration and the impact of DU at the JPG site.

3.1 BASINS 4.0

BASINS was developed by USEPA (2001a) to facilitate analysis of environmental and ecological systems and to support the investigation of various alternatives for improving watershed management. BASINS provides an integrated platform and streamlines watershed studies by bringing key data and resources together and make them work together seamlessly. BASINS 4.0 was used in this effort. The BASINS 4.0 GIS capabilities organize spatial information (e.g., soil types, land use, topography, stream flow network, point sources) so they can be displayed as maps, tables, or graphics, and permits quick and efficient changes in base layer data within the modeling files. BASINS helps delineate watersheds into smaller sub-basins (see Section 3.1.1), creates first set of input data files for the HSPF model and links various user supplied time-series input data to appropriate modules. This initial set of parameters for different modules supplied by BASINS is then refined during model calibration.

3.1.1 Stream Network and Watershed Delineation

Watersheds are generally heterogeneous and require subdivision into smaller units (sub-basins) of uniform characteristics to represent field conditions within the surface water model. Further subdivisions (generation of smaller sub-basins) are performed in areas of interest (i.e., the DU Impact Area). Auto-delineation based on the supplied elevation and hydrography datasets helped create stream reach shapefiles and watershed sub-basin boundaries.

The USGS high-resolution National Hydrography Dataset (NHD) provided a shapefile of streams/reaches used as a first approximation for the locations of streams within the surface water model domain. The auto-delineation process within BASINS 4.0 was used to calculate the flow pathways for the streams delineated in the NHD using the 6-m DEM.

Watershed sub-basins were initially defined through automatic delineation. Outlet points for sub-basins in and around the DU Impact Area were set to coincide with the automatic stream stage data recorders to enhance and facilitate accurate calibration. A minimum drainage area of 200 ac per sub-basin was specified. Manual delineation was used to refine sub-basins generated by automatic delineation. For example, the upstream and downstream segments of Big Creek and Middle Fork Creek, for which little or no data were available to define stream cross-sectional area, shape, and flow conditions, were combined into larger units. Marble Creek and Camp Creek also were combined into larger units. Delineation in this manner permits greater model resolution in the area of interest, namely the DU Impact Area, while permitting extension of the model area to natural boundaries (much like telescopic mesh refinement in groundwater flow modeling).

Fifty-seven individual sub-basins were defined for modeling efforts, as shown in Figure 3-1. Big Creek sub-basins are identified as 100 series sub-basins (i.e., sub-basin 100 through sub-basin 129); Marble Creek sub-basins are identified as 200 series sub-basins; Camp Creek sub-basins are identified as 300 series sub-basins; and Middle Fork Creek sub-basins are identified as sub-basin 1 through sub-basin 21 (Table 3-1). Sub-basin numbers generally increase from upstream to downstream flow (meaning lower numbered basins are typically upstream of higher numbered sub-basins); tributaries joining the main creek channels also are numbered in a similar manner.

THIS PAGE WAS INTENTIONALLY LEFT BLANK

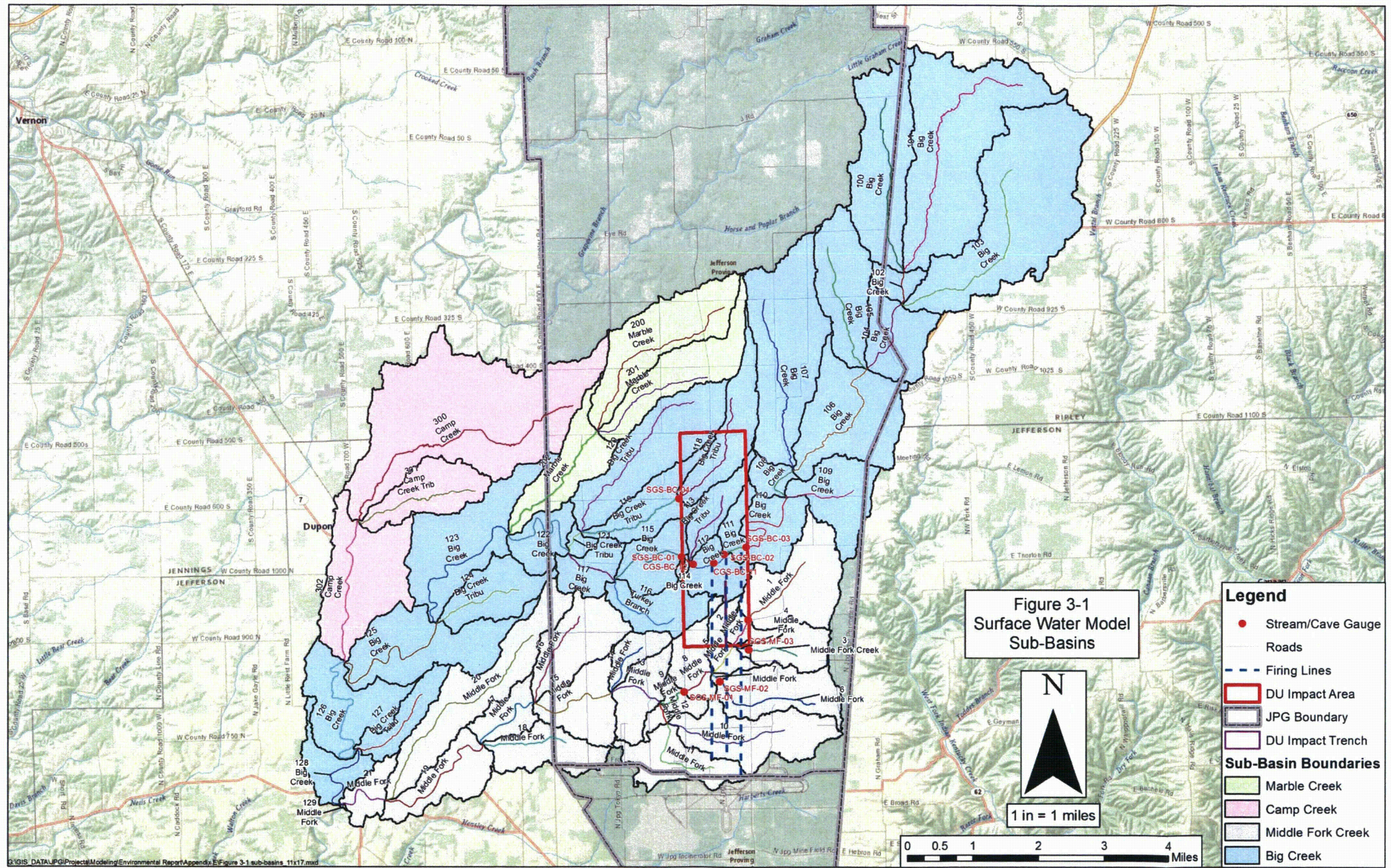


**Table 3-1. Sub-Basins Defined for Each Drainage Basin
Jefferson Proving Ground, Madison, Indiana**

Basin Name	Sub-Basin	Area (Acres)	# of Sub-Basins	Basin (acres)
Middle Fork Creek	1	1,093	21	10,886
	2	161		
	3	418		
	4	28		
	5	289		
	6	816		
	7	20		
	8	433		
	9	160		
	10	1,032		
	11	665		
	12	83		
	13	495		
	14	268		
	15	694		
	16	835		
	17	366		
	18	613		
	19	687		
	20	1,424		
	21	304		
Big Creek	100	1,540	30	25,168
	101	2,722		
	102	204		
	103	2,861		
	104	710		
	105	997		
	106	1,417		
	107	1,888		
	108	201		
	109	763		
	110	572		
	111	227		
	112	422		
	113	386		
	114	30		
	115	548		
	116	567		
	117	409		
	118	777		
	119	651		
	120	1,408		
	121	90		
	122	456		
	123	1,396		
	124	701		
	125	1,351		
	126	996		
	127	439		
	128	438		
129	3			
Marble Creek	200	1,299	3	3,053
	201	971		
	202	783		
Camp Creek	300	3,652	3	5,843
	301	765		
	302	1,425		
Total Big Creek (includes Marble and Camp Creeks)			36	34,064

3.1.2 Meteorological Data

The BASINS 4.0 library contains meteorological data from several weather stations near JPG. However, these data are limited to pre-2005, and are of little use in re-constructing the 2006 to 2011 timeframe for which stream gauging data were collected. Fortunately, an FWS weather station exists onsite, northeast of the DU Impact Area. This weather station served as the basis for meteorological data for the 2006 to 2011 period. Supplemental data from a nearby weather station in Butlerville, Indiana, was used to augment and fill data gaps identified within the onsite dataset.

3.1.3 Land Use

Land use plays a significant role in controlling components of a hydrologic cycle, such as evapotranspiration, runoff, infiltration, and groundwater recharge. Each land use input to the model requires additional parameters for that land use (e.g., permeable area, impermeable area, slope, soil classification). To balance input data requirements while still meeting model objectives, similar land use classifications with respect to their runoff characteristics were combined into a single category (e.g., all forest categories were combined into a single category). A total of six land use categories (i.e., grass, forests, farmland, bare soil, roads, and water) were defined for use in the HSPF-JPG model (Table 3-2). Grass represents shrub, scrub, and grass-covered land. Forest land use represents deciduous, coniferous, and mixed forest covered land. Farm land and bare soil both represent cultivated land, with bare soil representing a portion of cultivated land that was tilled/bare at the time of land use classification. Roads and water are self-explanatory. Almost 98 percent of the land surface within JPG surface modeling domain is permeable (except roads, buildings, and parking lots).

The relative abundance by area of the six land use types identified in the HSPF-JPG model is shown in Table 3-2. As shown in the comparison between sub-basins in Table 3-2(A), the entire model area consists of 70 percent forest (55 percent) and grass land (15 percent), 28 percent cultivated land (18 percent farmland and 10 percent bare soil), and 2 percent roads and water. The relative abundance by area also is shown for each of the drainage basins (Big Creek, Marble Creek, Camp Creek, and Middle Fork Creek). The relative land use abundances are similar (generally within a few percentage points) between the entire Big Creek, entire Middle Fork Creek, and the entire model area. Marble Creek, which entirely almost lies within the former JPG property, contains a much higher percentage of grass and forest combined (93 percent) and a lower percentage of cultivated land (6 percent) relative to the entire model area. Conversely, Camp Creek, which lies almost entirely to the west of the former JPG property, contains a much lower percentage of grass and forest combined (43 percent) and a higher percentage of cultivated land (51 percent combined between farmland and bare soil).

A comparison between sub-basins containing DU penetrators from within and adjacent to the DU Impact Area and sub-basins east and west of the former JPG property is shown in Table 3-2(B). Sub-basins containing DU penetrators are referred to as source areas, meaning the sub-basin contains a source of DU that can contribute DU mass to the surface water pathway (Section 6.1.1 provides a more detailed description of the DU penetrator mass within each source area sub-basin). Land use with the source area sub-basins is 96 percent (Big Creek) to 98 percent (Middle Fork Creek) grass and forest area combined and only 2 to 3 percent farmland. Land use east and west of the former JPG property shows a much higher percentage of cultivated (farmland plus bare soil) and a much lower percentage of grass and forested land. East of the former JPG, grass and forested land combined is 63 percent; and cultivated land is 36 percent. West of the former JPG, grass and forested land combined is 51 percent (Big Creek) to 53 percent (Middle Fork Creek); cultivated land is 41 percent (Middle Fork Creek) to 45 percent (Big Creek). The higher percentage of cultivated land (farmland plus bare soil) east and west of the former JPG property generates more sediment runoff per acre than the grass and forest land use comprising most of the area within the former JPG property.

**Table 3-2. Land Use Classification – HSPF-JPG Model
 Jefferson Proving Ground, Madison, Indiana**

A. Land use comparison between sub-basins										
	Entire Big Creek		Marble Creek		Camp Creek		Entire Middle Fork		Entire Model Area	
Land Use	Total (ac)	Total (%)	Total (ac)	Total (%)	Total (ac)	Total (%)	Totals (ac)	Totals (%)	Total (ac)	Total (%)
Grass	4,259	13	159	5	759	13	2,250	21	6,509	15
Forests	17,944	53	2,646	88	1,765	30	6,411	60	24,355	55
Farmland	6,747	20	125	4	1,679	29	1,250	12	7,997	18
Bare Soil	3,771	11	46	2	1,307	22	531	5	4,301	10
Roads	808	2	25	1	288	5	250	2	1,059	2
Water	125	0	8	0	36	1	36	0	161	0
Acreage	33,654	100	3,009	100	5,833	100	10,728	100	44,382	100
B. Land use comparison between source area sub-basins and off JPG sub-basins										
	Big Creek East of JPG (sub-basins 100-109)		Big Creek West of JPG (sub-basins 123-128)		Big Creek Source Areas (sub-basins 110-113, 116, 118)		Middle Fork Source Area (sub-basins 1,2, 5, 8)		Middle Fork West of JPG (sub-basins 17, 19 - 21)	
Land Use	Total (ac)	Total (%)	Total (ac)	Total (%)	Total (ac)	Total (%)	Total (ac)	Total (%)	Total (ac)	Total (%)
Grass	1410	11	940	18	528	18	572	30	528	19
Forests	6,744	52	1,725	33	2,269	78	1,314	68	954	34
Farmland	3,215	25	1,462	28	84	3	43	2	790	28
Bare Soil	1,442	11	892	17	1	0	0	0	348	13
Roads	211	2	257	5	8	0	6	0	135	5
Water	47	0	29	1	2	0	1	0	18	1
Acreage	13,068	100	5,306	100	2,891	100	1,936	100	2,773	100

One last note regarding Table 3-2, the total area shown for the model is 44,382 ac, which is ~1 percent less than the area presented in Section 2. This difference results from the use of the higher-resolution infrared analysis of land use. The difference in area is negligible, and the area information presented in Table 3-2 is used in the HSPF model.

Due to the relatively rural nature of the modeled area, most land uses were considered to have a relatively small fraction of impermeable surfaces, such as pavement, physical structures, or exposed bedrock. Therefore, for all land uses except roadways (100 percent impermeable) and water (0.0 percent), a default value of 2 percent of total area in each land use shown in Table 3-2 was assigned as impermeable (98 percent permeable).

3.1.4 Watershed Segmentation

Segmentation defines the level of discretization (refinement) of the model domain in HSPF. Model segments were created to account for the differences in meteorological data and/or other physical conditions, such as soil type, land use, surface topography, and channel characteristics over the study area. Model segments were subareas of watershed sub-basins with uniform properties and meteorological inputs connected by a stream network. Assigning appropriate meteorological stations and site-specific physical parameters to model segments provides a more accurate representation of site conditions within the model.

The JPG site is assumed to have a single meteorological segment (set of data); the weather data are the same for the entire model area and do not vary spatially. As noted in Section 2.2.4, precipitation data from neighboring stations were similar to data collected at the former Proving Ground for the same period, so assignment of a single meteorological segment is appropriate.

Land use and surface permeability are used to define segments within each sub-basin. Up to six different land uses are defined for PERLND or impermeable land segments (IMPLND) within each sub-basin, as shown in Table 3-3. Based on land use characteristics, BASIN 4.0 estimates and assigns acreage for each PERLND and IMPLND operation within each sub-basin (see Table 3-2).

**Table 3-3. PERLND and IMPLND Operations in HSPF-JPG Model
Jefferson Proving Ground, Madison, Indiana**

PERLND Operations (Permeable Surface)	IMPLND Operations (Impermeable Surface)
PERLND #101 (Grass)	IMPLND #101 (Grass)
PERLND #102 (Bare Soil)	IMPLND #102 (Bare Soil)
PERLND #103 (Forest)	IMPLND #103 (Forest)
PERLND #104 (Farm/New Growth)	IMPLND #104 (Farm/New Growth)
PERLND #105 (Water)	IMPLND #105 (Roads)

3.2 HSPF-JPG MODEL

HSPF uses meteorological data in conjunction with the characteristics of drainage basin such as soil types, surface topography, land use, stream configuration, and bed slope to generate runoff hydrographs and model sediment transport. The model also uses the physicochemical properties of DU to simulate corresponding DU levels in surface water and sediment over time.

3.2.1 Ftables

Each sub-basin requires an Ftable, which characterizes channel flow. Ftables are lookup tables listing stream flow depths (stage) and the corresponding water surface area, stream storage volume, and

the volumetric flow rate for each channel (also known as stream or reach). During simulation, HSPF uses Ftables to relate stage (depth) to volumetric flow rate, water surface area, and stream storage volume (during simulation, HSPF does not directly use the mathematical relationship between the flow rate and flow depth, bed slope, roughness, or shape of the stream segments, but instead only interpolates the tabulated values in Ftables to estimate compatible flow depths, stream volumes, surface areas, and flow rates). This considerably increases the computational efficiency of the surface flow module.

Manning's Equation (USGS 1987) provides a convenient method of relating flow depth to velocity (flow rate = velocity × stream cross-sectional water area). This equation relies on the knowledge of longitudinal (bed) slope, stream channel geometry, and the Manning's roughness coefficient to derive the relationship between stream depth and average flow velocity. Manning's coefficient is a function of the roughness of the surface (texture, stones, vegetation, and the hydraulic radius of the channel). Manning's roughness coefficients assumed for various streams at JPG ranged from 0.04 to 0.15 based on the observed stream channel conditions at JPG.

$$V = (1.49/n) \times R^{2/3} \times S^{1/2}$$

Where:

- V = Velocity (feet per second [ft/sec])
- n = Manning's roughness coefficient
- R = Hydraulic radius (cross-sectional area/wetted perimeter, feet [ft])
- S = Longitudinal slope (bed slope, ft/ft).

Multiplying average stream velocity by the cross-sectional area (square feet) will provide the volumetric flow rate in cfs. Surface water area and stream storage volume (the other components of the Ftables) are estimated from the defined geometry of the stream (segment length and cross-sectional configuration, such as side slopes and lateral extents to mimic floodplain accurately).

3.2.1.1 Ftables Development

The Ftables include representative stream cross-sections for every stream segment within the surface water domain. Each cross-section was approximated by a piecewise linear configuration consisting of a bottom width, maximum three side slopes, and a floodplain section (W11, W12) on each side of the channel, as shown in Figure 3-2 (USEPA 2001c).

Initially, Ftables were automatically generated in BASINS 4.0 for each sub-basin using the 6-m DEM and hydrography data. The Path Analyzer utility in BASINS 4.0 was used to draw a cross-section across each stream at several locations; a representative cross-section location was selected by visual inspection (Figure 3-3).

The 6-m DEM was not precise enough to determine representative cross-sections. The small creek size and topographic relief of the channels required updates to the initial Ftables to better represent the true characteristics of the channel for each of the streams defined. During low-flow conditions at the former Proving Ground, most flow was being carried through a smaller channel covering only a partial width of the stream. The simplified average cross-section (Figure 3-3) computed by Path Analyzer in BASINS 4.0 was modified. Under low-flow conditions, a small channel ranging up to 16.5 ft (most channels were less than 5 ft) in width and from 0.5 to 1 ft depth was assumed for each stream through which surface runoff was assumed to occur under these low-flow conditions).

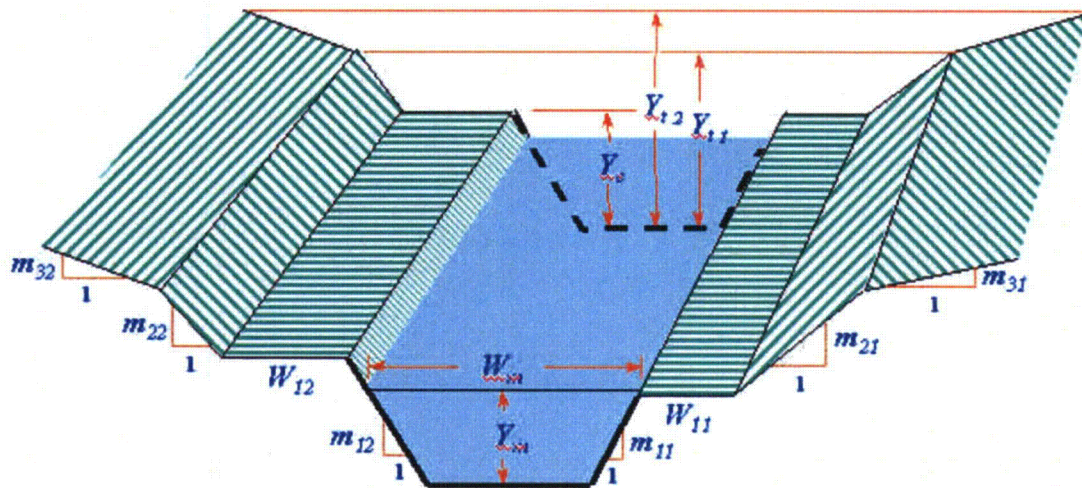


Figure 3-2. A Typical Stream Cross-Section (USEPA 2001c)

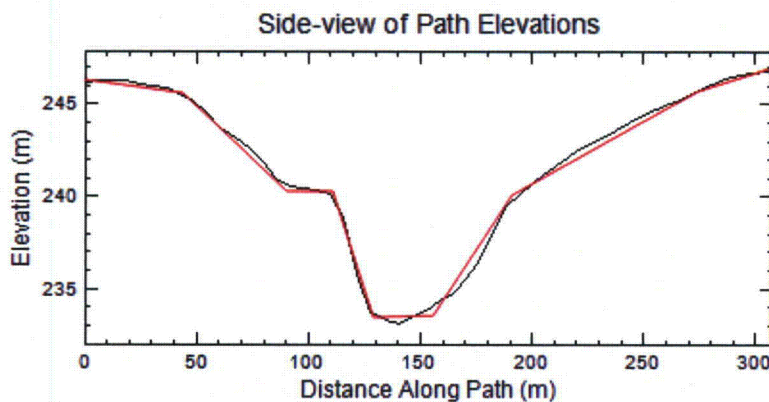


Figure 3-3. A Typical Stream Cross-Section Within Middle Fork (Black: From Path Analyzer, Red: Approximated for HSPF Model)

Each Ftable typically has four columns and several rows. The number of rows is determined by the cross-sectional geometry of the stream channel. Each row lists stream stage, and corresponding surface water area, stream storage volume, and volumetric flow rate. As noted previously, HSPF interpolates among these array of values to estimate prevailing flow depth, stream volume, water surface area, and the flow rate during simulation. Most Ftables deployed in the HSPF-JPG model have 13 rows and stream stage ranges from 0 to 30 ft (depth of flow increases with increasing row number). In addition, the observations below were noted during Ftable construction:

- Increases in stage value with increasing row number should be gradually increased – initial depth increments should be small (e.g., 0.1 to 0.2 ft); however, using a very small initial depth increment may result in extremely high simulated flow velocities ($V=Q/A$) due to small interpolated cross-sectional area.

- The maximum stream stage (first column, last row) in these tables is stream-specific and should always be larger than the depths likely to occur under the most severe storm expected within the design period (typically corresponding to 100-year and sometimes 1,000-year storm). However, using maximum stage values significantly greater than the highest expected depth of flow will likely result in less accurate interpolation.

3.2.2 *PERLND Segment Parameters*

BASINS 4.0 divides the model domain into smaller segments. Parameters are input for each model segment; recall that model segments are sub-areas of a watershed with uniform parameters and meteorological inputs connected by a stream network (each sub-basin has an associated stream, which is also known as reach). The JPG model domain consists of several PERLND and IMPLND (impermeable) categories (refer to Table 3-3). Data input to HSPF is undertaken in several blocks:

- GLOBAL BLOCK defines the start and end of the simulation; time series data (such as those for precipitation, temperature, potential evapotranspiration, and various external sources) are supplied for the complete duration of the simulation (HSPF-JPG model used the WDMUtil to format/create and supply various time series).
- FILES BLOCK lists the name and location of various input and output files.
- OPN SEQUENCE BLOCK defines the grouping and sequence in which various operations are performed.

HSPF stores the majority of the input parameters governing runoff and stream flow, and overland sediment transport within the PERLND and IMPLND sections of its input files. These sections describe various parameters assigned to PERLND and IMPLND, respectively. Permeable land uses comprise 98 percent and impermeable land uses comprise 2 percent of the total model area. Additional details on the required HSPF input parameters are provided in the program's documentation (USEPA 2001b).

Input parameters for PERLNDs are organized within the PERLND BLOCK. An explanation of the setup used in the JPG surface water model is provided below.

General PERLND parameters are used by HSPF to select the modules, such as ATEMP (temperature) SNOW, P WATER (runoff), SEDMNT (overland sediment) and PQUAL (overland contaminant transport) to be simulated (activated) and the frequency and units for reported parameters (results). The Activity Section consists of a series of flags for turning on/off different modules within HSPF. Air temperature, snowmelt, permeable water, and sediment transport modules were all simulated in the HSPF-JPG model. The quality component (DU) fate and transport is discussed in Section 6.

- The ATEMP module allows variation of air temperature with elevation. PERLND:ATEMP-DAT table requires specification of an elevation difference (ELDAT) between each PERLND and the temperature gauge. Because of the large spread of the PERLNDs across the domain and the limited relief of the domain, all ELDATs were set to 0.
- The PERLND:SNOW module simulates runoff due to the fall, accumulation, and melting of snow, and accounts for surface runoff to be stored in snow banks and released into streams during melting events and forms an important component of the hydrologic cycle.
- PERLND:SNOW-FLAGS table/dialog box is used to specify the method of computing snowmelt events. Setting SNOPFG in this table equal to 1 invokes a degree-day factor method to determine snowmelt as opposed to an energy balance approach. This method was chosen due to the simplicity of data needs and the relatively small difference expected between both methods. The energy balance method needs solar radiation, humidity, dew point, and cloud cover time series, and such data were unavailable.

- PERLND:SNOW-PARM1 dialog box is used to specify parameters governing the snowmelt module. Latitude was set at 40 degrees N, while mean elevation of 800 ft was assumed for all PERLNDs. Other variables include:
 - SHADE (fraction of the PERLND shaded from solar radiation such as by tree coverage)
 - SNOWCF (factor by which recorded precipitation was multiplied to account for poor catch efficiency)
 - COVIND (maximum pack at which the entire PERLND will be covered with snow, inch)
 - KMELT (degree-day snowmelt factor)
 - TBASE (base temperature) was set at 32°F, since the melting temperature of water is generally accepted at this value.

3.2.2.1 PERLND Overland Flow

PWATER is the key member of the PERLND module and helps to calculate components of the water budget used in prediction of runoff from permeable areas. Several other PERLND members (e.g., SEDMNT – simulates overland sediment transport) depend on the results of this section. These modules are important in determining overland flow and erosion characteristics, and overall water budget of the model:

- PERLND:PWAT-PARM1 contains flags for turning off/on modules such as those simulating snow accumulation and melt, overland flow routing through stream network, and to allow several different parameters to vary monthly as opposed to being held constant (including various parameters used in evapotranspiration processes).
- PERLND:PWAT-PARM2 (see HSPF Parameters Section 4.5.2) defines parameters governing infiltration, overland, and groundwater flow. For various land use types, forest coverage fraction likely to transpire in winter (FOREST), nominal Lower Zone storage capacity (LZSN, in), infiltration capacity (INFILT, inches per hour [in/hr]), average overland flow length (LSUR, ft) and slope of overland flow plane (SLSUR), and groundwater recession curve parameters (KVARY 1/in, and AGWRC, 1/d) are specified.
- PERLND:PWAT-PARM3 (see HSPF Parameters Section 4.5.2) contains parameters used in defining infiltration, deep percolation, and potential evapotranspiration adjustment during HSPF simulation such as INFEXD (exponent in infiltration equation) and INFILD (ratio of maximum to mean infiltration capacity), DEEPFR (fraction of recharge to inactive groundwater), BASETP and AGWETP (fraction of potential EF supplied from base-flow and active groundwater, respectively).
- PERLND:PWAT-PARM4 (see HSPF Parameters Section 4.5.2) contains parameters used by HSPF to simulate moisture storage in upper zone (UZSN, in), evapotranspiration from lower subsurface zone (LZETP), Manning's roughness coefficient for overland flow (NSUR), and interflow (INTFW) and interflow recession parameter (IRC, 1/d).

3.2.2.2 PERLND Overland Sediment Transport

Soil erosion and transport to surface water bodies is one of the most common causes of pollutants originating from urban, agricultural, and forested lands. Sediment can facilitate transport of many inorganic and organic contaminants, including radionuclides and many heavy metals. Sediment transport involves the following processes:

- Soil particles are detached from soil matrix by impact of raindrops; kinetic energy of rain particles frees soil particles from the top soil layer

- Detached soil particles are carried by overland flow downstream toward the closest intercepting reach (stream/channel); during this process, a significant part of the detached particles could deposit within the sub-basin before ever reaching the intercepting reach.

HSPF uses the SEDMNT module to simulate the production and removal of sediment from pervious land segments. The module SOLIDS is used to model the removal of sediment from impervious land segments. The sediment transport within reaches is simulated using the SEDTRN module.

The sediment detachment (scour) and attachment (deposition) from pervious segments occurs by two mechanisms: wash off and scour. The wash off involves the following two steps: 1) detachment/attachment of the sediments to and from the soil matrix, and 2) removal/transport of sediments with the overland flow. The parameters governing these processes (KRER, JRER, and AFFIX) are discussed in Section 5. Soil particles transport by overland flow is governed by transport capacity (see parameters KSER, JSER in Section 5). The scouring of soil surface matrix and transport are lumped and expressed as an exponential function (intercept KGER and exponent JGER, see Section 5).

3.2.3 IMPLND Segment Parameters

Parameters for the IMPLNDs for each land use category are collectively defined and organized within IMPLND BLOCK. The cumulative impermeable land area under all types of land use within HSPF-JPG modeling domain was about 2 percent of the total modeling domain area. An explanation of the setup used in the HSPF-JPG model is provided below:

- General IMPLND parameters are used by HSPF to determine the modules, such as ATEMP (temperature), SNOW, IWATER (runoff), SOLIDS (sediment), and IQUAL (contaminant transport) to be simulated (activated) and the frequency and reporting units for various parameters (results). The Activity Section consists of a series of flags for turning on/off different modules within HSPF. Air temperature, snowmelt, impermeable overland water flow, and sediment transport modules were simulated in the HSPF-JPG model. DU quality component (IQUAL section) was not explicitly simulated in IMPLND; IMPLND consists of roads, buildings, and parking lots; buildings and parking lots are not present within the DU Impact Area. Roads within and around the perimeter of the DU Impact Area were free from penetrators.
- The ATEMP module allows variation of air temperature with elevation. IMPLND: ATEMP-DAT table requires specification of an elevation difference (ELDAT) between each IMPLND and the temperature gauge; similar to corresponding PERLND, all ELDAT were set to 0.
- The IMPLND: SNOW module simulates runoff due to the fall, accumulation, and melting of the snow and accounts for surface runoff to be stored in snow banks and released into streams during melting events, and forms an important component of the hydrologic cycle.
- IMPLND: SNOW-FLAGS table is used to specify the method of computing snowmelt events. Setting SNOFG in this table equal to 1 invokes a degree-day factor method to determine snowmelt, as opposed to an energy balance approach. This method was chosen due to the simplicity of data requirements and the relatively small difference expected between both methods.
- IMPLND: SNOW-PARM1 table (see HSPF Parameters Section 4.5.2) is used to specify parameters governing the snowmelt module. Latitude was set at 40 degrees N, while mean elevation of 800 ft was assumed for all IMPLNDs. Other variables include, SHADE (fraction of the IMPLND surface shaded from solar radiation such as by tree coverage), SNOWCF (factor by which recorded precipitation was multiplied to account for poor catch efficiency), COVIND (maximum pack at which the entire IMPLND will be covered with snow, inch),

KMELT (degree-day snowmelt factor), and TBASE (base temperature) was set at 32°F, since the melting temperature of water is generally accepted at this value. These parameters have been discussed and tabulated in Section 4.5.2.

- IMPLND:IWAT-PARM1 table contains flags for turning off/on modules for simulating snow accumulation and melt, routing overland flow through stream network, and to allow several different parameters to vary monthly as opposed to being held constant.

3.2.3.1 IMPLND Overland Flow

IMPLND:IWAT-PARM2 table (see Section 4.5.2) defines various parameters governing behavior of overland flow and retention storage capacity (RETSC, in) of the surface. For various land use types, the average overland flow length (LSUR, ft) and slope of overland flow plane (SLSUR), and Manning's roughness coefficient (NSUR) are tabulated.

3.2.3.2 IMPLND Overland Sediment Transport

Soil mass deposits on impermeable surfaces are transported (may redeposit) by the overland flow and can be expressed by an exponential power function, (parameters include – an intercept KEIM and exponent JEIM are the required inputs, see Section 5.1).

4. FLOW CALIBRATION

The surface water pathway involves DU entering into the surface streams as dissolved, adsorbed, or solid particles carried by overland runoff into the streams. Once in the streams, DU physicochemical properties (such as K_d), stream flow rate and water velocities, sediment load, and channel characteristics influence sediment transport and determine the ultimate fate of the mobilized DU. Due to the high specific gravity (18.9) of DU, its transport as solid particles was assumed primarily local and spatially restricted within sub-basins. Most streams at JPG have significant natural vegetation, debris, and/or natural rocks resulting in relatively high surface roughness, which in addition to DU's specific gravity, will likely arrest and limit migration of DU particles downstream. As noted in Section 2.1.5, transport of smaller fragments from corrosion products may occur, as these particles are smaller and less dense. However, the corrosion products are more susceptible to dissolution and are likely to break down further and transport in solution or be adsorbed to sediments. Land use within the DU Impact Area is primarily forested, which also will limit the amount of sediment (including DU fragments or fragments of corrosion products) runoff following precipitation events.

To make predictions of DU fate and transport, it is important to be able to predict surface water runoff and stream flow. To accomplish this, model predictions of stream flow volumes and velocities are compared to observed data for similar conditions and adjustments made to model parameters to bring simulated values in line with observations. This section describes the calibration methodology and selection of calibration targets, and results of HSPF-JPG calibration. Since the total area of impervious land uses (primarily roads) is only about 2 percent of all of the land uses described within the model, refinement of the impervious (IMPLND) parameters during calibration was not performed.

4.1 CALIBRATION TARGETS

The first step in surface runoff and stream flow calibration is to establish target values. These targets should be (wherever possible) based on real observed data for a time period that can be simulated by the model. During calibration, model parameters are adjusted to minimize the difference between simulated and observed variables (targets such as stream stage, flow rate) versus time.

Continuous stream gauges have been in place since September 2006 at seven stream locations (three on Big Creek and four on Middle Fork Creek) recording stream stage for the period. Near the transducers (often up to several hundred feet downstream), field measurements of stream flow were made at different stream stages if the stream conditions were safe (i.e., flow was low enough to enable safe wading). The cross-section of the stream and velocity were measured at multiple points. A trapezoidal approximation then was used to calculate the stream flow rate. Stream flow and depth were recorded concurrently from 7 to 10 times per station, all representing low-flow conditions (the maximum stage where flow measurements were made is 2.25 ft) due to safety concerns.

The data from the stream stage transducers were valuable in establishing many qualitative components of the stream flow, as well as serving as a proxy for flow rates at high flows. The peak stage (height) and recession slopes recorded by stream transducers establish characteristics of the stream flow hydrographs, giving clues to the quantities of interflow and base flow, and the speed (time lag) with which the stream responds to a precipitation event and then returns to the base flow conditions.

With the data availability and limitations described above and in Section 4.3, three main calibration goals were established:

- Predicted cumulative flow from the model should mirror the annual water budget, both in total quantities and as separate components such as surface runoff, base-flow, and evapotranspiration (see Section 4.2)

- At low-flow (stage) conditions, the model should exhibit a close degree of match and correlation between predicted stage (or flow rates, see below) and the corresponding observed values (or flow rates) (see Section 4.3)
- At high stream flows, when no manual flow measurements were made, the predicted stage over time should match the character of the observed stage reported by the stream transducers (see Section 4.4).

At low-flow conditions for the streams where transducers were located and flow measurements were recorded, the first few rows of Ftables were based on the manually measured flow depth (stage) and flow rates. Therefore, at low-flow rates, the stage and flow rates were highly dependent variables and either could be used to calibrate the model.

Three years of hydrologic data, including precipitation and stream stage measured continuously, were used to calibrate the flow model. These are 1 October 2006 to 30 September 2007 (hydrologic year [HY]2007), 1 October 2007 to 30 September 2008 (HY2008), and 1 October 2008 to 30 September 2009 (HY2009). Development of the calibration goals are described below.

4.2 WATER BUDGET

HSPF uses meteorological data and watershed characteristics to simulate various components of surface and subsurface flow. When rainfall and/or snowmelt occur, several factors determine what percentage of the total precipitation evaporates or transpires, is intercepted by vegetation, partitions into groundwater, and/or remains on the surface and eventually runs off into stream channels.

Over the course of a year, an estimation of the total volume of precipitation (as rainfall or snow) that has fallen on the model domain can be calculated by simply multiplying the total rainfall (and snow) by the surface area of the model domain. A certain percentage of this will appear as stream flow and can be measured at outlet points within the domain. Total stream flow is composed of direct surface runoff, interflow (primarily an unsaturated zone phenomenon and occurs when vertical percolation is retarded by a shallow, less permeable soil layer), and base flow from active groundwater. This total stream flow should be equal to the total volume of precipitation plus the changes in various surface and subsurface storages, less the fractions that are lost through evapotranspiration and infiltration into deep groundwater that is unavailable for base flow within the modeled area.

At JPG, observed data consist of continuous stage recordings at seven stream locations and manual stage measurements at an eighth location. At each of these stations, direct flow measurements were taken during low-flow conditions and provide a means to relate stream stage to flow under low-flow conditions. The transducer measurements record a wide range of flow conditions that are useful for comparing the characteristics of the modeled versus observed stages but cannot be relied on to give an accurate picture of flow under higher flow (higher stage). Therefore, the water budget for JPG as calculated in the Final Well Construction and Surface Water Data Report (SAIC 2008) is used for comparison against the modeled surface water budget.

The water budget analysis (SAIC 2008) determined for an average precipitation year of 47 in, 56 percent (26.3 in) is lost to evapotranspiration, 8 percent (3.8 in) becomes groundwater, and the remaining 36 percent (16.9 in) is runoff. Weather data collected at Madison, Indiana (1976 to 2007) and from FWS on JPG were used to determine evapotranspiration rates. During this period, annual precipitation ranged from 33.24 to 60.93 in and actual evapotranspiration ranged from 17.2 to 29.7 in/y (SAIC 2008). Groundwater recharge rates were determined from base flow studies conducted for the neighboring Brush Creek and the larger Muscatatuck River (to which Big Creek and all JPG streams are tributary). For comparison, published estimates indicate groundwater recharge at 4 to 8 in/y for southern Indiana (Bechert and Heckard 1966). Brush Creek in particular demonstrates the extremely flashy nature that is observed within the JPG streams; Brush Creek is similar in size and hydrology to the JPG streams.

Large runoff volumes are observed quickly following a precipitation event followed by a rapid fall off to base flow conditions. The SAIC (2008) water budget assumes most of groundwater reemerges as base-flow into streams. Therefore, percolation losses to deep groundwater are insignificant.

The recorded precipitation at the FWS weather station for HY2007 through HY2010 (1 October 2006 through 30 September 2010) was 45.4, 56.2, 54.7, and 40.4 in, respectively. A weather station at nearby Butlerville, Indiana, was used for proxy data in the event that FWS data were missing (see Section 2.2.2).

Using the average water budget percentages determined by SAIC (2008) for HY2007 results in 25.4 in lost to evapotranspiration and 16.3 in becoming runoff (direct surface runoff + interflow). An additional 3.63 in percolated into groundwater (re-emerges as base flow), and an insignificant portion of which infiltrated to deep groundwater (unavailable as base flow). Similarly, the HY2008, HY2009, and HY2010 water budget details are presented in Table 4-1.

**Table 4-1. Water Budget Estimates HY2007 Through HY2010 (Based on SAIC 2008)
Jefferson Proving Ground, Madison, Indiana**

Hydrologic Year	Precipitation PREC (in)	Evapotranspiration SAET (in)	Runoff (in) SURO+IFWO	Groundwater AGWO (in)
Average	49.18	27.54	17.70	3.93
HY2007	45.4	25.42	16.34	3.63
HY2008	56.2	31.47	20.23	4.50
HY2009	54.7	30.63	19.69	4.38
HY2010	40.4	22.62	14.54	3.23

The water budget (SAIC 2008) is calculated for an average year of 47 in of rainfall. Actual amounts (various components as percentages of total) for other years may differ. For example, review of annual precipitation and evapotranspiration for the period 1976 to 2007 shows evapotranspiration ranges from 34 to 66 percent of the annual precipitation. For example, the intensity and frequency of rainfalls, air temperature, wind velocity, the relative dryness of the soil root zone, and vegetative cover can all influence various components of the water budget, especially the evapotranspiration (actual evapotranspiration cannot exceed the potential evapotranspiration).

4.3 STAGE VERSUS FLOW AT LOW-FLOW CONDITIONS

Stream flow measurements were made at each of the gauging stations under low-flow conditions. These flow measurements can only be reliably correlated to the range of stream depths under which they were recorded. Due to safety concerns and technical limitations, field personnel did not record stream flow measurements at higher stream stages (greater flow depths). Therefore, under higher flow conditions, stage versus flow rating curves could not be reliably developed.

Observed stage and stream flow rates at low-flow conditions represent the most comprehensive field data collected for flow model calibration. Low- or base-flow conditions represent the majority of time at JPG. While low flows are not expected to carry very much sediment or adsorbed DU, matching the observed low-flow data are nonetheless important in the overall characterization of the streams and provides confidence in extrapolating model predictions to higher flow conditions.

The first step in establishing these low-flow calibration targets was to understand the limitations and assumptions associated with the stage transducer data and how the data were used in HSPF-JPG model predictions. The assumptions invoked in HSPF-JPG to simplify the complex field conditions also must be understood. For any given stream segment, HSPF-JPG assumes a uniform bed slope between the entry and exit points. In reality, slope is variable along these segments, which may result in some

overestimation or underestimation of stream depth. Since creating Ftables within HSPF relies on the nonlinear Manning's Equation to relate stream flow to depth, any nonzero reported depth of flow has a corresponding associated nonzero stream flow. However, observations show that this is not always true, as field observations often would show very shallow manually measured depths accompanied by insignificant or zero flow, while the stage transducers were concurrently reporting half a foot or more of depth. Such discrepancies introduce differences between the simulated and observed results at low-flow conditions.

The stage transducers are located at points along Big Creek and Middle Fork Creek where they were easy to access, typically near bridges. These bridges tend to collect debris around their pylons, which can alter the hydrodynamics of the stream and bias the stage results. In addition, the raw stage data do not necessarily represent the actual depth of stream flow, as the transducers were sometimes placed within shallow depressions in the stream channel or pressed into gravel and sediment. However, several stage measurements were made by field technicians concurrently with the transducer measurements that could be used to correct the transducer data to more accurately reflect stream flow conditions.

The field data (manual) were not collected at the exact same locations as the stream transducers, which helped to minimize distortions in manual flow and depth measurements from the turbulence caused by the bridges and debris that often were found near the transducers. During field events, technicians measured the stream profile, depth, and velocity of the water, and used simple trapezoidal approximations to estimate the flow (rates). By comparing the measured depths versus the reported transducer depths at concurrent times, a corrective equation (correlation) was derived to apply to the transducer stage data to calculate the flow depth.

Graphical representations and correlation between the transducer stages versus measured depths for each of the seven transducers were developed. Figure 4-1 shows the correlation of the raw transducer data to field measured depth. Figure 4-2 shows the correlation of the corrected transducer data versus the measured field depth to show the relative variability between all transducers and their corresponding manual field measurements.

Figure 4-1 shows that most of the field (manual) flow and depth observations were recorded when transducer stage was less than 2.25 ft (for various gauging stations it ranged from 0.8 to 2.25 ft). The trend line equations on Figure 4-1 show the relationship between the field depth and the raw transducer stage over the range of flow measurements made at each gauging station. The data also reflect the uncertainty in the manual measurements of flow and stream depth under low-flow conditions. The trend line equations on Figure 4-1 are used to correct the stage transducer data at low-flow conditions.

Transducer recorded stage at higher flow conditions (at stages above those where manual stream flow measurements were made) were adjusted using the correction at lower-flow conditions. The correction at low-flow conditions was linearly dropped to zero over a short transition depth (1 ft or less) to avoid a discontinuity in recorded stage at higher flow conditions. Beyond this transition depth, no adjustments to transducer stage data were made.

Figures 4-3 through 4-10 illustrate the flow versus stage (corrected) relationship (rating curves) for each of the seven gauging stations with continuous recorders. Measured flow data under low-flow conditions are shown for each station (by orange square symbols). The corresponding best fit line also is shown through the measured flow data (orange line color; the exponential relationship in Figures 4-3 and 4-4 shows the trend line for the measured data under low-flow conditions). The best fit Manning's curve is shown by the blue line and extends over higher observed stage data. Two figures are shown for BC-01; one at stages up to 4 ft to better illustrate the manual measurement data, and one with stages up to 16 ft to illustrate the relationship between stage and flow over the expected flow depths at BC-01. Figures 4-3 through 4-10 clearly demonstrate the fact that manual flow measurements were collected under low-flow conditions at the low end of the expected stream stages (flow depths) anticipated at JPG.

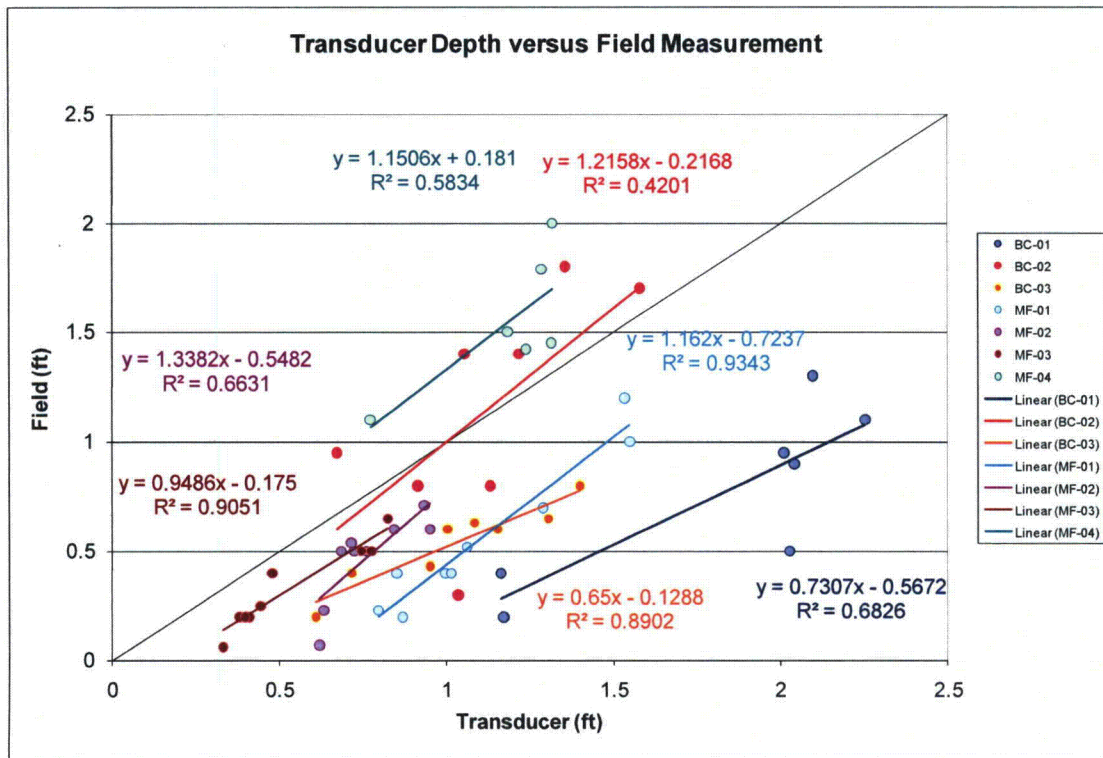


Figure 4-1. Correlation of Raw Transducer Data to Field Measured Depths

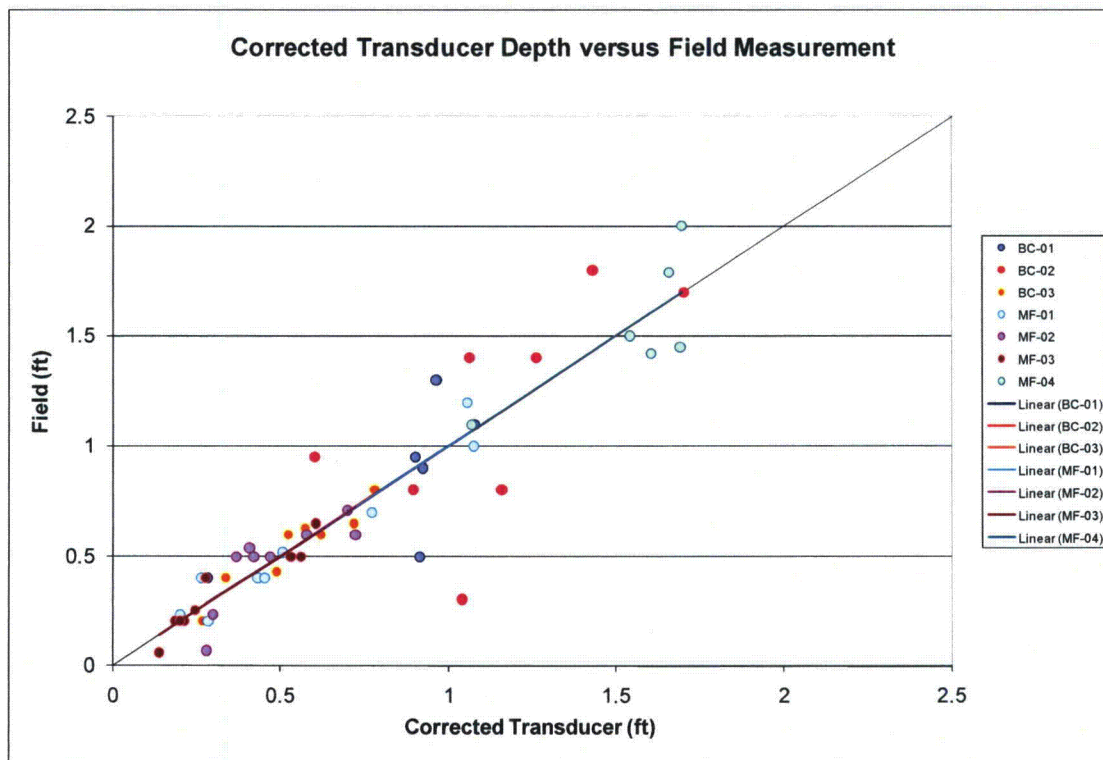


Figure 4-2. Correlation of Corrected Transducer Data to Field Measured Depths

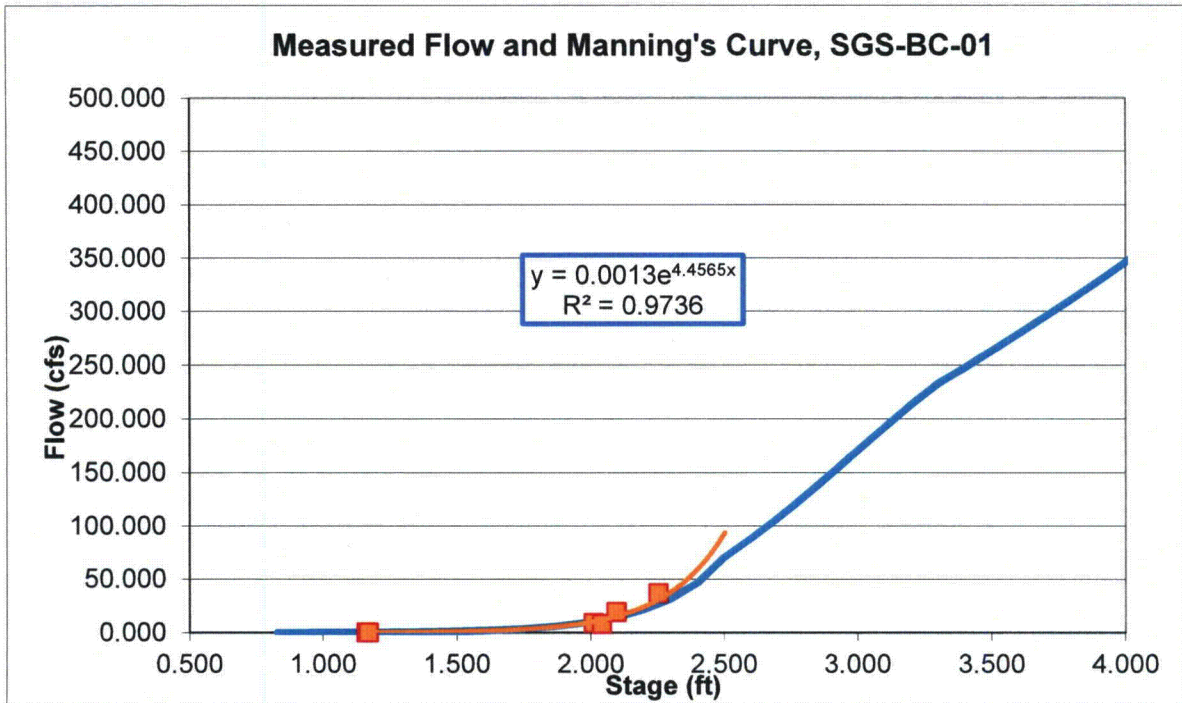


Figure 4-3. Flow Versus Stage at BC-01 (Stage 0 to 4 Feet) With Measured Flow Data

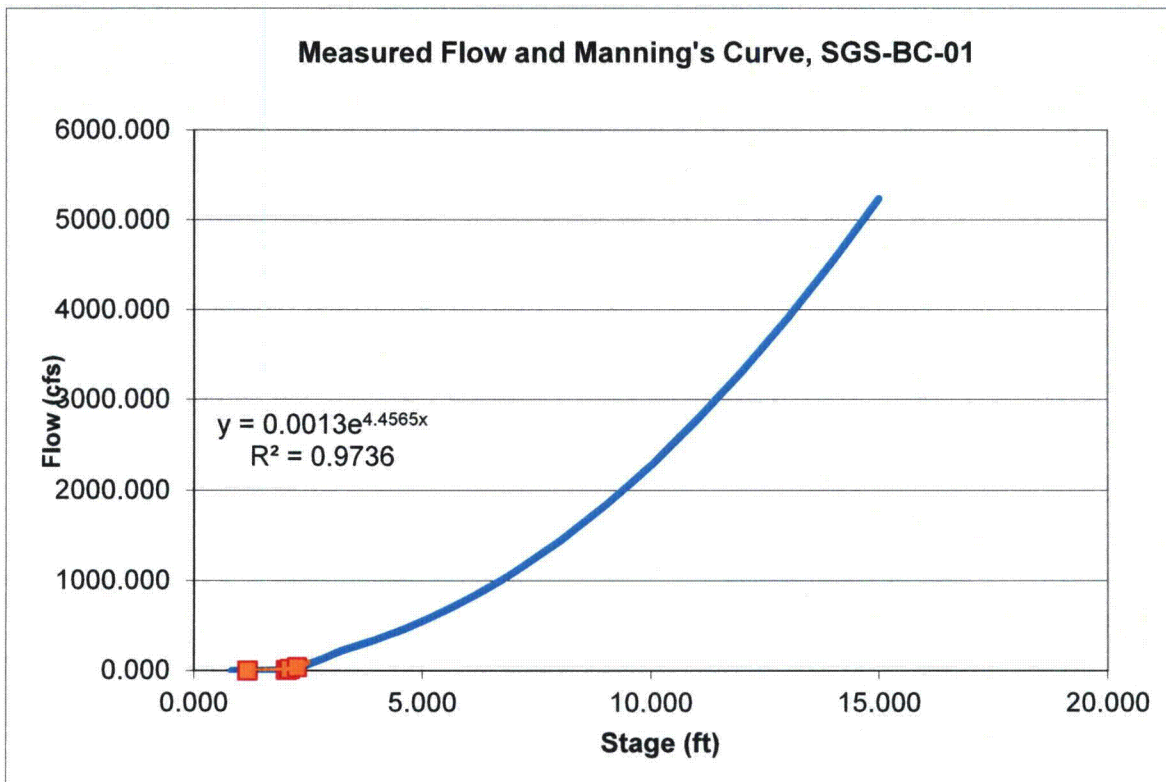


Figure 4-4. Flow Versus Stage at BC-01 (Stage 0 to 16 Feet) With Measured Flow Data

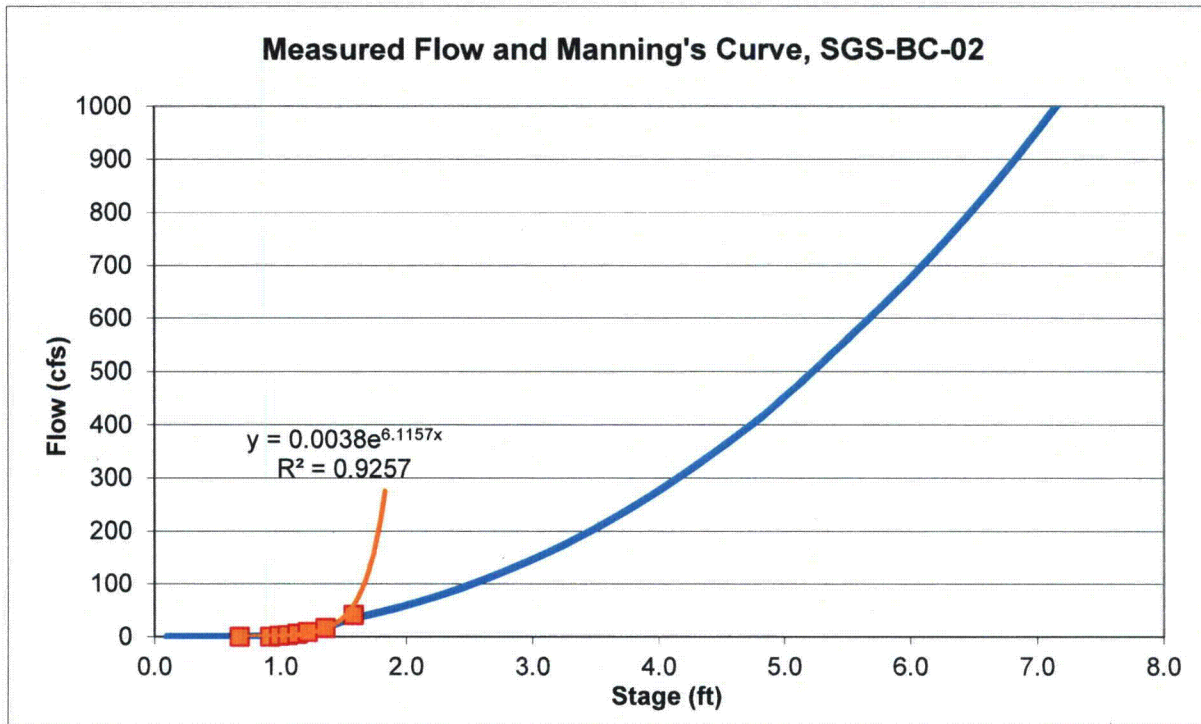


Figure 4-5. Flow Versus Stage at BC-02 With Measured Flow Data

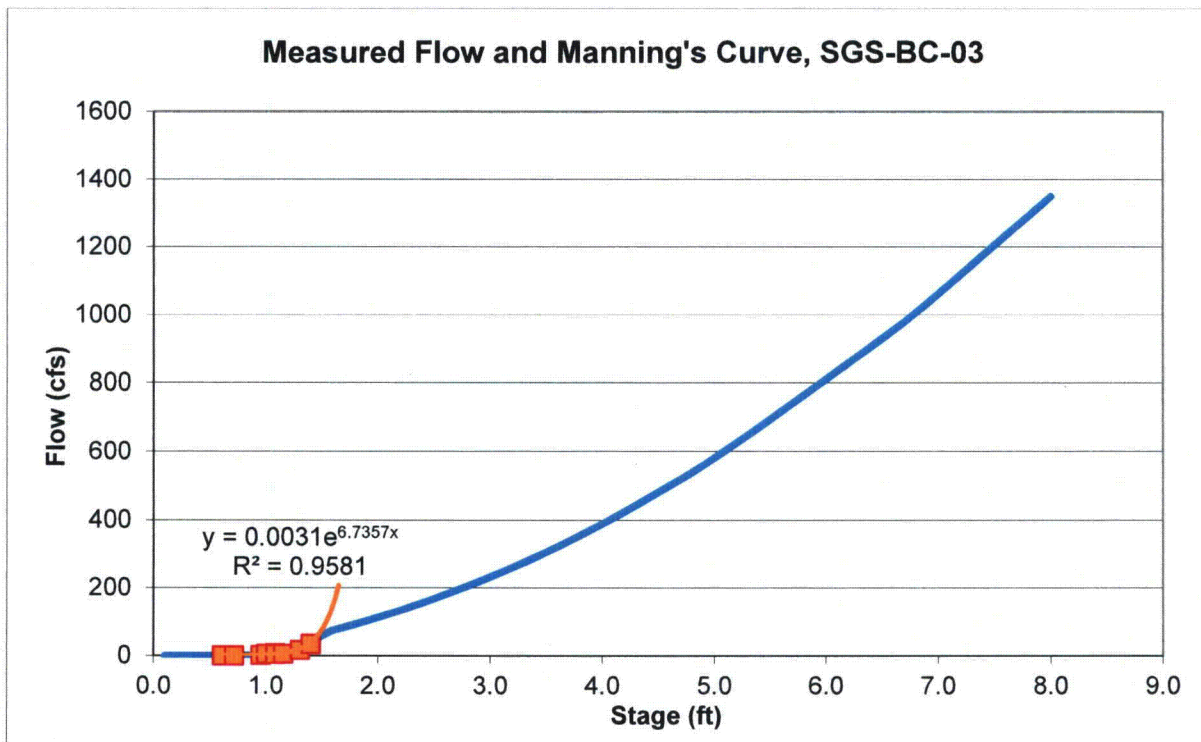


Figure 4-6. Flow Versus Stage at BC-03 With Measured Flow Data

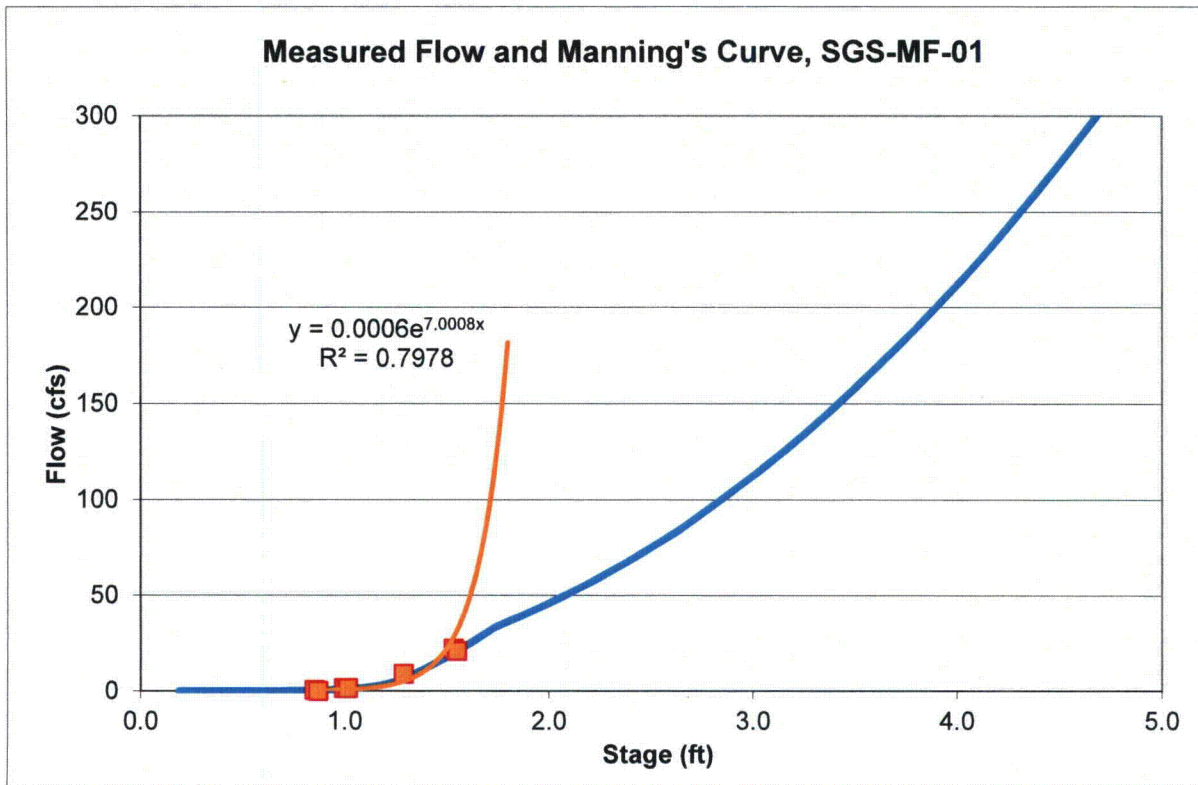


Figure 4-7. Flow Versus Stage at MF-01 With Measured Flow Data

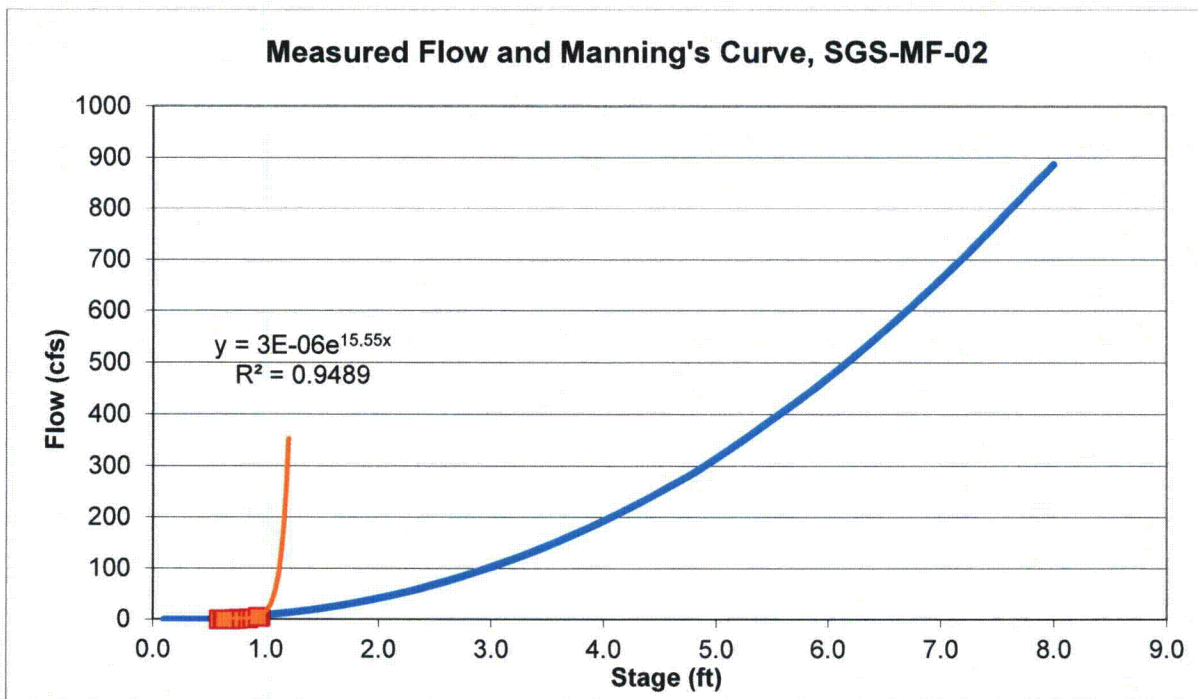


Figure 4-8. Flow Versus Stage at MF-02 With Measured Flow Data

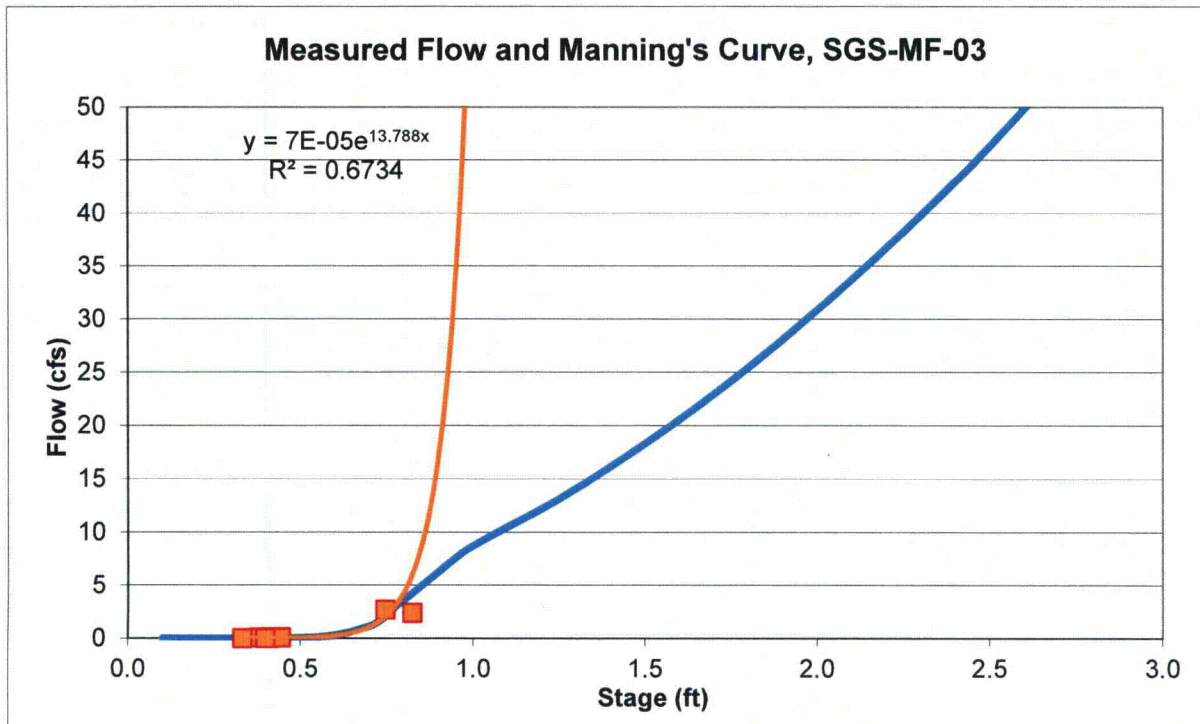


Figure 4-9. Flow Versus Stage at MF-03 With Measured Flow Data

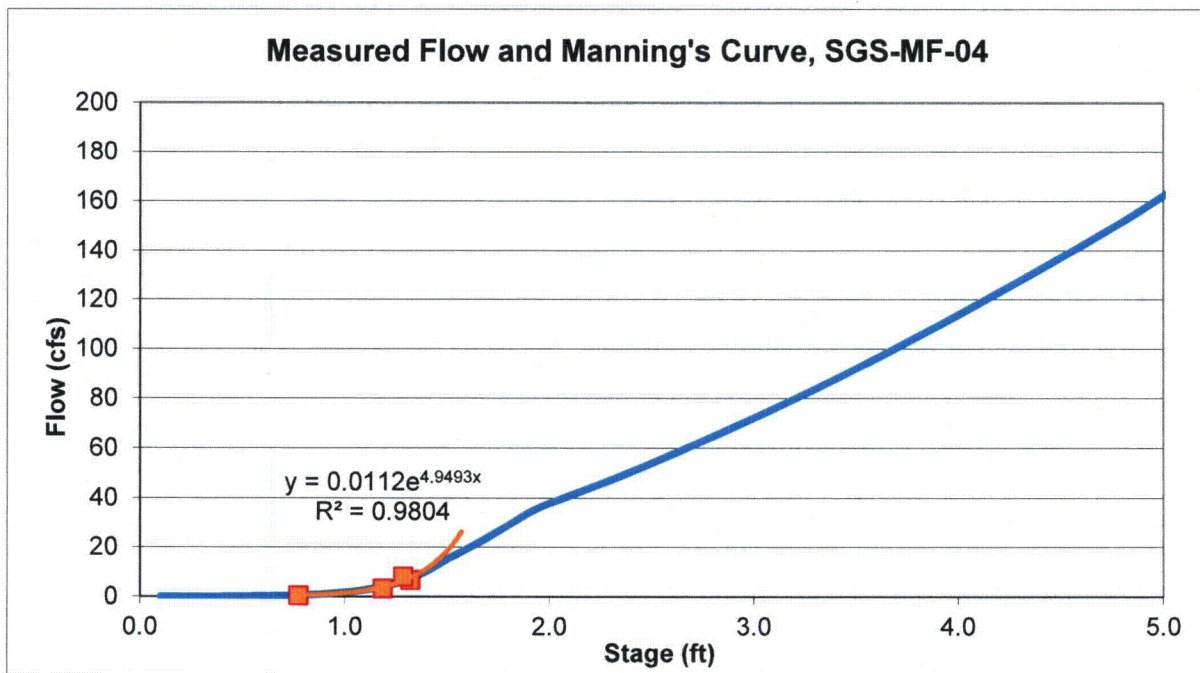


Figure 4-10. Flow Versus Stage at MF-04 With Measured Flow Data

Similarly, the following strategy was used to modify Ftables (see Section 4.5.1) to be consistent with the low-flow field measurements and the corresponding rating curves.

- For the seven streams (those with transducer), the Ftables were updated to match measured low-flow conditions depicted in the rating curves.
- At four locations, (BC-01, BC-03, MF-01, and MF-03), the Ftables were updated to reflect the corrected stage at higher flow conditions (to account for adjustments in the transition depth range, above which the recorded stage was used). Transition depths for each are as follows:
 - BC-01, 2.5 to 3.2 ft
 - BC-03, 1.4 to 1.575 ft
 - MF-01, 1.487 to 1.737 ft
 - MF-03, 0.8 to 0.95 ft.

During calibration and under low-flow conditions (stage \leq manual measured flow depths), simulated stream stages and/or flow rates could be matched with the corresponding observed values. At high-flow conditions where no direct flow or depth field (manual) measurements were made, the corrected transducer stage represents the calibration criteria to be matched with the simulated stream stages.

During simulations, HSPF-JPG uses Ftables to relate stream flow rate, stage, and channel storage volume to find a combination of values that satisfy the mass balance. By matching HSPF-JPG (Ftables based) simulated results to the observed low-flow conditions, the assumption is made that under high-flow conditions, matching modeled stream stage (or depths) with observed stream stage (or depths) produces a reasonable match between simulated and observed flow rates. At high-flow conditions, the calibration goal is therefore to match the model predicted stream stage to the observed stream stage.

4.4 HYDROGRAPH STAGE AND SHAPE

When calibrating HSPF-JPG and comparing simulated and measured stages, it is important to realize that these results are based on the approximations inherent in representing a complex stream configuration by a straight channel with a uniform bed slope and invariant cross-section along its length. However, the real world channels are likely to exhibit nonuniform characteristics such as bed slope, side slopes, Manning's roughness, and so forth. These variations are lumped into averaged parameters in the HSPF model and may represent significant sources of uncertainty in the model results.

For these reasons, matching the qualitative character of the flows reflected in the shape of the hydrographs (such as slope of the rising and falling limbs, time to peak flow, and area under the hydrographs) and response to precipitation events also are selected as calibration criteria.

Figure 4-11 shows observed response of Big Creek at gauging station BC01 to precipitation events for the period 21 November 2007 through 21 May 2008. Creek stage response varies with storm intensity, but generally occurs almost simultaneously with the beginning of the precipitation event with peak stage within a few hours of the precipitation event. Stage decline occurs at a slower rate, with a slightly longer period of decline following the event that represents a combination of interflow and groundwater discharge. Hydrograph stage and shape are affected seasonally and by the number and timing of precipitation events. For example, a storm event in the summer may generate no or very little stream stage response due to depleted soil moisture and plant uptake, while in the late fall or early spring, a similar storm event may produce a marked stream response because soils are at near saturation and plant growth is at a minimum. Similarly, snowfall during winter months may not result in an observed stage response until the snow melts (see precipitation events from 27 January to 1 February 2008 and the lack of stream stage response).

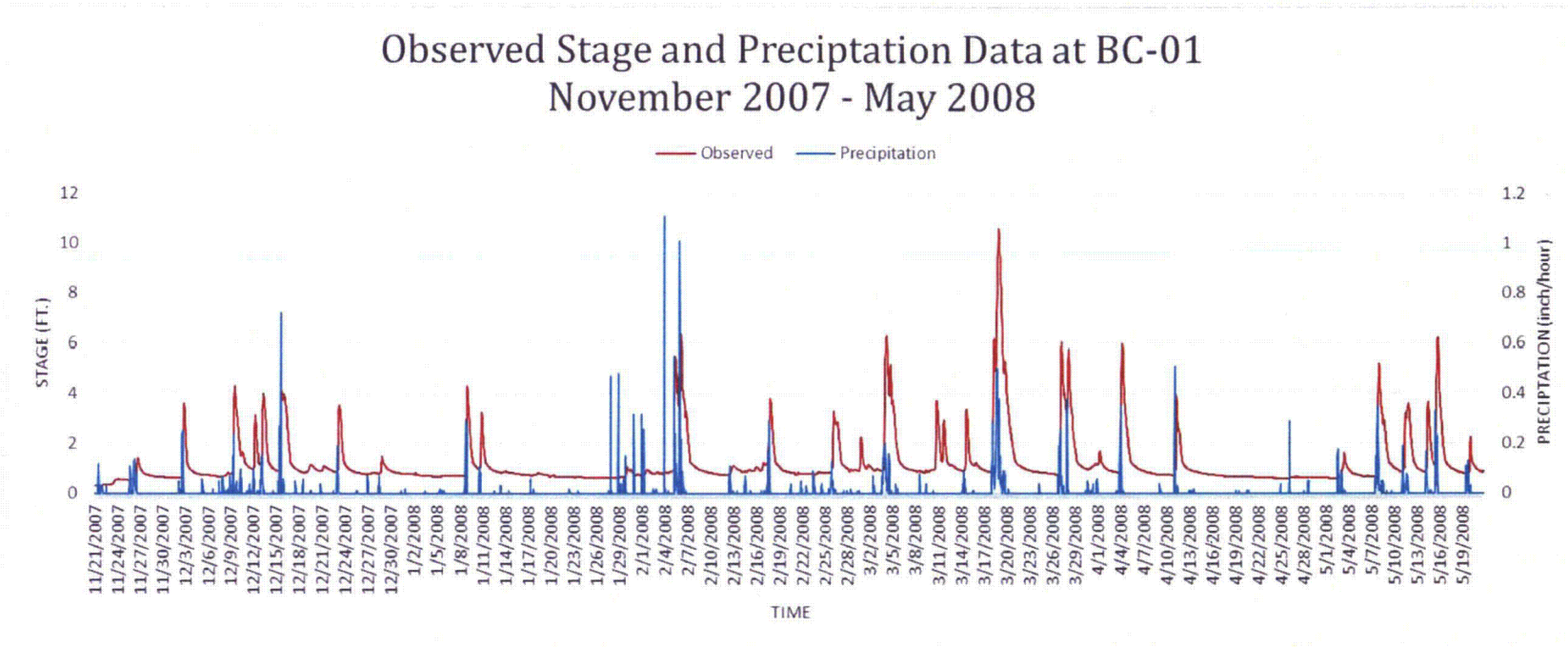


Figure 4-11. Observed Stage and Precipitation Data at BC-01 November 2007 Through May 2008

4.5 CALIBRATION PARAMETERS

HSPF-JPG invokes simplified representation of otherwise highly complex physical, chemical, and biological processes. The watershed domain is discretized into sub-basins and parameters are lumped so that each sub-basin can be analyzed and simulated efficiently. During calibration, parameters are adjusted to obtain results that reproduce observed data.

This section describes the key parameters examined during the process of calibrating runoff and various stream flow components of the model, how those parameters were changed, and the effects on the modeled results. This is followed by a discussion on the calibration, including a description of how the calibrated base case model compares to the identified targets, results, and discrepancies and limitations of the model to accurately predict flow and stage.

4.5.1 Ftables

As described in the model setup (Section 3.2.1), Ftables are the lookup tables describing the relationship between stream depths (stage), water surface area, stream storage volume, and the volumetric flow rate for each channel (which is also known as stream or reach). During simulation, HSPF interpolates these tabulated values to relate stage (depth) to volumetric flow rate, water surface area, and stream storage volume, and determines compatible values for these parameters in various reaches versus time. This considerably decreases computational time of several surface flow modules.

The assumption that a single Ftable can accurately describe an entire stream reach is inherently flawed due to the variability of the described reaches. Variability in side slopes, floodplain heights and lateral extents, channel depths and widths, and the bed slope of the streams have to be encompassed by these tables. This obviously introduces uncertainty into any attempt to match predicted model depths with field observations. For example, the stage versus flow rating curve can exhibit large changes at the side slope inflection points defining floodplain lateral extents. Therefore, once an HSPF model has been created by BASINS, Ftables must be refined to reflect the true characteristics of the channel for each sub-basin that has been defined in the river reach or reservoir (RCHRES) module.

However, it is important that these changes are made without disrupting the carefully constructed relationship between depth and flow at low flow, as these relationships are based on field observed data. The relationship at higher flow conditions is open to considerable interpretation due to the uncertainty introduced by having no correlated flow measurements for high measured (transducer) stages.

4.5.2 HSPF Parameters

HSPF subdivides the parameters in various groups within the PERLND module. Parameter values are assigned for each land use.

The PERLND:SNOW-PARM1 dialog box is used to specify parameters governing the snowmelt module. Table 4-2 provides the values used for these parameters in the HSPF-JPG model.

**Table 4-2. Parameters Governing Snowmelt Used in HSPF-JPG
Jefferson Proving Ground, Madison, Indiana**

Land Use	SHADE (fraction)	SNOWCF (factor)	COVIND (in)	KMELT (in/d.F)
Grass	0.1	1.1	10	0.5
Bare Soil	0.1	1.1	10	0.5
Forest	0.9	1.1	10	0.5
Farm/New Growth	0.2	1.1	10	0.5
Water	0.01	1.1	10	0.5

- SHADE is the fraction of the land surface that is shaded from solar radiation
- SNOWCF is the factor by which recorded precipitation data will be multiplied if the simulation indicates it is snowfall, to account for poor catch efficiency under snow conditions
- COVIND (in) is the maximum pack (water equivalent) at which the entire PLS will be covered with snow
- KMELT is the degree-day snowmelt factor (in/d.F); minimum value is zero.

The category of primary interest to runoff and stream flow for pervious land is PWATER, with PWAT-PARM2, PWAT-PARM3, and PWAT-PARM4 tables containing the main drivers behind dynamic flow calculations. Each component is assigned per land usage, although many of the parameters will have the same value across all land usages. Each of the components is described below, and the calibrated values are tabulated in this section.

- PERLND:PWAT-PARM2 (Table 4-3) defines parameters governing infiltration, overland, and groundwater flow and includes:

**Table 4-3. PERLND:PWAT-PARM2 Parameters Used in HSPF-JPG Model
Jefferson Proving Ground, Madison, Indiana**

Land Use	FOREST (fraction)	LZSN (in)	INFILT (in/hr)	LSUR (ft)	SLSUR (%)	KVARY (1/in)	AGWRC (1/d)
Grass	0.10	5	0.015	350	0.05	3	0.10
Bare Soil	0.10	5	0.015	350	0.05	3	0.10
Forest	0.80	8	0.015	350	0.05	3	0.10
Farm/New Growth	0.10	5	0.015	350	0.05	3	0.10
Water	0.01	5	0.015	350	0.05	3	0.10

- FOREST describes the fraction of each land use that will continue to transpire during the winter months (generally coniferous plants). This parameter is not important in the calibration process, as it primarily affects evapotranspiration during the winter months when rates are low.
- LZSN (inches) describes the nominal lower zone (subsurface) soil moisture storage capacity, which sets an upper limit on the amount of precipitation that is allowed to be partitioned into the lower zone. This parameter can be used to force more precipitation to be partitioned to interflow, surface runoff, or evapotranspiration. Other parameters have greater influence on these processes and are described below. After some initial adjustments, the LZSN was not fine-tuned during calibration refinement.
- INFILT (in/hr) is the index to the infiltration capacity of the soil and controls partitioning of the net precipitation (after interception is considered) into various surface and subsurface hydrologic components. Higher values will cause less water to be available for direct surface runoff and more for interflow and groundwater recharge. Conversely, low values produce higher direct surface runoff and less interflow and groundwater recharge. Less interflow and groundwater recharge corresponds to lower base flows and, therefore, INFILT is of high importance both in matching the water budget calibration goals and accurately depicting the character of stream flows between precipitation events.
- LSUR (feet) describes the length of the assumed overland flow plane. This is important in the timing of surface water runoff entering the streams but is represented in HSPF-JPG as a lumped average parameter for each land use. Due to the highly variable nature of the land use areas within each basin, and the necessary coarseness of the model basins due to the

large area being modeled, direct methods of calculation for the LSUR were impractical. However, variations in the LSUR were not observed to cause large differences in peak flow or timing within the modeled hydrographs, so LSUR was set at an intermediate value of 350 ft for all land uses (for comparison, the possible range described by BASINS Technical Note 6 was 100 to 700 ft, while the typical range is 200 to 500 ft).

- SLSUR describes the average slope of the assumed overland flow plane. As with LSUR, the lumping of land uses into a generalized parameter made it impractical to calculate a slope, but variations in the slope produced no noticeable effects in the quality of the hydrographs. Overland slope was set to an intermediate value of 0.05 (for comparison, the possible range of 0.001 to 0.3 and typical range of 0.01 to 0.15 described by BASINS Technical Note 6; and the range in slopes from soil survey descriptions is 0 to 35 percent) for all land uses.
- KVARV (1/in) is used to allow the exponent in the groundwater recession equation to vary allowing the recession rate to vary with groundwater level. This component had little effect on either the water budget or the hydrograph qualities, and was set at 3.0 (typical range 0 to 3, possible range 0 to 5).
- AGWRC (1/d) is the base groundwater recession rate, described as the ratio of current groundwater discharge to those 24 hours earlier. Due to the highly flashy nature of the JPG streams, values at the lower end of the range, which allow a quick recession (falling limb) to base flow conditions, are representative. A value of 0.1 was selected; higher values resulted in overestimated base flows following storm events.
- PERLND:PWAT-PARM3 (Table 4-4) contains parameters used in defining infiltration, deep percolation, and potential evapotranspiration adjustment during HSPF simulation and include:

**Table 4-4. PERLND:PWAT-PARM3 Parameters Used in HSPF-JPG Model
Jefferson Proving Ground, Madison, Indiana**

Land Use	INFEXP	INFILD	DEEPPFR	BASETP	AGWETP
Grass	3	1.5	0	0.03	0.03
Bare Soil	3	1.5	0	0.03	0.03
Forest	3	1.5	0	0.03	0.03
Farm/New Growth	3	1.5	0	0.03	0.03
Water	3	1.5	0	0.20	0.70

- INFEXP is an exponent in the infiltration equation and can significantly influence the direct surface runoff volume and hydrograph characteristics (the HSPF recommended range is 0 to 10). A higher INFEXP value results in high peak runoff hydrographs. A value of 3 was used for all land uses to match the observed hydrograph characteristics.
- INFILD is an infiltration function parameter and defines the ratio of the maximum to mean infiltration rates. INFILD significantly influences the direct surface runoff volume and hydrograph characteristics (HSPF recommended range, 1 to 2). A value of 1 produces steep rising and falling limb hydrographs; higher values produce lower peaks and relatively slower rising and falling limbs. A value of 1.5 was used for all land use types to match the observed hydrograph characteristics.
- PETMAX and PETMIN are the parameters defining the temperature range and are used to allow potential evapotranspiration rates to vary. PETMAX is the temperature below which evapotranspiration will be established as a fraction of the calculated value. This represents a decrease in potential evapotranspiration as the temperature approaches the freezing point of water. PETMIN is the minimum temperature at which any potential evapotranspiration

is allowed. The freezing point is the logical choice here, representing zero potential evapotranspiration due to the water freezing instead of evaporating. PETMAX and PETMIN were assigned values of 40 and 32°F, respectively.

- DEEPFR describes the fraction of groundwater inflow that will enter deep groundwater and be lost from the system, as described by HSPF. This separates active groundwater (=1 - DEEPFR), which contributes to stream base flow, from inactive groundwater that has no further effect in the surface water modeling (this can be thought of as recharge to deeper regional groundwater flow paths that leave modeled area). DEEPFR also has a large effect on the hydrographs at low flow due to its role in establishing how much water is available for base-flow conditions. In the HSPF-JPG model, DEEPFR was assumed equal to 0.
- BASETP describes what fraction of the remaining potential evapotranspiration is allowed to be satisfied from the base flow. BASETP represents evapotranspiration by riparian vegetation and only occurs when groundwater outflow is occurring. Variation of this parameter has minor influence on matching the water budget at JPG.
- AGWETP is the fraction of remaining potential evapotranspiration permitted from active groundwater storage, traditionally represented by marshy or wetland areas where the groundwater surface is in contact with the land surface. Variation of this parameter also has minor influence in matching the water budget at JPG.
- PERLND:PWAT-PARM4 (Table 4-5) contains parameters used by HSPF to simulate moisture storage in the upper zone, evapotranspiration from the lower subsurface zone, Manning's roughness coefficient for overland flow, and interflow and interflow recession parameter (IRC, 1/d).

**Table 4-5. PERLND:PWAT-PARM4 Parameters Used in HSPF-JPG Model
Jefferson Proving Ground, Madison, Indiana**

Land Use	UZSN (in)	INTFW (in)	IRC (1/d)	LZETP (no units)
Grass	1.0	3	0.03	0.60
Bare Soil	0.8	3	0.03	0.50
Forest	2.0	3	0.03	0.90
Farm/New Growth	1.8	3	0.03	0.70
Water	0.1	3	0.03	0.60

- CEPSC (inches) describes the amount of rainfall that can be retained by vegetation and evaporated, never reaching the surface. For a model area with great seasonal variation in vegetative cover, this is best allowed to vary monthly using the MON-INTERCEP table. Variation of this parameter is important in the initial matching of the water budget, as this water is completely removed from the possibility of becoming runoff, interflow, or groundwater. Interception storage capacity (CEPSC) for various land use types was allowed to vary over each month (range 0 to 0.35 in).
- UZSN (inches) is the nominal upper zone soil moisture storage, and is highly dependent on soil and land surface characteristics. This parameter also is often allowed to vary monthly, especially for land that experiences high variability in tillage and growth such as agricultural land. Higher values of UZSN reduces direct overland flow by allowing the water to be retained and available for evapotranspiration or infiltration, while lower values have the opposite effect. Overall water balance is typically minimally affected, but the character of overland flow can be altered by this parameter.

- NSUR is the average Manning’s roughness coefficient for the assumed overland flow plane, and is considerably higher than published values for typical channel flow conditions with low density of vegetation and roughness. This factor is highly dependent on vegetation, and is often allowed to vary monthly. Little to no effect was noticed on either the water budget or hydrograph shapes by varying this parameter. NSUR was allowed to change over each month (range 0.02 to 0.3).
- INTFW (inches) describes the amount of water that enters groundwater from surface detention and becomes interflow. Interflow is one of the most important factors in attempting to match the hydrograph peaks. By dividing surface water into interflow and direct surface runoff, a portion of what would have been surface runoff entering the streams is delayed. The same volume of water enters the streams but over a longer period of time (thus not affecting the overall water budget). A high INTFW coefficient therefore will reduce the height of peak stages by “stretching” the flow volume over longer periods, whereas a low value will allow more of the water to directly runoff and increase the peak flows and stages.
- IRC (1/d) is the interflow recession coefficient. Like AGWRC and INTFW, this parameter has little effect on the overall water budget but a large effect on the shape and character of the hydrographs. The interflow recession coefficient describes that ratio of current interflow outflow to those occurring 24 hours earlier. A high IRC value will force the interflow to enter the stream more slowly resulting in a slower, return from peak values to base-flow conditions. A lower IRC value will force the interflow to quickly enter the stream, acting almost like surface water. Lower IRC values result in steep hydrograph slopes following peak events and a quicker return to base-flow conditions.
- LZETP is the lower zone evapotranspiration parameter. It is an index to the density of deep-rooted vegetation (range 0 – 1.5), units = none.

For impervious land, the IMPLND:IWAT-PARM2 (Table 4-6) defines various parameters governing behavior of overland flow and retention storage capacity (RETSC, inches) of the surface. For various land use types, the length (LSUR, feet) and slope of overland flow plane (SLSUR) and Manning’s roughness coefficient (NSUR) are tabulated.

Table 4-6. Parameters Used for Impervious Land Use Overland Flow and Retention Storage Capacity in HSPF-JPG Jefferson Proving Ground, Madison, Indiana

Land Use	LSUR (ft)	SLSUR (%)	NSUR (Manning’s Coef.)	RETSC (in)
Grass	350	0.05	0.03	0.05
Bare Soil	350	0.05	0.03	0.05
Forest	350	0.05	0.03	0.05
Farm/New Growth	350	0.05	0.03	0.05
ROAD	350	0.05	0.03	0.05

4.6 CALIBRATION PROCESS

The first step in calibrating the HSPF-JPG model consisted of matching the modeled flow (runoff) to the established annual water budget goals. Matching the water budget ensures the correct amount of flow is in the system on an annual basis and enhances confidence in the stage and hydrograph calibration efforts. If both overall flow and stage/hydrograph matches are achieved, modeled flow velocities are assumed similar to what would be observed in the field.

The second step involves the semi-quantitative comparison of stream hydrographs. This is especially important for matching both stage and flow at low-flow conditions, as this is the window under which observations of both flow and stage exist. Ftable adjustments through Manning's coefficients along with adjustment of the key watershed parameters such as AGWRC, INTFW, and IRC were the most important processes in matching observed low-flow measurements and hydrograph shape.

4.7 CALIBRATION RESULTS

The results of the calibration process in comparison with the goals established earlier in this section are presented. Each of the calibration targets is evaluated against simulated results. A discussion of the limitations of the calibrated model is also included. The calibration targets include:

- Water budget
- Measured low-flow data at stream gauging stations
- Measured stage at high-flow conditions
- Stream hydrograph stage and shape.

The HSPF flow calibration initially was performed using 2006 to 2009 meteorological data (HY2007 to HY2009). The simulated stream stages were compared with the observed values and various parameters were adjusted to improve the calibration. The model was verified with an independent set of 2010 to 2011 (HY2010) meteorological data and stream stage was compared against the observed values. The simulated and observed results for the 2006 to 2011 periods show a reasonable agreement within the range of observed values. These results, along with the water balance analysis reported in Section 4.2, enhance confidence in the flow model calibration/verification and in the predictive capability of the model.

4.7.1 Water Budget

For the calibrated model, output results matched the water budget criteria well (Table 4-7). The HSPF budget for the period is within 3.6 percent of the precipitation falling within the model area. Differences between the HSPF flow budget and annual precipitation are expected and result from changes in storage (e.g., water moving into and out of storage depending upon soil moisture). The sum from HSPF of evapotranspiration, runoff, and groundwater percolation for HY2007 (Table 4-7) was equal to 49.67 in compared to precipitation of 45.4 in. The additional 4.27 in were derived from decrease in storages (subsurface and surface) within PERLND segments under different land uses.

HY2008 and HY2009 were wetter and HY2010 was drier than the average rainfall year and vary more from the water budget for HY2007. The results below treat interflow as surface runoff, since the percolating water almost immediately enters back into the stream network, as exhibited by the very flashy nature of the stream flows.

As shown in Table 4-7, modeled runoff (average total surface and interflow runoff [SURO+IFWO]) matches water budget runoff (36 percent of annual precipitation) for the period. Modeled evapotranspiration (SAET) is slightly less (53 percent versus budget of 56 percent) and is within the range of observed annual variability. Modeled shallow groundwater recharge (AGWO) is greater (14 percent versus budget of 8 percent), but is within the range of published literature for southern Indiana. The average evapotranspiration estimates in Table 4-1 were almost equal to the average potential evapotranspiration (PETX) values used in HSPF-JPG simulations (Table 4-7) and are the likely reason for under predicted evapotranspiration (SAET, Table 4-7) and could be resulting in higher groundwater recharge (base flow).

**Table 4-7. Simulated Water Budget Components (Inches) for Reach 129
Jefferson Proving Ground, Madison, Indiana**

Year	PREC (in)	HSPF total (in)	Dif (PREC minus HSPF)	% Dif	SAET (in)	SURO (in)	IFWO (in)	SURO + IFWO (in)	AGWO (in)	PETX (in)
Average	49.18	50.95	-1.77	-3.60	26.03	10.33	7.59	17.92	7	27.83
HY2007	45.4	49.67	-4.27	-9.41	26.4	8.5	8.02	16.52	6.75	28.5
HY2008	56.2	56.59	-0.39	-0.69	25.1	13.8	9.62	23.42	8.07	26.8
HY2009	54.7	49.76	4.94	9.03	25.6	10.3	6.65	16.95	7.21	26.8
HY2010	40.4	47.75	-7.35	-18.19	27	8.7	6.08	14.78	5.97	29.2

Note: Values in Tables 4-1 and 4-7 above were based on 0 percent (DEEPPFR=0.0) percolation.

PREC = annual precipitation total

HSPF total = total flow budget

SAET = calculated evapotranspiration

SURO = surface runoff

IFWO = interflow

AGWO = shallow groundwater recharge

PETX = potential evapotranspiration

4.7.2 Stage Versus Flow at Low-Flow Conditions

With the water budget relatively well-matched across the site, the next step is to examine the quality of match between simulated and observed hydrographs for the model segments where observed stage data were available. This is especially important in low-flow conditions where the stage transducers can be directly correlated against actual field measurements of stream flow. At low-flow conditions, the Ftables incorporate the rating curves developed at each gauging station, as shown in Section 4.3, implying that under such conditions the stage and flow rates were highly dependent variables and either could be used in model calibration and verification. Therefore, the flow model reproduces the observed flow and stage within the uncertainty of the field measured values.

Gauging station BC-01 is on Big Creek at the western boundary of the DU Impact Area. BC-01 corresponds with sub-basin 114 within the surface water model domain. Figure 4-12 compares simulated stage at sub-basin 114 (RCH114) with observed values for BC-01 (SGSBC01). Gauging station BC-03 is on Big Creek on the eastern boundary of the DU Impact Area. BC-03 corresponds with sub-basin 110. Figure 4-13 compares simulated stage at sub-basin 110 (RCH110) with observed values for BC-03 (SGSBC03). The measured and modeled stages agree very well with each other. At stage heights less than 1 ft, the simulated stage shows a more spiky nature than the observed, likely due to uncertainties within the stream cross-sectional area. Periods of low flow (May 2007 to October 2007 except for an 8 to 9 August storm event, June 2008 to first half of December 2008, last half of August 2009 to September 2009, and July 2010 to November 2010) have been observed. These periods are associated with below average monthly precipitation. Precipitation falling during these periods (Figure 4-14) replenishes stored moisture but is not of sufficient intensity or duration to generate a rise in stage above 1 ft in either the measured or modeled flows at BC-01 or BC-03.

In the January (2007, 2009) timeframe, the observed and modeled stage do not match well; however, this is an easily explained anomaly introduced by the way that HSPF handles snow and snowmelt. Depending on the temperature at the time of the precipitation event, HSPF will assume that it is snow or rain, which may differ from actual observations. Likewise, melting events may occur at different times than HSPF predicts.

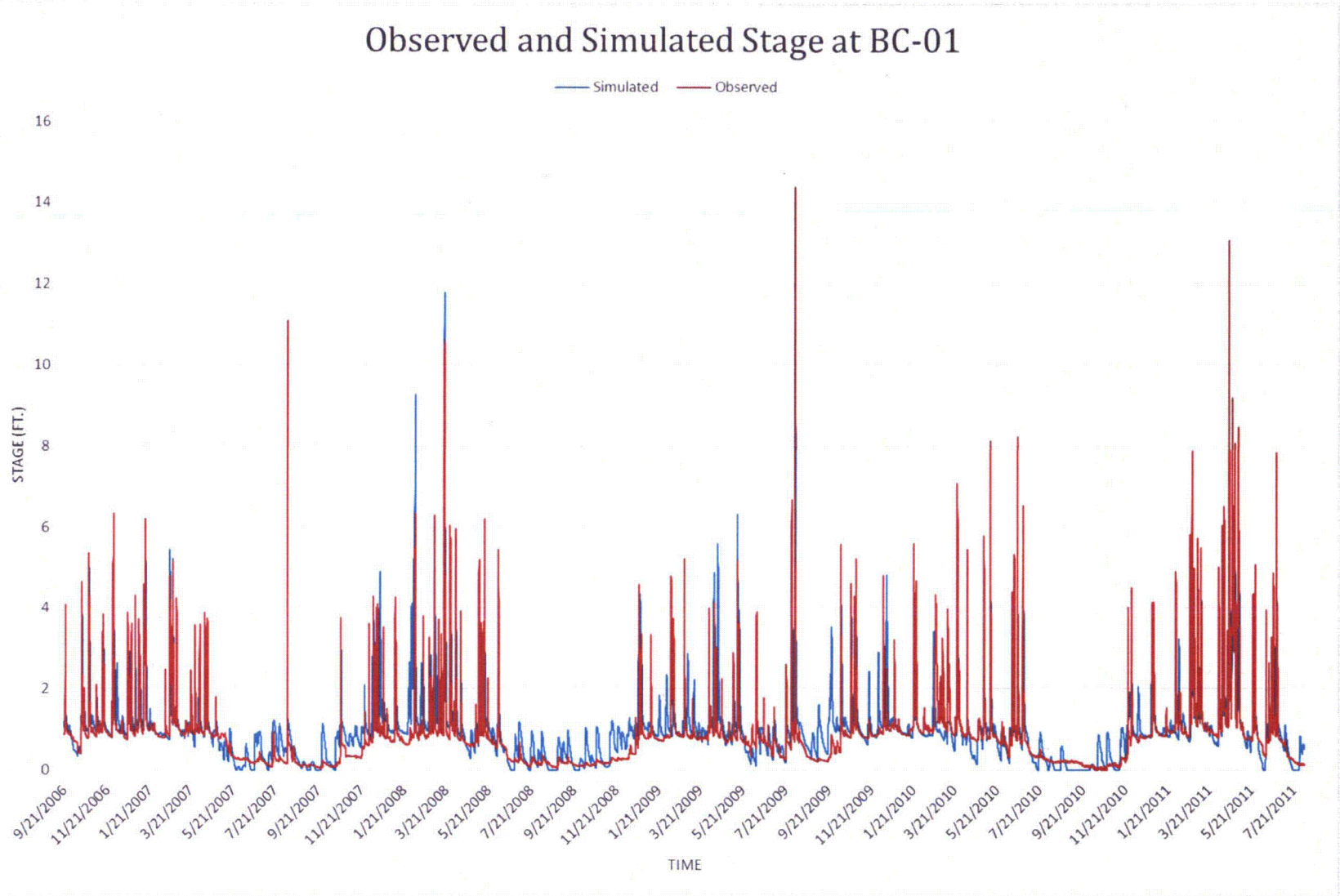


Figure 4-12. Observed and Simulated Stage at BC-01

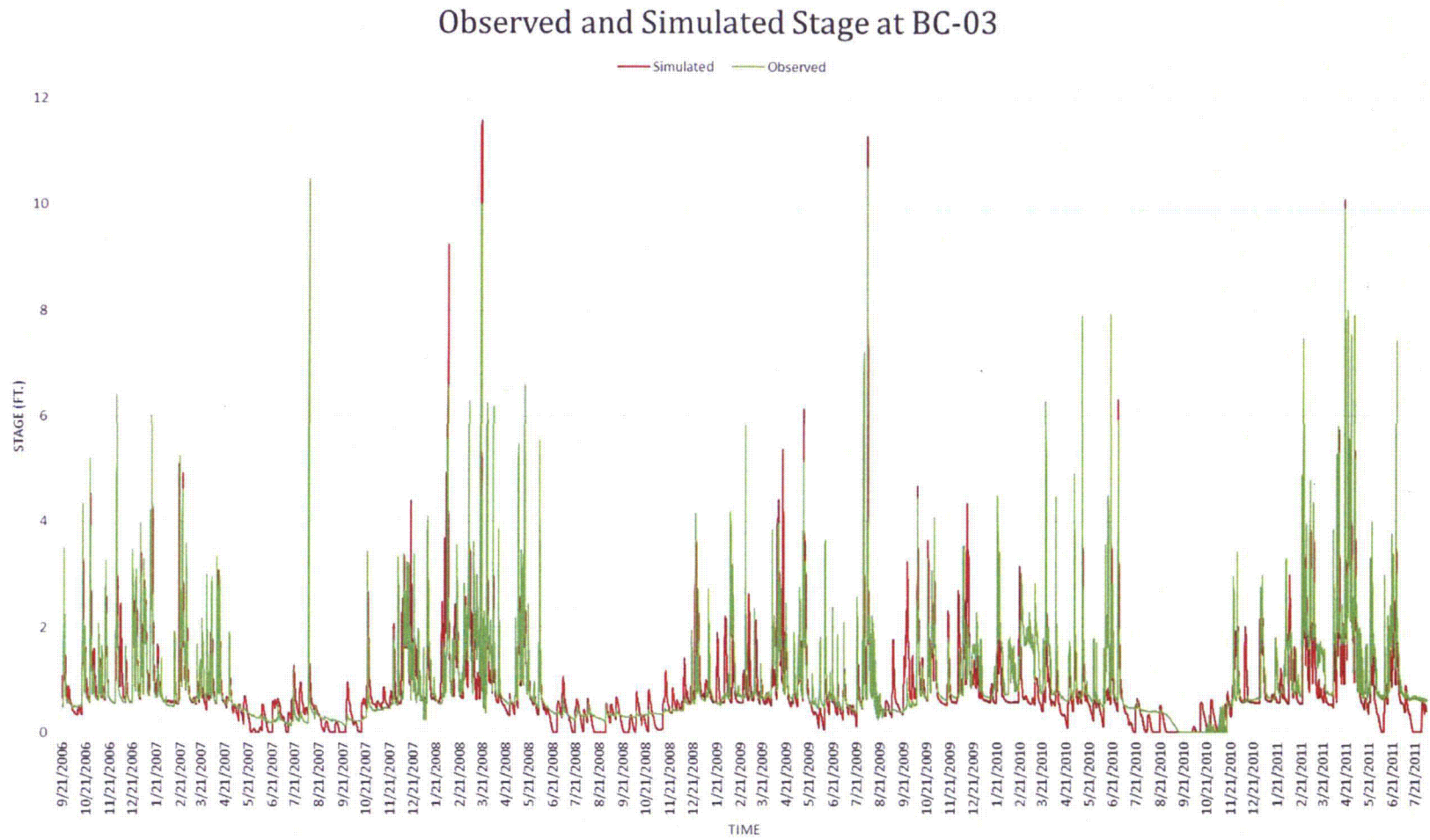


Figure 4-13. Observed and Simulated Stage at BC-03

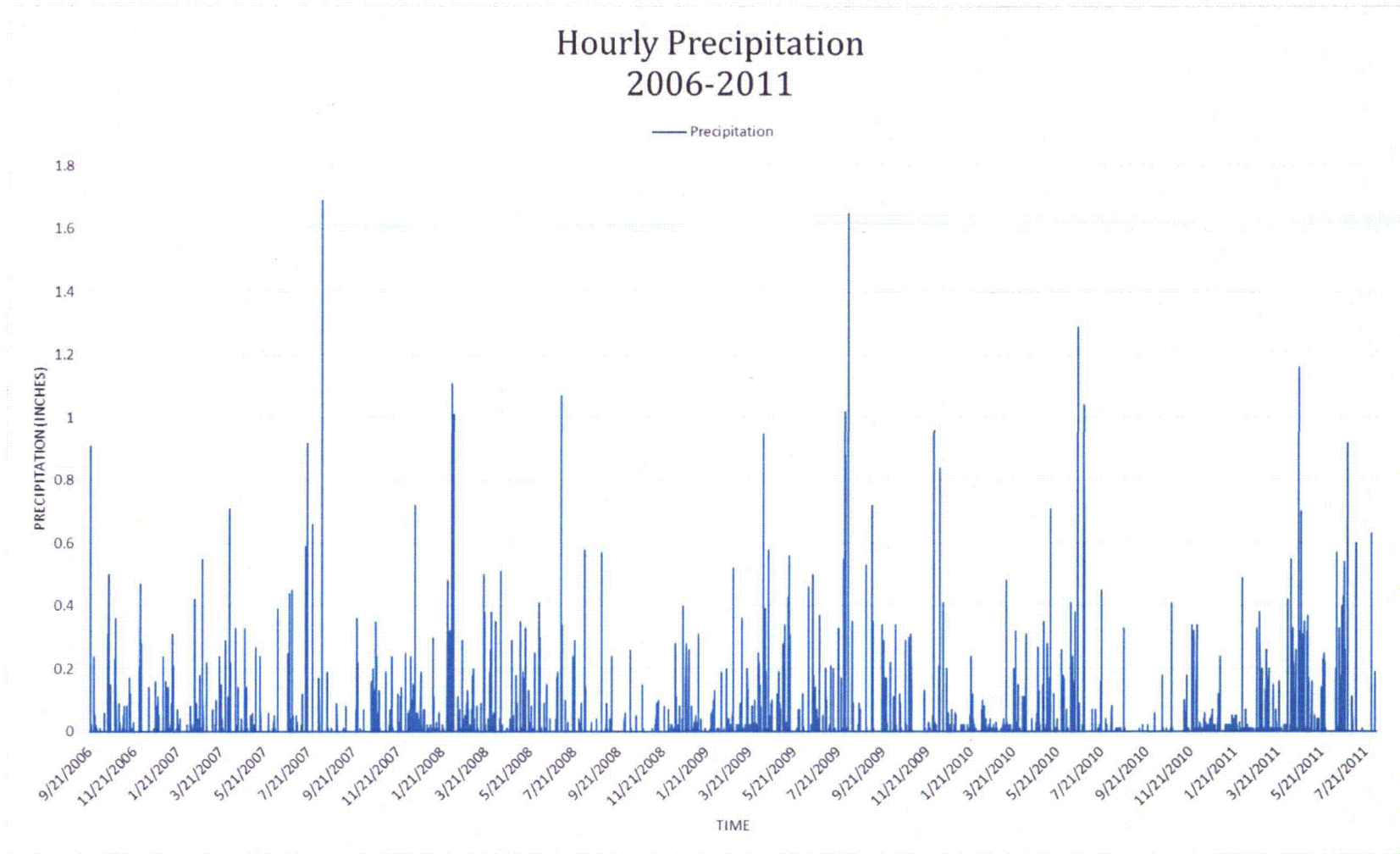


Figure 4-14. Hourly Precipitation 2006-2011

One other anomaly on Figures 4-12 and 4-13 occurs between 21 July 2007 and 21 September 2007. The observed stage shows a short-duration storm event with nearly an 11-ft rise in stage while the model shows very limited rise in modeled stage. Examination of hourly precipitation data (Figure 4-14) shows the highest intensity storm event for the period 21 September 2006 through 6 August 2011 at nearly 1.7 in per hour on 8 August 2007, corresponding with the observed rise in stage. Stream stage rose over 10 ft in less than 5 hours on Big Creek (recorded stage data at BC-01 and BC-03), before dropping back down to less than 1 ft 20 hours later on 9 August. A similar intensity storm occurred in early August 2009 with rainfall exceeding 1.6 in per hour and results in observed stage rise to more than 14 ft at BC-01 and nearly 11 ft at BC-03. The modeled stages at BC-01 and BC-03 for this event are roughly 11 ft. So, these are two similar intensity storm events, one where the simulated stage does not reproduce the observed stage (August 2007) and one where the simulated stage is similar to the observed stage (August 2009). Examination of precipitation data shows below normal monthly precipitation leading up to and following the August 2007 event; conversely, monthly precipitation was above normal leading up to and including the August 2009 event. Based upon this review, modeled results for the August 2007 event appear to overestimate the amount of water going into storage to replace moisture lost from below average monthly precipitation preceding and following this event.

Examination of modeled flow at BC-01 (Figure 4-15) shows very low simulated flow rate (<100 cfs) associated with the August 2007 event compared to highest flow rate of 4,800 cfs associated with the August 2009 event. So, the model is underpredicting flow and stage for the August 2007 event.

4.7.3 Hydrograph Stage and Shape Matching

With good water budget matching and stage/flow matching at low-flow conditions, the last remaining calibration criteria to demonstrate is the ability of the model to match the general shape and character of the observed hydrographs. Since an accurate relationship between flow and stage at higher flow conditions could not be developed due to lack of data, the matching of observed and simulated stages at high-flow conditions was done qualitatively.

As depicted in Figure 4-16, overall the model does a good job of matching the timing of flow peaks within the stream segment #114 where gauging station BC-01 was located. The model does tend to exhibit a slightly slower recession back to base flow conditions than observations indicate. One notable difference occurs in late January to early February 2008, where simulated stages show several peaks that were not observed in the gauge data. This difference is most likely due to precipitation falling as snow with later melting to produce the observed stage response relative to the simulated stage response.

4.8 MODELED FLOW BY SUB-BASIN

Simulated flow by sub-basin is shown in Table 4-8 for calendar years 2007 through 2010. Modeled flow is proportional to the area drained. Big Creek comprises 76 percent of the model area and 76 percent of the modeled flow. Annual precipitation ranges from a low of 36.6 inches in 2010 to a high of 58.4 inches in 2009. Simulated flow is shown from upstream to downstream at select sub-basins with flow increasing with the area drained (see Figure 3-1 for sub-basin locations). For Big Creek, flow is shown for sub-basin 110 at the eastern boundary of the DU Impact Area through sub-basin 128, west of JPG just upstream from the confluence with Middle Fork Creek. Sub-basin 110 contains the flow from nearly 14,000 ac upstream of the DU Impact Area. Sub-basin 114 is at the western boundary of the DU Impact Area, sub-basin 117 is near the western boundary of JPG, and sub-basin 122 is the first sub-basin west of JPG. Flow down Middle Fork Creek is shown for sub-basin 1 through sub-basin 21, the last sub-basin before confluence with Big Creek.

Simulated Flow at BC-01 2006-2011

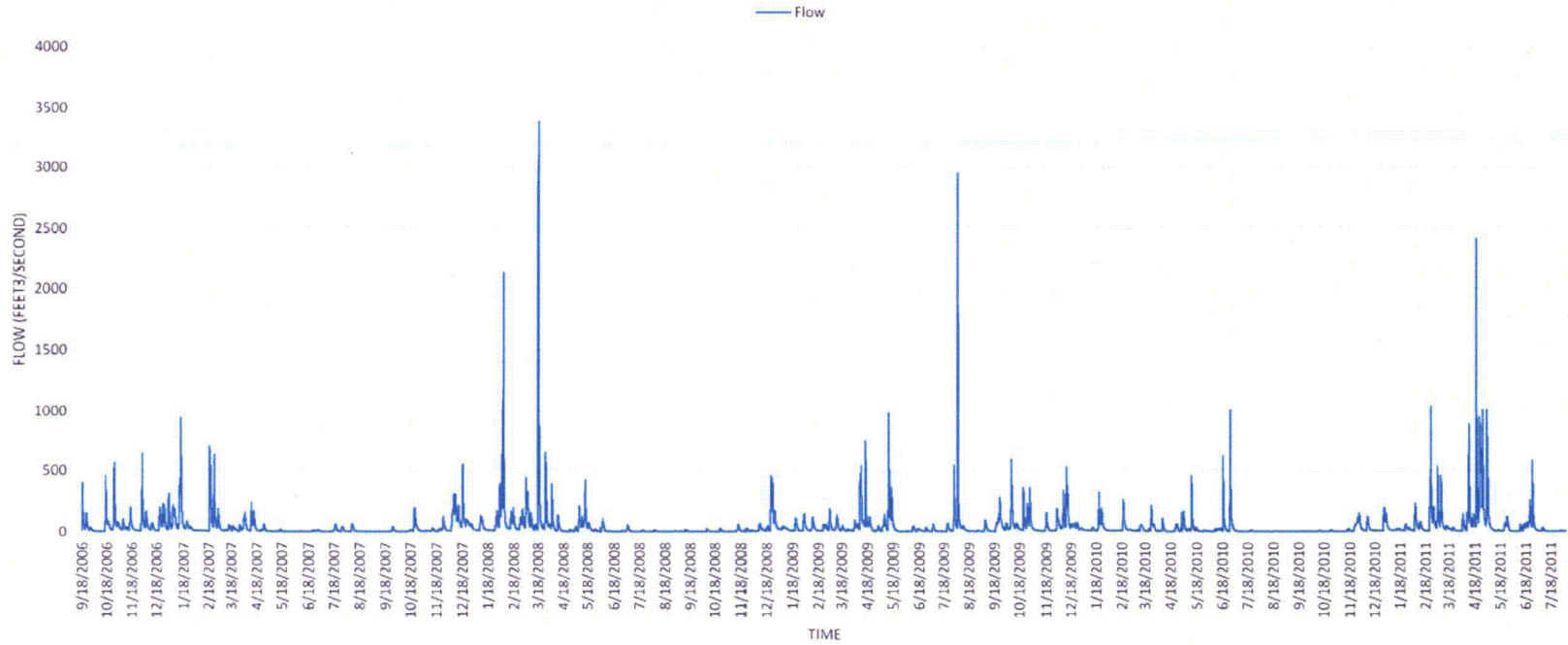


Figure 4-15. Simulated Flow at BC-01 2006-2011

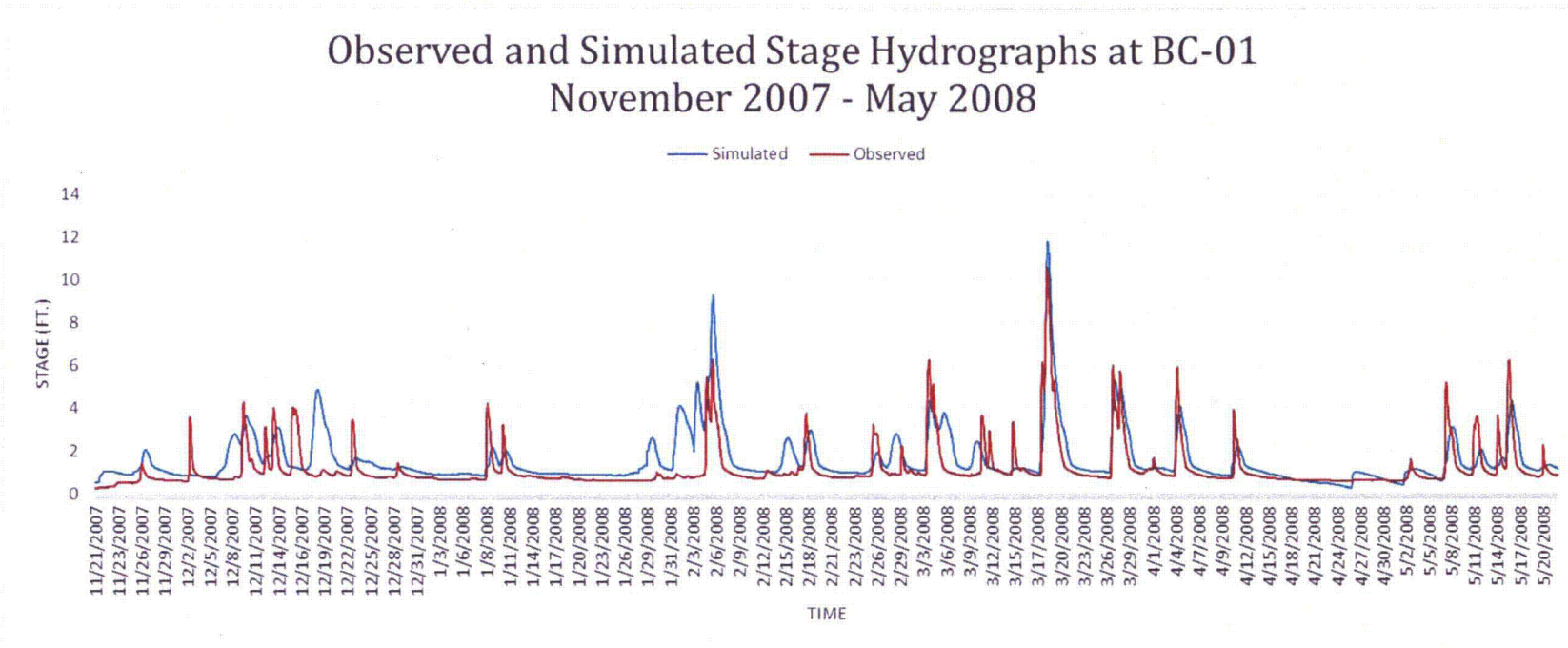


Figure 4-16. Observed and Simulated Stage Hydrographs at BC-01 November 2007 Through May 2008

**Table 4-8. Simulated Flow for Calendar Years 2007-2010
Jefferson Proving Ground, Madison, Indiana**

Annual Precipitation (in)			2007	2008	2009	2010
			45.5	51.8	58.4	36.6
Basin Name	Sub-Basin	Area (ac)	Total Flow Volume (ac ft)			
			2007	2008	2009	2010
Big Creek	110	13,873	24,790	33,750	36,100	15,440
Big Creek	114	14,938	25,970	35,360	37,780	16,130
Big Creek	117	16,462	29,270	39,910	42,670	18,170
Big Creek	122	22,897	40,290	55,280	59,140	25,070
Big Creek	128	34,060	61,510	83,530	89,370	38,480
Basin Name	Sub-Basin	Area (ac)	Total Flow Volume (ac ft)			
			2007	2008	2009	2010
Middle Fork	1	1,093	1,811	2,540	2,729	1,115
Middle Fork	2	1,254	2,083	2,923	3,139	1,322
Middle Fork	5	1,989	3,292	4,622	4,965	2,091
Middle Fork	8	3,258	5,359	7,518	8,083	3,403
Middle Fork	15	6,656	11,190	15,590	16,740	7,099
Middle Fork	21	10,886	19,050	26,211	28,150	12,130
Total		44,946	80,560	109,741	117,520	50,610
Big Creek % of Total		76	76	76	76	76
Middle Fork % of Total		24	24	24	24	24

4.9 SENSITIVITY ANALYSIS

Simulations were performed to assess sensitivity of results (flow budgets and hydrograph shape) to various parameters. One of these parameters was changed at a time (other parameters retained base case calibrated values) and its impact on the overland flow and stream flow characteristics was assessed.

4.9.1 Critical Flow Parameters

Sensitivity of the model results to several critical flow parameters was investigated. Critical flow parameters are those parameters having the biggest influence on predicted surface water runoff. The parameters assessed were:

- INFILT is the infiltration capacity index of the soil (in/hr)
- INFILD is the ratio between the maximum and mean infiltration capacities over the PERLND
- INFEXP is the exponent in the infiltration equation
- IRC is the interflow recession parameter; under zero inflow, this is the ratio of interflow outflow rate today/rate yesterday
- AGWRC is the basic groundwater recession rate (rate of flow today/rate yesterday)
- LZSN is the lower zone nominal storage (inches)
- UZSN is the upper zone nominal storage (inches).

The adjusted variables and their base case values are provided in Table 4-9.

**Table 4-9. Flow Parameters Adjusted During Sensitivity Evaluation
Jefferson Proving Ground, Madison, Indiana**

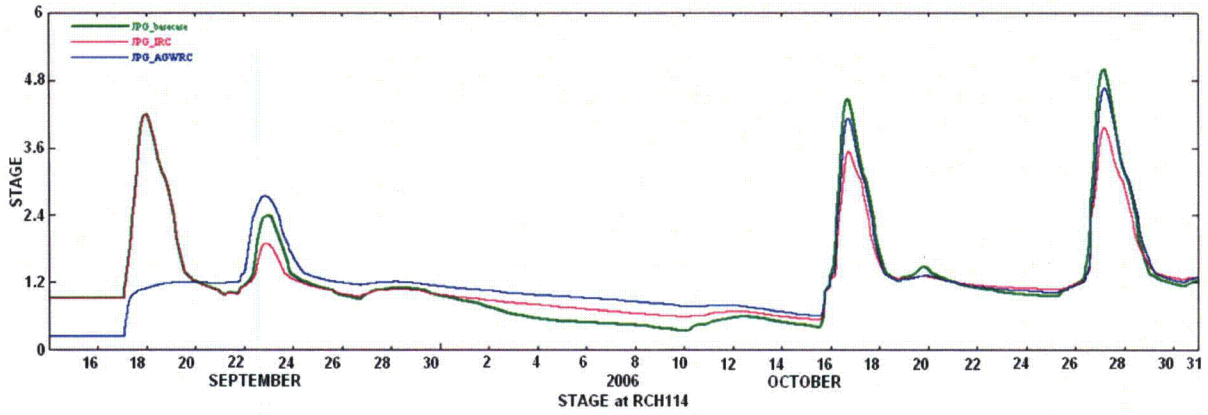
Variable	Perturbed Values	Base Case Values
INFILT (in/hr)	0.03	0.015
INFEXP (-)	4.50	3.00
INFILD (-)	2.00	1.50
IRC (-)	0.90	0.03
AGWRC (-)	0.90	0.10
LZSN range (in)	2.5-4	5-8
UZSN (in)	0.05-1.0	0.1-2.0

The annual water budget components for various sensitivity simulations were compared for HY2007 (1 October 2006 to 30 September 2007) and they are shown in Table 4-10. The annual evapotranspiration (SAET) was not sensitive to parameters assessed in the sensitivity analysis discussed here. Individual components of the runoff (SURO, IFWO, and AGWO) were sensitive (responded actively) to parameter adjustments (Table 4-10). However, the total runoff (SURO + IFWO + AGWO) is relatively insensitive to these changes.

**Table 4-10. Annual Water Budget Components (Inches) for Sensitivity Simulations – HY2007
Jefferson Proving Ground, Madison, Indiana**

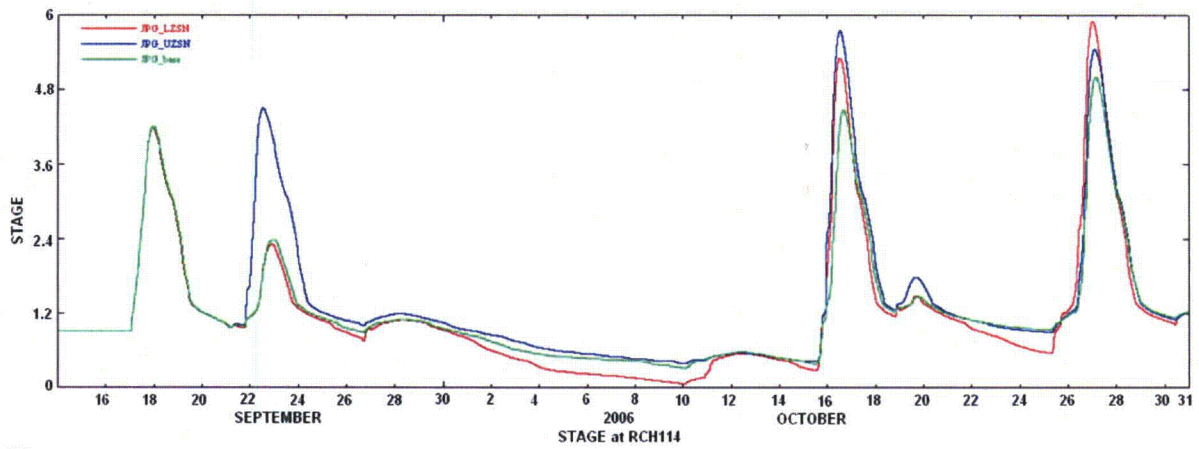
Variable	SURO (Overland Flow)	IFWO (Interflow)	AGWO (Baseflow)	Total Runoff (SURO+IFWO+ AGWO)	SAET (Evapotranspiration)
Base Case	8.5	8.02	6.75	23.27	26.2
INFILT	5.07	8.86	9.16	23.09	26.2
INFEXP	10.2	6.77	6.41	23.38	26.2
INFILD	8.9	7.53	6.80	23.23	26.2
IRC	8.49	8.09	6.75	23.33	26.2
AGWRC	8.52	8.03	6.76	23.31	26.3
LZSN	16.0	7.15	2.64	25.79	25.9
UZSN	9.63	9.36	5.77	24.76	25.6

Figures 4-17 and 4-18 show the impact of changes in IRC, AGWRC, LZSN, and UZSN on the stage at BC-01 during the September to October 2006 period. Note the 2-month period was selected to permit illustration of the effect on the hydrograph for discrete storm events. The impact of INFILT, INFEXP, and INFILD on the shape of runoff hydrograph was relatively small.



IRC: interflow recession parameter
 AGWRC: groundwater recession rate

Figure 4-17. Sensitivity of Stage (BC-01) to Changes in IRC and AGWRC



LZSN: lower zone nominal storage (inches)
 UZSN: upper zone nominal storage (inches)

Figure 4-18. Sensitivity of Stage (BC-01) to Changes in LZSN and UZSN

THIS PAGE WAS INTENTIONALLY LEFT BLANK

5. SEDIMENT TRANSPORT CALIBRATION

As noted in Section 3.2.2.2, HSPF uses the SEDMNT module to simulate the production and removal of sediment from pervious land segments. The module SOLIDS is used to model the removal of sediment from impervious land segments. Sediment transport within reaches is simulated using the SEDTRN module. Very limited data exist for sediment transport calibration. The available data consist of point measurements of total suspended sediment (TSS) in nearby Brush Creek and Vernon Fork (Section 2.2.6) with concurrent flow information. Both creeks are similar to Big Creek and Middle Fork Creek. Therefore, sediment transport calibration efforts consist of developing modeled suspended sediment loads in Big Creek and Middle Fork Creek that are similar in magnitude to those measured at Brush Creek and Vernon Fork.

5.1 OVERLAND SEDIMENT TRANSPORT

The parameter values used to calibrate overland sediment transport in pervious and impervious land use segments are provided in this section. Soil particle size (texture) data are important to overland sediment transport and are presented in Section 2.2.2. The average sand, silt, and clay mass fractions of collected soil samples were 0.205 ± 0.118 , 0.490 ± 0.075 , and 0.305 ± 0.105 , respectively. More energy is required to mobilize and transport coarser (sands) mass fractions than finer (silt and clay) mass fractions.

Overland sediment transport may begin by sediment detachment from the soil matrix initiated by the impact of a raindrop (Figure 2-2) and can be expressed as a power function of the rainfall intensity by an intercept (KRER) and exponent (JRER). The attachment (deposition) of detached particles occurs only on days when there is no rainfall. The rate of attachment (deposition) is specified by parameter AFFIX, and the surface sediment storage mass is diminished by multiplying with $1.0 - \text{AFFIX}$, representing a first-order reduction rate of the detached soil mass available in the surface storage. The detachment of soil particles by rain can be significantly affected by the availability of surface cover (COVER, fraction). HSPF also supports soil management practices through a specified erosion reduction factor. The parameters used in the calibrated base case model are listed in Table 5-1.

**Table 5-1. Pervious Overland Sediment Transport Parameters – PERLND:SED-PARM2
Jefferson Proving Ground, Madison, Indiana**

Land Use	KRER	JRER	AFFIX (1/d)	SMPF	Average COVER (%)
Grass	0.07	2	0.01	0.5	0.70
Bare Soil	0.35	2	0.03	1	0.10
Forest	0.07	2	0.01	0.4	0.95
Farm/New Growth	0.35	2	0.03	0.7	0.652
Water	0.07	2	0.01	1	0.10

*The COVER parameter was changed monthly for each land use – a range of 0.10 (water) to 0.95 (forest) was used.

Soil particles are transported by overland flow downstream toward the closest intercepting reach or stream segment (Figure 5-1); soil particles also can deposit within the sub-basin before reaching the stream segment. The transport capacity (expressed as an exponential power function; the intercept KSER and an exponent JSER are the required inputs) of the overland flow is estimated and compared to the amount of detached sediment mass available. When transport capacity exceeds the detached sediment, overland flow will wash off all of the detached sediment, otherwise the sediment transported will be limited to the transport capacity, and the excess detached soil will remain within the sub-basin. The parameters (KSER, JSER) lump effects of slope, overland flow length, particle size, and surface roughness. The parameters for the calibrated base case model are listed in Table 5-2.

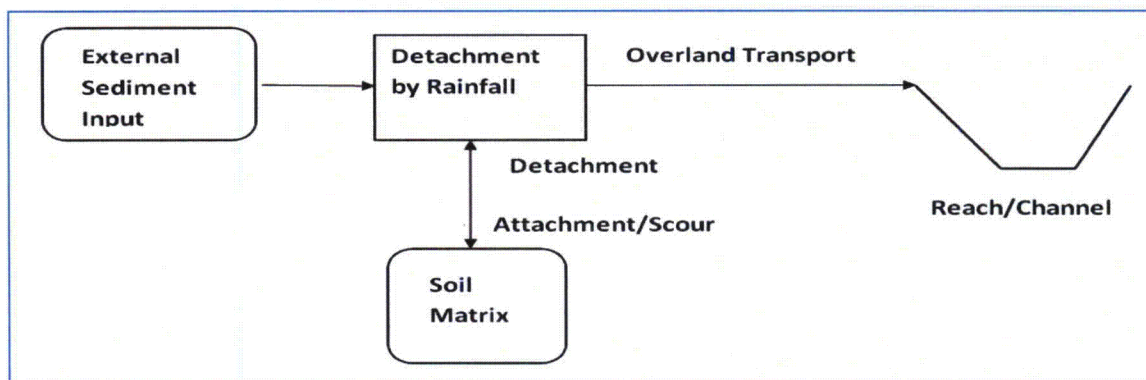


Figure 5-1. Sediment Detachment and Overland Sediment Transport (USEPA 2001b)

Table 5-2. Pervious Overland Sediment Transport Parameters – PERLND:SED-PARM3 Jefferson Proving Ground, Madison, Indiana

Land Use	KSER	JSER	KGER	JGER
Grass	0.25	2.5	0	1
Bare Soil	1.50	2.5	0.001	1
Forest	0.25	2.5	0	1
Farm/New Growth	1.50	2.5	0.001	1
Water	0.25	2.5	0.001	1

The scouring of the matrix soil includes sediment pickup (scour) from the surface and its transport, and both processes are lumped into a single exponential power function expressed as an intercept (KGER) and exponent (JGER); both are the required inputs parameters to HSPF. The scour processes are only invoked when gully erosion-like conditions are involved. The sediment transport associated with the wash-off phase described earlier is primarily of sheet and rill type erosion. The parameters used in the calibrated base case model are listed in Table 5-2.

Similar to transport over pervious (permeable) soils, soil particles are transported on impervious land segments by the overland flow downstream toward the closest intercepting reach or stream segment; soil particles also may deposit within the sub-basin before reaching the stream segment. The transport capacity (expressed as an exponential power function, parameters with an intercept KEIM and an exponent JEIM are the required inputs) of the overland flow is estimated and compared to the amount of sediment mass available within the surface storage. If transport capacity exceeds the detached sediment mass within the storage, overland flow will wash off all of the sediment, otherwise the sediment transported will be limited to the transport capacity and the excess sediment load will remain within the sub-basin.

Within HSPF, the IMPLND:SLD-PARM1 table (refer to HSPF User's Guide) includes the flag to activate overland sediment transport. The IMPLND:SLD-PARM2 table contains parameters to define wash-off (KEIM and JEIM noted above), sediment deposition (ACCSDP, tons/ac-day), and the fraction of solids removed (REMSDP, 1/day). The parameters used for the calibrated base case model are listed in Table 5-3.

Parameters in Tables 5-1 through 5-3 were adjusted to ensure that the accumulated sediment on the land surface was not continually increasing or decreasing; final parameter values are shown in each table.

**Table 5-3. Parameters Used in Impervious Overland Sediment Transport – IMPLND:SLD-PARM2
Jefferson Proving Ground, Madison, Indiana**

Land Use	KEIM	JEIM	ACCSDP	REMSDP
Grass	0.03	2	0.0005	0.02
Bare Soil	0.15	2	0.0005	0.02
Forest	0.03	2	0.0005	0.02
Farm/New Growth	0.15	2	0.0005	0.02
ROAD	0.05	2	0.0005	0.02

5.2 IN-STREAM SEDIMENT TRANSPORT

Soil mass entering intercepting reaches from various sub-basins are transported through a network of conduits (streams). During this process, different size soil particles could remain in suspension, deposit on the channel bed, and/or re-suspend (scour) and be transported downstream through the channel network (see Figure 5-2).

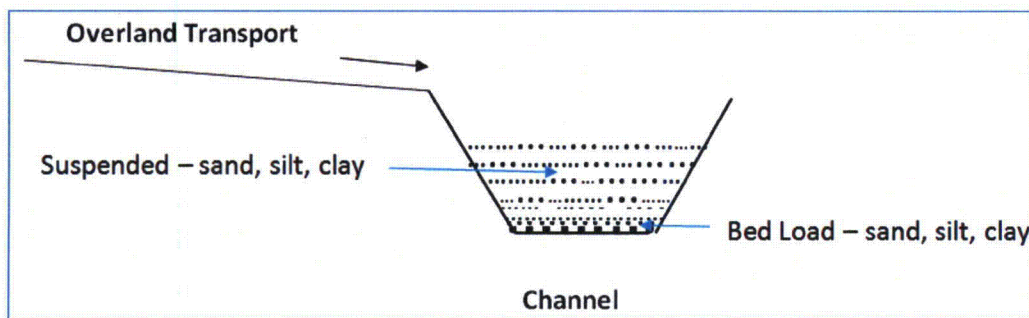


Figure 5-2. In-Stream Suspended and Bed Load Sediment Fractions (USEPA 2001b)

In-stream sediment transport assumptions include suspended sediment is uniformly dispersed throughout the water column in the channel, completely entrained by the flow, and transported (convective transport of all three fractions – sand, silt, and clay) at the same horizontal velocity as the water. HSPF does not model the horizontal movement of bed sediments. HSPF further assumes:

- Scour and deposition do not affect the hydraulic behavior of the channel
- Sand, silt, and clay fractions deposit in different sections of the bed, and there are no sediment mass transfer/exchanges between these areas.

To initiate this procedure, the eroded material is partitioned into sand, silt, and clay fractions prior to entering a model reach. The average sand, silt, and clay fractions entering the channel network were determined from the particle size analysis completed for 32 sediment samples (estimated at 0.205, 0.49, and 0.305, respectively). The approach used assumes these fractions are equal to those determined for the samples collected from various sub-basins. This assumption should be valid under most conditions. However, for some individual storms, a larger fraction of fine material (silt, clay) and less coarse material (sand) could be transported to streams as some of the coarse parent material is likely to settle out within the sub-basins during overland transport (sand particles are more likely to be deposited in the overland flow plane, in swales, ditches, and natural depressions relative to the finer silt and clay).

The transport and retention (adsorption) characteristics of eroded soil particles vary significantly with the particle size. Therefore, HSPF divides the sediment load into three components (sand, silt, and clay), and requires distinct properties for each fraction.

5.2.1 In-Stream Sand Fraction Transport Parameters

HSPF offers three methods to simulate transport of sand (noncohesive) particles: the Toffaleti, Colby, and Power Function methods. The Power Function method is the most widely used and was selected for this investigation.

The transport, deposition, and scour of the sand fraction are estimated based on the sediment carrying capacity of the flow in a channel. The transport capacity of a channel is expressed as an exponential function: $KSAND \times (\text{average velocity})^{EXPSND}$. The intercept $KSAND$ and the exponent $EXPSND$ are the required inputs. The sediment transport load is compared with the channel transport capacity; the transport, deposition, and scour are estimated as follows:

- If the amount of sand transported is less than the carrying capacity of flow, sand will be scoured from the channel bed until the amount of sand transported equals the carrying capacity or until all of the available bed sand is scoured
- If the amount of sand transported exceeds the carrying capacity of flow, sand deposition occurs.

The parameters used for the calibrated base case model are presented in Table 5-4. The sand particle density and settling velocities were assumed equal to 2.65 grams per cubic centimeter (g/cm^3), and 0.4 inch per second (in/sec), respectively.

**Table 5-4. Parameters Used for In-Stream Sand Fraction Transport
Jefferson Proving Ground, Madison, Indiana**

Reach #	KSAND	EXPSND
1-21	0.06	1.20
100	0.10	1.60
101	0.20	1.70
102	0.90	2.40
103	4.00	0.40
104	0.70	2.20
105	0.10	1.60
106	0.30	1.90
107	0.04	1.10
108	0.70	2.20
109-110	0.04	1.10
111	0.10	1.60
112	0.20	1.70
113	0.04	1.10
114	0.035	1.05
115-116	0.04	1.10
117	0.20	1.70
118-121	0.04	1.10
122	0.70	2.20
123	1.10	2.60
124	0.04	1.10
125	0.35	1.90
126	0.30	1.80
127	0.04	1.10
128	0.50	2.10
129	0.15	1.49
200-202	0.05	1.10
300	0.20	1.70
301-302	0.05	1.10

5.2.2 Silt and Clay Fraction Transport Parameters

For silt and clay fraction in-stream transport, the mass (sediment) transfer between the suspended and the bed cohesive material is dependent upon the shear stresses being exerted upon the bed surface. Therefore, the transport, detachment (scour), and attachment (deposition) of the silt and clay fractions are controlled by the shear stress distribution within various reaches. In a typical system, sediments should deposit on the channel bed during low flows and detach (scour) and transport during the high-flow conditions. During average flow conditions, most of the sediment influx is transported through the channel without significant scour and deposition. The parameters selected for various reaches ensure that there are no persistent sediment depositions and/or scours within the reach network. HSPF can output the prevailing shear stress (defined as the bed slope \times specific weight of water \times hydraulic radius) time series to identify the deposition and scour conditions within various streams.

If simulated bed shear stress (TAU) is less than the critical shear stress for deposition (TAUCD), deposition of cohesive material occurs. If TAU is greater than the critical shear stress for scour (TAUCS), scour of cohesive material occurs. If the shear stress falls between the critical scour and deposition values, the incoming suspended material is transported through the reach without deposition.

Ftables play a critical role in these computations. Using the simulated hydraulic radius (based on simulated discharge), HSPF uses information in these look-up tables to determine the shear stress distribution within the corresponding channel. In cases where simulated bed shear stresses appeared unreasonable, the channel cross-section configuration, bed slopes, and Manning's roughness coefficient were checked for accuracy and adjusted to improve results during model calibration. Shear stresses (TAUCD and TAUCS) were adjusted for various reaches to ensure no persistent deposition and/or scour in the corresponding channel. Generally, TAUCS values are greater than TAUCD, and the values of both parameters for silt are greater than or equal to those for clay. During high-flow periods, the amount of scour is adjusted with an erodibility factor for silt and clay. During low-flow periods, the silt and clay fall velocity parameter can be adjusted to improve the agreement. TAUCD and TAUCS for silt and clay fractions were adjusted so that the model calculates scour during high-flow events, deposition and settling during low-flow periods, and transport with neither scour nor settling for moderate flow rates.

For the calibrated base case model, the particle density (g/cm^3), particle diameter (inches), and settling velocities (in/sec), and the erodibility coefficient ($\text{lb/ft}^2 \cdot \text{d}$) were assumed equal to 2.65, 0.0004, 0.0004, and 0.01, respectively. The critical shear stress parameters (TAUCD and TAUCS) for silt and clay fractions for various reaches are reported in Tables 5-5 and 5-6, respectively.

Channel velocity is the driver for transport of the noncohesive (sand) fraction and is indirectly related to the shear stress (function of slope, hydraulic radius) that controls the transport behavior of cohesive fractions (silt and clay). Therefore, the cohesive (sand) and noncohesive (silt and clay) materials are expected to show different responses to changes in the flow conditions in the reach.

5.3 SEDIMENT TRANSPORT CALIBRATION

A qualitative sediment transport calibration was completed using the suspended sediment versus flow rate and/or channel velocities observed at the Brush Creek and Vernon Fork (of Muscatatuck River) as calibration targets. The data reported for Brush Creek and Vernon Fork were collected at discreet points in time and, therefore, should be used carefully. Following a precipitation event, actual and simulated suspended sediment and stream flow vary continuously over a wide range as the runoff travels through the stream network to an outlet. Differences in land cover, frequency, and intensity of precipitation events also will affect the suspended sediment load. Sediment transport input parameters were adjusted to ensure modeled suspended sediment values were similar (in the same range or lower) to the point measurements at Brush Creek and Vernon Fork.

**Table 5-5. Silt Fraction Transport Parameters
Jefferson Proving Ground, Madison, Indiana**

Reach #	TAUCD (lb/ft ²)	TAUCS (lb/ft ²)
1-7	0.25	0.400
8	0.20	0.400
9-14	0.25	0.400
15	0.10	0.25
16	0.25	0.40
17	0.10	0.25
18-21	0.25	0.400
100	0.15	0.25
101	0.05	0.15
102	0.025	0.06
103	0.05	0.12
104	0.10	0.30
105	0.15	0.25
106	0.05	0.15
107	0.35	0.50
108	0.10	0.20
109	0.35	0.50
110-111	0.15	0.30
112	0.1	0.25
113-116	0.35	0.50
117	0.05	0.15
118-121	0.35	0.50
122	0.10	0.20
123	0.10	0.30
124	0.35	0.50
125	0.20	0.35
126	0.25	0.45
127	0.30	0.50
128	0.15	0.30
129	0.30	2.25
200-202	0.35	0.50
300	0.07	0.20
301	0.10	0.20
302	0.20	0.35

**Table 5-6. Clay Fraction Transport Parameters
Jefferson Proving Ground, Madison, Indiana**

Reach #	TAUCD (lb/ft ²)	TAUCS (lb/ft ²)
1-14	0.20	0.400
15	0.10	0.25
16	0.20	0.40
17	0.10	0.25
18-20	0.20	0.40
21	0.25	0.40
100	0.15	0.25
101	0.05	0.15
102	0.025	0.06
103	0.05	0.12

**Table 5-6. Clay Fraction Transport Parameters
Jefferson Proving Ground, Madison, Indiana (Continued)**

Reach #	TAUCD (lb/ft ²)	TAUCS (lb/ft ²)
104	0.10	0.30
105	0.15	0.25
106	0.05	0.15
107	0.30	0.50
108	0.10	0.20
109	0.30	0.50
110-111	0.15	0.30
112	0.1	0.25
113	0.30	0.50
114	0.35	0.50
115-116	0.30	0.50
117	0.05	0.15
118-121	0.30	0.50
122	0.10	0.20
123	0.10	0.30
124	0.30	0.50
125	0.20	0.35
126	0.25	0.45
127	0.30	0.50
128	0.15	0.30
129	0.30	2.25
200-202	0.30	0.50
300	0.07	0.20
301	0.10	0.20
302	0.20	0.35

Figure 5-3 illustrates the modeled stage versus the TSS concentrations in milligrams of sediment per liter of water in sub-basin 114. Recall sub-basin 114 is on Big Creek at the western boundary of the DU Impact Area at the location of gauging station BC-01 (refer to Figure 3-1 for locations of the sub-basins). The maximum modeled TSS is 1,300 mg/L in sub-basin 114 on Big Creek, which is roughly half of the maximum TSS in the data from Brush Creek. Most of the modeled TSS is less than 200 mg/L, similar to the data from Brush Creek and Vernon Fork under lower flow conditions. Figure 5-4 illustrates the modeled TSS on sub-basins 21 (RCH21) and 114 (RCH114). Sub-basin 21 is on Middle Fork Creek west of JPG and is the last sub-basin prior to confluence with Big Creek. Modeled TSS results in Middle Fork Creek are generally less than those in Big Creek because Big Creek drains a larger area and also contains substantial farm land upstream (east) of JPG. Middle Fork Creek originates on the former JPG where land cover is predominantly forested or grass land, which has lower sediment runoff than farmland.

5.4 MODELED SEDIMENT LOAD BY LAND USE

The calibrated model provides the sediment load generated by different land uses. Land use categories in the model consist of grass, bare soil, forest, farm, water (consisting of wetlands and surface water bodies), and roads. The majority of the modeled area land use (more than 97 percent) consists of grass, bare soil, forest, or farm land uses; of these, forest land use is most widespread, covering 55 percent of the model area, including nearly all of the former Proving Ground. The predicted annual sediment load generated from different land use categories is summarized in Table 5-7; note that roads and water land use are not shown as both cover a small area of the model and generate negligible sediment load. Bare soil generated the highest sediment load, on average 2.28 tons per acre-year over the period 2007 to 2010. Forested land generated the lowest sediment load, on average 0.02 tons per acre-year for the same period.

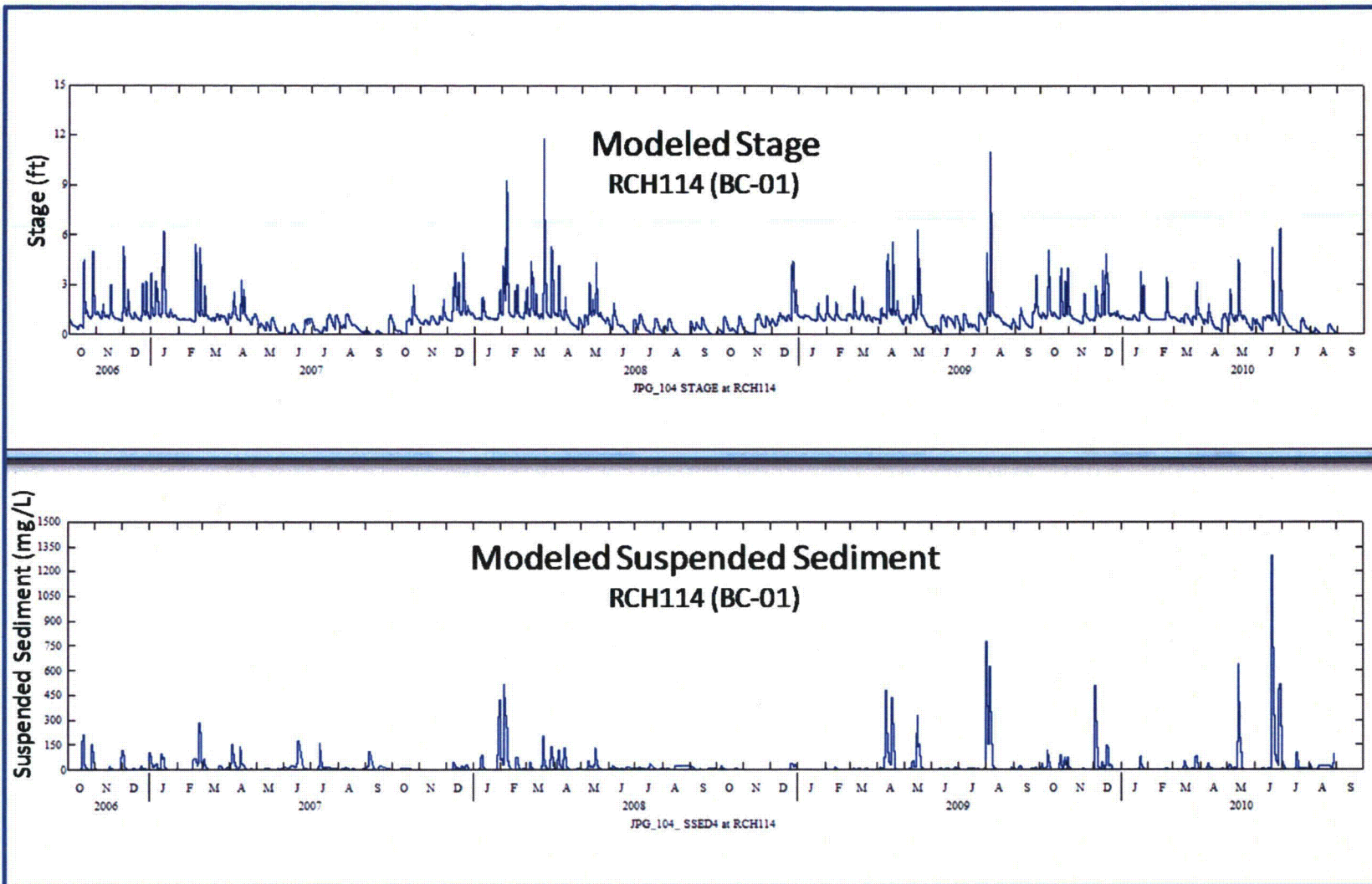


Figure 5-3. Modeled Stage and Suspended Sediment on Big Creek at Gauging Station BC-01 (RCH114)

Simulated Total Suspended Sediment for Sub-Basins #21 and #114

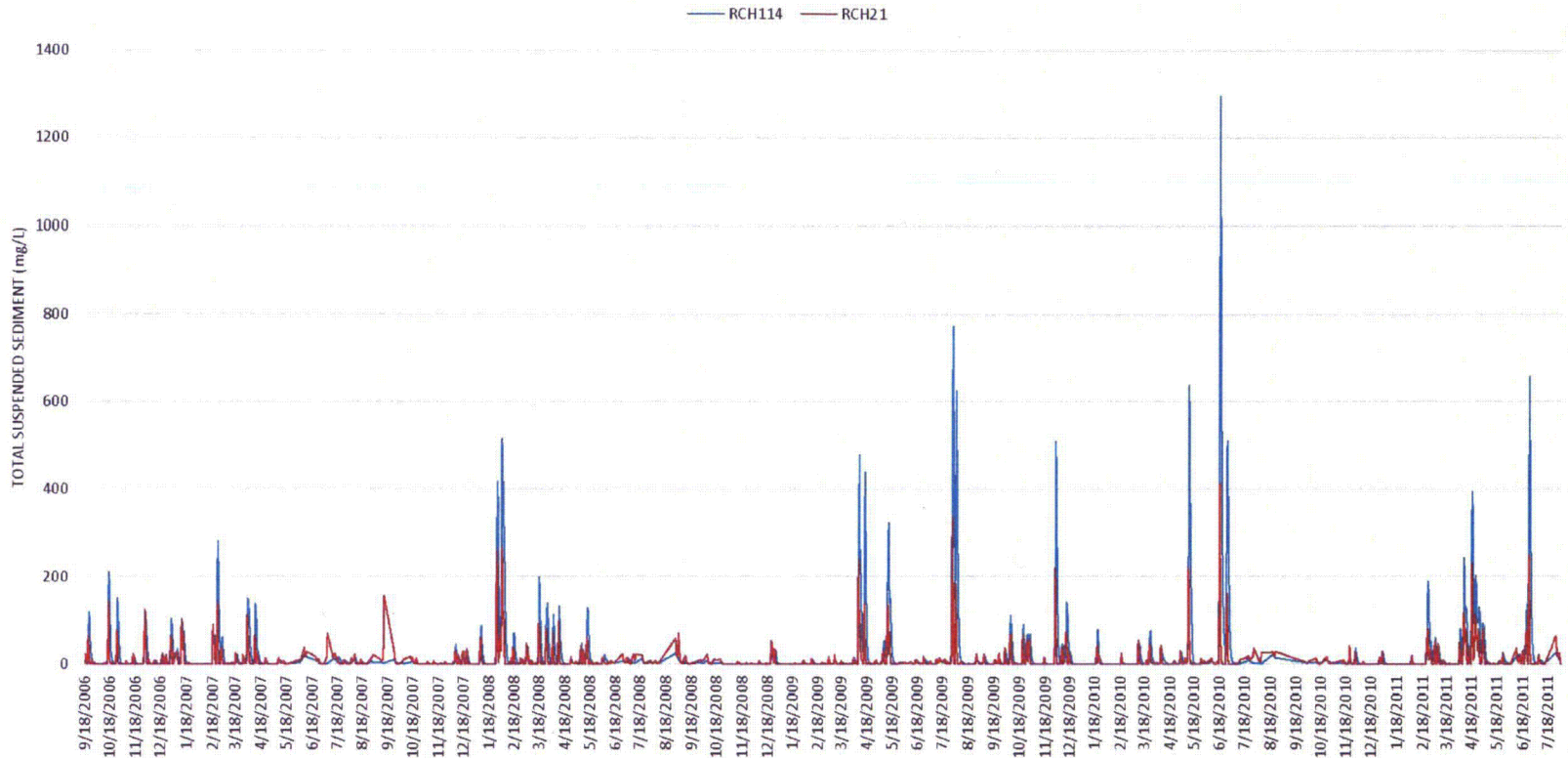


Figure 5-4. Simulated Total Suspended Sediment for Sub-Basins 21 and 114

**Table 5-7. Annual (Calendar Year) Sediment Yield by Land Use (Tons per Acre)
Jefferson Proving Ground, Madison, Indiana**

Land Use	Grass	Bare Soil	Forest	Farm
PERLND	P101	P102	P103	P104
2007	0.067	0.525	0.042	0.277
2008	0.117	2.360	0.017	0.806
2009	0.179	3.860	0.023	1.060
2010	0.088	2.380	0.012	0.492
Average	0.11	2.28	0.02	0.66

Farm land and bare soil land uses cover a smaller area (28 percent) but generate much more sediment load per acre. The net effect is a high sediment load coming onto JPG from offsite areas to the east, mixing with the relatively small sediment load on JPG; west of JPG, the sediment load increases due to greater areas under farming (includes bare soils plus farm land and less forested area).

5.5 SENSITIVITY TO CRITICAL PARAMETERS

Simulations were performed to assess sensitivity of sediment transport results to various parameters. Normally one parameter (and sometimes a few parameters as a group) was changed at a time and the impact on the overland and in-stream sediment transport characteristics was assessed. The following parameters were changed and their impacts are analyzed and summarized below.

5.5.1 Overland Sediment Transport Parameters

Overland sediment transport from various sub-basins to respective reaches was highly sensitive to KRER and JRER (see Section 5.1 for definition). The sediment load increased with an increase in KRER, and it decreased with an increase in JRER. Table 5-8 illustrates the sensitivity in sediment yield from the base case calibrated model for JRER (one half calibrated value) and KRER (twice calibrated value) for the HY2006 to HY2009. Decreasing JRER by a factor of two increased the average sediment yield by a factor of 1.4 (bare soil) to 2.5 (grass). Increasing KRER by a factor of 2 had a similar but somewhat less impact on sediment yield with increased yield ranging from a factor of 1.3 (forest) to 1.8 (both grass and farm land uses). The sediment transport was significantly less sensitive to the changes in KSER and JSER. The sediment load decreased only slightly when AFFIX (Section 5.1) was increased five times.

5.5.2 In-Stream Transport Parameters

The sediment transport in various reaches (in-stream) was investigated for sensitivity to various parameters. Sand fraction transport was highly sensitive to the transport capacity parameters KSAND and EXPSND (see Section 5.2.1 for definition). An increase in these parameters significantly increased the transport capacity of the flow enhancing scour in respective channels. Results also were sensitive to TAUCD and TAUCS (Section 5.2.2), significantly impacting the silt and clay deposition and scour tendencies in the channel network. An increase in TAUCD increased the deposition while an increase in TAUCS decreased the scour tendencies in respective channel.

**Table 5-8. Sediment Yield Sensitivity to JRER and KRER (Tons per Acre)
Jefferson Proving Ground, Madison, Indiana**

A. Calibrated base case (hydrologic year)				
Land Use PERLND	Grass P101	Bare Soil P102	Forest P103	Farm P104
2006	0.102	0.761	0.0537	0.471
2007	0.117	2.36	0.0158	0.808
2008	0.142	3.56	0.0207	0.808
2009	0.127	2.69	0.0165	0.760
Average	0.12	2.34	0.03	0.71
B. Scenario: JRER half of base case (hydrologic year)				
Land Use PERLND	Grass P101	Bare Soil P102	Forest P103	Farm P104
2006	0.126	0.761	0.0789	0.69
2007	0.366	4.34	0.053	2.19
2008	0.383	5.5	0.0551	1.74
2009	0.311	2.95	0.0545	1.53
Average	0.30	3.39	0.06	1.54
C. Scenario: KRER twice base case (hydrologic year)				
Land Use PERLND	Grass P101	Bare Soil P102	Forest P103	Farm P104
2006	0.126	0.761	0.0592	0.601
2007	0.228	4.07	0.0314	1.51
2008	0.283	5.5	0.0396	1.57
2009	0.239	2.95	0.0337	1.36
Average	0.22	3.32	0.04	1.26

THIS PAGE WAS INTENTIONALLY LEFT BLANK

6. DU FATE AND TRANSPORT

Surface runoff of DU dissolved in surface water or adsorbed to soil particles (primarily silt and clay) to streams and migrations of DU within streams (either dissolved or adsorbed) represents the primary transport pathway for DU transport. As noted previously (Section 2.1.5), transport of DU fragments is believed unlikely due to the high density and size of the fragments and is supported by a literature review of field studies pertaining to DU oxidation and environmental fate (Parkhurst et al. 2012). Transport of smaller fragments from corrosion products may occur, as these particles are smaller and less dense. However, uranyl species dominate in oxidizing environments (such as surface water, sediment, and near surface soils) and, as such, the corrosion products are more susceptible to dissolution and are likely to break down further and transport in solution or be adsorbed to sediments (Kaiser-Hill, 2002; Parkhurst et al. 2012). Analysis of groundwater, surface water, and sediments shows little to no physical DU transport outside the DU Impact Area over the past 25 years. Land use within the DU Impact Area is primarily forested, which also will limit the amount of sediment (including DU fragments or fragments of corrosion products) runoff following precipitation events.

The calibrated flow model provides the basis (the modeled surface water and sediment runoff to streams and then within streams) for the DU fate and transport modeling. The location of DU within the model, the rate of DU release, dissolution of DU in water, and sorption to soil and sediment particles govern DU transport within the calibrated flow model.

6.1 SOURCE TERM EVALUATION

The source term, as defined here, represents the rate of DU mass released over time for transport via the surface water pathway. The source term depends on the location of the DU penetrators and the processes that affect the weathering (corrosion and dissolution) of penetrators.

In most geologic formations, +4 (IV), and +6 (VI) are the most important oxidation states of uranium present. Uranium (VI) and (IV) species dominate in oxidizing and reducing environments, respectively. Uranium is most mobile in oxidizing environments (uranyl species U(VI)); in reducing environments, U(IV) forms very low solubility precipitates, reducing its concentration and mobility in aqueous solutions (Kaiser-Hill 2002, Parkhurst et al. 2012). Surface waters at JPG are likely well oxygenated. Mottling of near surface, poorly drained soils within the DU Impact Area indicates periodic reducing conditions; reducing conditions also may occur along riparian corridors. Spatial and temporal variations in reducing conditions are not explicitly simulated in the surface water model. The fate and transport of uranium in soil and aqueous environments is largely controlled by its adsorption and desorption to/and from porous media into the dissolved phase. Available research (USEPA 1999) shows that pH and dissolved carbonate concentrations are the two most important factors influencing the adsorption behavior of uranium. Table 6-1 lists processes affecting uranium distribution and mobility in the environment.

DU is created as a byproduct of the uranium enrichment process. Although metallic uranium is essentially immobile, corrosion reactions of DU can yield oxidized products that can dissolve, adsorb to the soil matrix, and complex with natural organic matter (Chen and Yiacoumi, 2002). Geochemical reaction codes and surface complexation models have been used to investigate mobility of uranium within various co-existing media (e.g., soil, surface water, and groundwater) generally at small scales. For large sites such as the JPG surface water model, a feasible approach is to use the K_d , defined as the ratio of adsorbed concentration to aqueous (or dissolved) concentration to represent sorption and dissolution and mobility of DU. The K_d model works fine where concentrations are relatively low (such as at locations away from the DU source) and the geochemical conditions remain fairly constant.

**Table 6-1. Soil and Water Geochemical Processes Affecting Uranium Mobility and Distribution
Jefferson Proving Ground, Madison, Indiana**

Geochemical Factors and Uranium Distribution	
Soil	
1.	Natural uranium in soil and rock U-234 and U-238 in secular equilibrium (identical activities).
2.	Uranyl ion (U^{6+} or UO_2^{2+}) or ligand complexes, listed below, dissolved in water can be reduced to insoluble uranous precipitates by humus and peat in the soil matrix, and once reduced are relatively insoluble and not reversible.
3.	Uranyl ion or complexes in solution readily partition to organic matter; iron and manganese oxides and clays in soil matrix within pH range of 5.0 - 8.5 and is reversible.
4.	Naturally occurring microbes can: 1) speed DU corrosion and once corroded and dissolved in shallow precipitation, 2) promote reduction of uranyl to insoluble uranous bearing minerals uraninite and coffinite.
Water	
1.	In natural waters, U-234 slightly more soluble than U-238 due to natural decay of U-238 to Th234 to Pa234, which are more soluble, so U-234 appears to move while U-238 remains sparingly soluble.
2.	The acidity or pH of waters controls mobility of uranyl ion; UO_2^{2+} complex dominates in oxidizing acidic waters, whereas carbonate complexes dominate in near-neutral and alkaline oxidizing waters. Iron oxide and clay exchange sites decline as pH declines below 5.0.
3.	Alkalinity of pore fluids can limit or inhibit uranyl ion/complex partitioning, having an inverse relationship with K_d values.
4.	ORP: the uranyl ion (U^{6+} , or $U[VI]$; UO_2^{2+}) and weaker uranyl ligands like uranyl carbonate and less so uranyl nitrate, uranyl sulfate, uranyl fluoride and uranyl phosphate are most soluble and therefore mobile in oxidizing waters, with a reduced potential for partitioning, especially where pH is > 5.0 .
5.	ORP: the uranous ion (U^{4+} or $U[IV]$), reduced from the uranyl ion and complexes in the presence of fulvic and humic acids in solution or anaerobic conditions, is essentially insoluble in a reducing environment like a wetland or swamp or oxygen deficient groundwater system, forming precipitates like uraninite or coffinite, that in turn are not very soluble or reversing.
6.	Dissolved organic carbon can complex with both uranous and uranyl, increasing solubility and mobility and reducing partitioning.
7.	Uranyl bound to colloids, complexants, ligands and chelators can undergo facilitated transport, particularly in fracture/conduit flow.

6.1.1 Penetrator Distribution

The distribution of penetrators remaining within the DU Impact Area is uncertain. Penetrators were test fired from 1984 through 1994. During this period, penetrators were recovered twice each year to ensure the total DU mass remained below permitted levels.

Science Applications International Corporation (SAIC) reviewed available literature, conducted field surveys, and developed methodology to estimate the spatial distribution of penetrators remaining within and near the DU Impact Area. An estimated total of 73,500 kg of DU remains unrecovered within the surface modeling domain. The spatial distribution was used to determine DU mass in the surface water model sub-basins, as shown in Figure 6-1. Additional details are provided in Appendix C.

The surface water model domain has 57 sub-basins. DU was estimated to occur in 17 sub-basins with nearly all of the DU mass occurring within the DU Impact Area. Seven of the sub-basins have less than 1 percent of the total mass; 98 percent of the DU mass is located in 10 sub-basins. The mass from sub-basins with less than 1 percent mass was added to the nearest sub-basins, resulting in six Big Creek sub-basins and four Middle Fork Creek sub-basins acting as DU sources within the model (see Table 6-2). Sixty-seven percent of the DU mass lies within Big Creek sub-basins; 33 percent lies within Middle Fork Creek sub-basins.

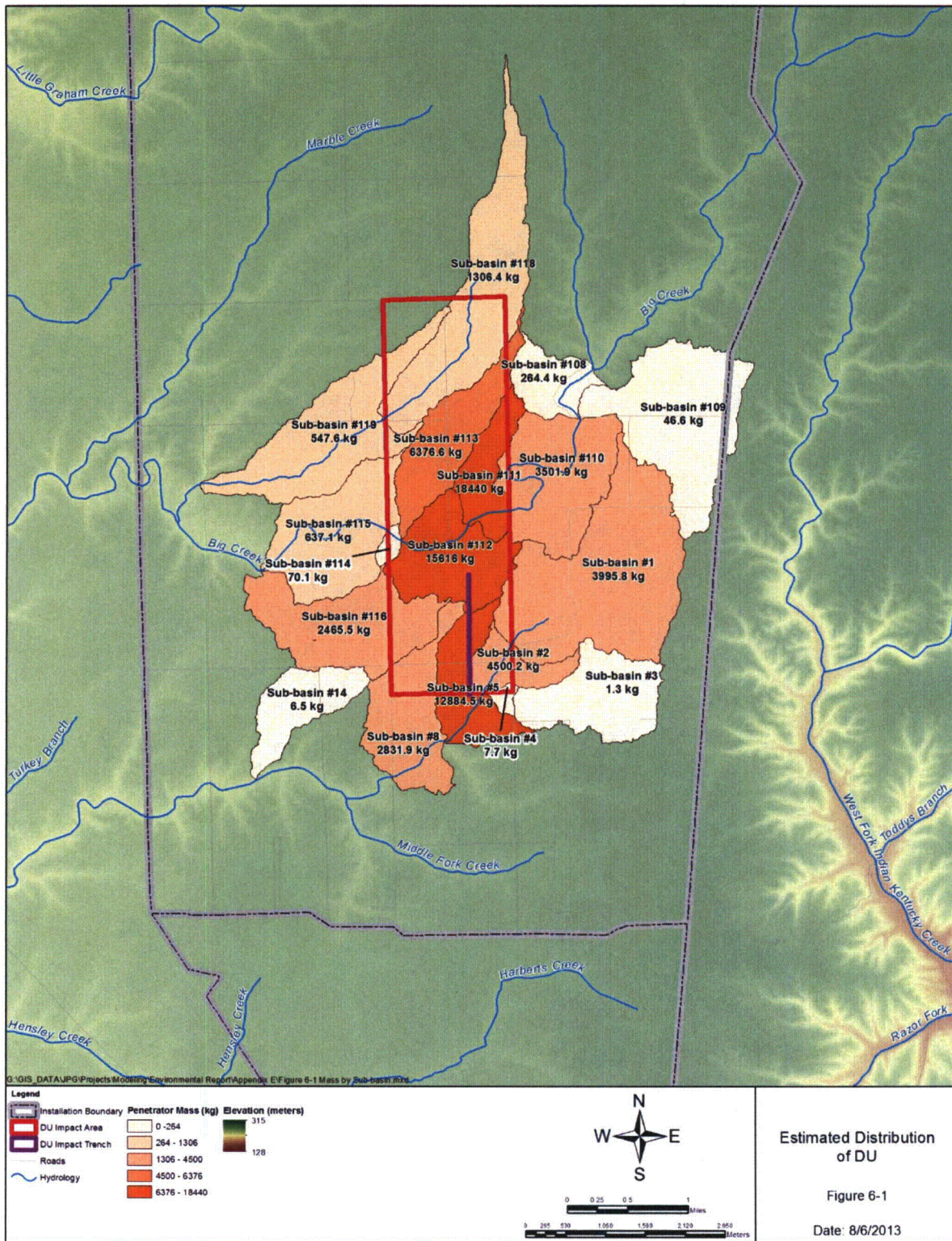


**Table 6-2. DU Mass (kg) Distribution at JPG
Jefferson Proving Ground, Madison, Indiana**

Sub-Basin #	DU Mass (kg)
1 (Middle Fork)	3,988
2 (Middle Fork)	4,491
5 (Middle Fork)	12,867
8 (Middle Fork)	2,843
Total DU Mass (Middle Fork)	24,189
110 (Big Creek)	3,806
111 (Big Creek)	18,400
112 (Big Creek)	15,906
113 (Big Creek)	6,999
116 (Big Creek)	2,461
118 (Big Creek)	1,851
Total DU Mass (Big Creek)	49,423
Total DU Mass JPG	73,612

6.1.2 Laboratory Derived K_d Values

The K_d was measured at JPG to characterize how DU may adsorb to or desorb from site soils during fate and transport (Appendix D). Two basic tests (sorption and desorption) were used to estimate the site-specific K_d for DU. Sorption tests were performed for site soils and glacial till. Rainwater collected at the site was spiked with uranyl nitrate hexahydrate at known concentrations and mixed with representative soils collected from background locations to determine what fraction of uranium would adsorb to the soils. Similarly, groundwater spiked with uranyl nitrate hexahydrate at known concentrations was mixed with glacial till samples to determine uranium sorption to glacial till in the saturated zone. Desorption-dissolution tests consisted of passing rain water collected at the site through impacted soil samples (collected beneath penetrators) to determine the fraction of uranium that could desorb or leach from impacted soils as rain water comes in contact with the soils. Results from the tests are summarized in Table 6-3. In summary, sorption tests showed lowest K_d (lowest fraction of uranium partitioning onto the till) for groundwater in glacial tills. Sorption tests for soils at the surface showed high K_d (uranium strongly sorbed to soils). Desorption-dissolution tests indicated a higher fraction of uranium will partition to rain water in contact with highly impacted soils beneath or near the penetrators.

The laboratory results show a wide range in potential K_d for uranium at JPG, which is consistent with reported K_d in the literature for uranium. Near surface soils are expected to have relatively high K_d s for uranium due to the low alkalinity and acidic soil conditions. Twenty-six soil samples collected at the surface for K_d testing had an average pH of 5.5 and ranged from pH 4.4 to 7.6. Eight soil/glacial till samples collected from depths of 6 to 18 ft had higher alkalinity with an average pH of 8.6 and ranged from pH 7.4 to 10.4.

6.1.3 DU Corrosion and Dissolution Rates

The rate of uranium released from penetrators to the environment is dependent upon the penetrator corrosion rate and the subsequent dissolution of the corrosion products. Uranium metal is unstable when in contact with oxygen and water. The uranium is oxidized, and in the presence of water the oxides are hydrated to form minerals such as schoepite ($UO_3 \cdot nH_2O$), which exists as uranium (VI). As discussed in Appendix G, Updated Conceptual Site Model, the corrosion rate and subsequent dissolution of the corrosion products were estimated from similar studies published in the literature and from laboratory studies on a per penetrator basis.

**Table 6-3. Summary of Sorption Test Results
Jefferson Proving Ground, Madison, Indiana**

Soil Type	Adjusted K_d (mL/g)	
	Individual Test	Average
Desorption/Leaching by Loess Soil Types		429
Avonburg/Cobbsfork	189	
Cincinnati/Rossmoyne	591	
Grayford/Ryker	507	
Groundwater Sorption for Glacial Till		8
Avonburg/Cobbsfork	0.93	
Avonburg/Cobbsfork	1.03	
Avonburg/Cobbsfork	0.96	
Cincinnati/Rossmoyne	11.7	
Cincinnati/Rossmoyne	--	
Grayford/Ryker	16	
Grayford/Ryker	20	
Rainwater Sorption for Loess Soil Types		1,954
Avonburg/Cobbsfork		2,290
Avonburg/Cobbsfork	2,501	
Avonburg/Cobbsfork	2,435	
Avonburg/Cobbsfork	1,646	
Avonburg/Cobbsfork	1,058	
Avonburg/Cobbsfork	3,831	
Avonburg/Cobbsfork	3,132	
Avonburg/Cobbsfork	2,024	
Avonburg/Cobbsfork	1,347	
Avonburg/Cobbsfork	1,610	
Avonburg/Cobbsfork	3,315	
Cincinnati/Rossmoyne		2,363
Cincinnati/Rossmoyne	3,069	
Cincinnati/Rossmoyne	2,234	
Cincinnati/Rossmoyne	4,470	
Cincinnati/Rossmoyne	2,284	
Cincinnati/Rossmoyne	57	
Cincinnati/Rossmoyne	2,436	
Cincinnati/Rossmoyne	2,270	
Cincinnati/Rossmoyne	1,500	
Cincinnati/Rossmoyne	656	
Cincinnati/Rossmoyne	2,347	
Grayford/Ryker		1,208
Grayford/Ryker	1,089	
Grayford/Ryker	1,073	
Grayford/Ryker	1,248	
Grayford/Ryker	1,421	

As shown in Table 6-4, the best estimate of the penetrator corrosion rate is 0.25 grams of DU per square centimeter each year. The dissolution rate of the corrosion products is estimated at 0.15 grams of DU per square centimeter of the corroded penetrator. The calculated time to complete corrosion and dissolution of the penetrator is 107 years and peak loss of mass is 56.8 grams per year (g/y) in years 18 through 24. Figure 6-2 shows the calculated time-dependent source of uranium into the soil based on these values. The figure displays the mass of DU entering the soil per year per penetrator and the estimated range in rates.

**Table 6-4. Best-Estimate Values for Corrosion and Dissolution Rates
Jefferson Proving Ground, Madison, Indiana**

Parameter	Best-Estimate Value	Notes
DU Corrosion Rate	0.25 g/cm ² -yr	Calculated per unit surface area of remaining DU metal
Dissolution Rate	0.15 g/cm ² -yr	Calculated per unit surface area of corroded penetrator (outer surface)

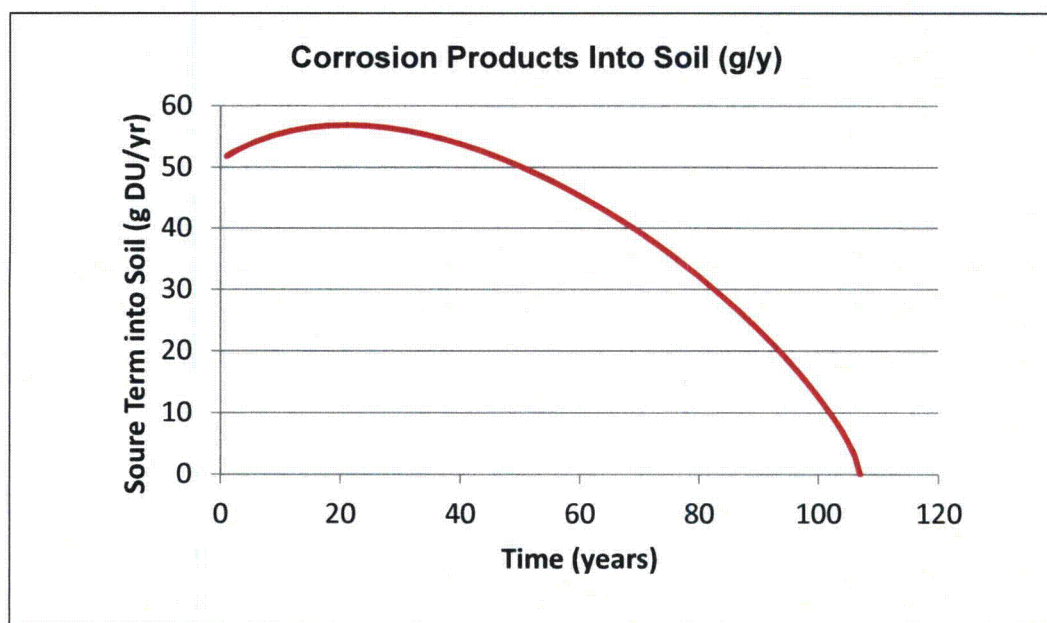


**Figure 6-2. Estimated DU Mass Release Into the Soil per Penetrator
From Corrosion and Dissolution**

The estimated mass of DU entering the soil per year per penetrator (Figure 6-2) was developed assuming a 4.0 kg penetrator. However, different penetrator models of varied mass and surface area were test fired at JPG. Therefore, they will exhibit slightly different dissolution rates than the estimated rates shown above. It is assumed that dissolution rate from such penetrators is proportional to their mass and surface area. The equivalent total number of penetrators remaining within JPG watershed was estimated by dividing the total penetrator mass of 73,500 kg by 4.0 kg/penetrator = 18,375. The distribution of DU mass within each sub-basin (Table 6-2) has been estimated from operational history, field surveys, etc. and using this information, the number of penetrators within each sub-basin can be estimated. DU transport calibration is performed by adjusting the rate of DU entering the soil per penetrator over time to match observed conditions from surface water and sediment sampling.

One last note regarding the estimated rates of penetrator corrosion and subsequent dissolution; DU penetrators were test fired during the period 1984 to 1994. The best estimate rate shown in Figure 6-2

indicates the rate of DU mass release to soil should be near the maximum rate if assumptions regarding development of the rates (oxidizing conditions) are valid. As noted in Section 2.2.2.1, greater than 55 percent of the soils in the DU Impact Area are somewhat poorly drained and exhibit redoximorphic features (soil mottling) that indicate a reducing environment exists in the shallow (<3 ft) subsurface for some period of time during the growing season. The rates presented here do not take into account this effect. Therefore, the values presented here represent the upper end of corrosion and dissolution rates. The rates (DU mass released to soil over time) used to calibrate DU transport in the JPG model are expected to be lower (less mass each year) and occur over longer period of time as a result of the periodic seasonal reducing conditions. The seasonal reducing conditions also will reduce dissolved mass transport as uranium (VI) is reduced to uranium (IV), which as noted above tends to form insoluble precipitates.

6.1.4 Specification of DU Source

HSPF offers several options to specify spatial distribution of the DU source at JPG. Each option has advantages, disadvantages, and limitations. Some of the options selected during the screening process for further research and assessment are discussed below:

- **Option 1**—Specify the location of the DU source within the sub-basin. DU is assumed to be sediment associated, and a potency factor (the DU mass associated with each size fraction) defining the ratio of DU mass to sediment mass transported is specified. HSPF uses the potency factor and the simulated sediment loads to estimate the DU transport (HSPF does not explicitly simulate DU transport) to various streams. A dissolved DU source within the sub-basin also may be specified, but wash-off factors need to be input to simulate DU fate and transport in the overland flow. No long-term field data were available at JPG to determine potency factor and the wash-off characteristics of the overland flow; therefore, this option was not pursued.
- **Option 2**—Add DU directly to the stream passing through the sub-basin having DU penetrators. DU can be specified as sediment associated and/or as a dissolved source. Several test runs were performed (assuming hypothetical DU source areas within sub-basins 21 and 114). Results showed that when DU was specified as an adsorbed source time series, HSPF gives an error if the source was specified during an hour when no sediment load was delivered (simulated) to the stream. In addition, during a nonsediment hour, this option will not specify and simulate DU transport into stream as dissolved phase (in surface and/or base-flow and/or interflow). During the period September to December 2006, of the 2,522 hours simulated, only about 55 to 60 hours had simulated sediment delivery to streams 21 and 114, for the rest of the period, the modeled sediment discharge to these streams was zero. Specifying DU as a sediment associated component poses logistical difficulties when the number of DU source sub-basins increases. Flow and sediment transport simulation must be performed first to determine the hours when sediment load discharges to streams (needed to create sediment associated DU time series). This will be followed by performing a complete simulation that includes the DU transport simulation. There are about 10 DU source sub-basins and nonsediment hours for each sub-basin could be slightly different. Each DU sub-basin will need its own time series. As rainfall pattern changes, such as expected during longer-term simulations, the task of creating the DU source time series input data would be resource intensive.
- **Option 3**—DU is added to the stream as dissolved source. User specified mass transfer rates between adsorbed (suspended and bed load sediment fractions) and dissolved phases control the mass transfer kinetics between these phases – high rates establish equilibrium concentrations between these phases (dissolved and adsorbed) more quickly. In this option, the dissolved mass is added to the stream partitions to the sediment within the stream channel (sediment that has been transported to the stream channel). During test simulations of these

source term options, using high mass transfer rates between adsorbed (suspended and bed-load sediment fractions) and dissolved phases was observed to allow fairly quick equilibrium between these phases. This helps to reduce the difference between scenarios where DU source was specified as sediment associated versus a dissolved source. Such differences are likely to be reduced further when the source was diffused (spatially distributed) and when greater numbers of DU source sub-basins are involved (such as those at JPG). DU sources could be specified each day. Fortunately, hourly precipitations are the same (JPG has one meteorological station) for all sub-basins, which simplifies creation of DU time series compared to the other options. Cumulative DU mass is allocated proportionate to the number of penetrators estimated in each sub-basin. This option is implemented in the HSPF-JPG model because:

- The DU Impact Area is heavily vegetated, limiting the amount of surface erosion (both sediment and particulate transport) from the DU Impact Area
- The dissolved DU added to the streams quickly partitions between dissolved and sorbed phases within the stream channels
- The distribution of penetrators and impacted soils within each sub-basin is uncertain and specification of a dissolved and sediment associated source for long-term simulations adds complexity to the surface water model that does not appear warranted based upon the currently available data
- Source term specification in this manner facilitates long-term modeling.

6.2 TRANSPORT CALIBRATION

The calibrated flow and sediment transport model provides the framework within which DU transport modeling is performed. Calibration of DU transport was completed by adjusting the source term (DU mass released) within each sub-basin until an overall match with observed average DU concentrations in surface water and sediment was achieved. Timing is also an important consideration. DU penetrators were test fired from 1984 to 1994 with penetrator recovery efforts completed twice per year during that period. The average concentrations observed in surface water and sediment today is the result of transport that began between 18 and 29 years in the past. So, transport model calibration efforts attempted to match the average observed concentrations between 18 and 29 years after the start of the model simulation. As noted in Section 2.2.7, the average concentrations of uranium in Big Creek surface water are 3 µg/L (1 µg/L upstream of and downstream from the DU Impact Area and 5 µg/L within the DU Impact Area) and 3.6 mg/kg in sediment. Middle Fork Creek surface water contains < 1 µg/L uranium and on average 2.8 mg/kg uranium in the sediment. These average values represent our calibration targets for uranium in surface water and sediment within Big Creek and Middle Fork Creek.

At the start of the model simulation, all penetrator DU mass is assumed available for release into the model. In other words, the model did not attempt to increase the DU mass in the system over the period 1984 to 1994 to reflect operations at the site. Rather, the model starts with the entire estimated mass remaining in the system. Transport simulations also assume the same mass release rate (source term) per penetrator for each sub-basin within the Big Creek or Middle Fork Creek watersheds, but allows a different rate between the watersheds to achieve calibration. Different rates may result from a number of factors, including variability in penetrator burial depths (e.g., those impacting on an upslope may be buried deeper and weather at a slower rate than those impacting on a downslope), temporal and spatial variability in geochemical conditions (e.g., due to variability in seasonal high water in site soils), or differences in the penetrator surface area or fragments exposed to weathering to name a few. One last assumption was made with respect to the weather data used in transport calibration efforts. Weather data from calendar year 2007 were assumed representative of the temporal (hourly) precipitation distribution (hourly precipitation as percentage of the annual value; see Section 7 for details) over the period

calibration is performed (from 1984 through the 2007 to 2012 timeframe where average uranium concentrations in surface water and sediments are measured). This same assumption was made for predictive transport simulations (Section 7). The model start date was set at 1 January 2013. For transport calibration purposes, predicted model results 18 to 29 years after the start of the simulation (model simulation time 2031 to 2042) are comparable to observed concentrations today. Parameters are adjusted to achieve this match (calibration) with observed concentrations.

6.3 CRITICAL PARAMETERS

The K_d (Section 6.1.2) and DU corrosion and dissolution rates (Section 6.1.3) are the most critical parameters for calibration of DU fate and transport. Both parameters were adjusted until modeled uranium levels in surface water and sediment matched average observed conditions in Big Creek and Middle Fork Creek. Table 6-3 presents the range of K_d values for various soil types at the JPG site. Since Grayford/Ryker soil type is the most abundant soil type in the stream valleys including Big Creek and Middle Fork Creek, a value of 7,421 milliliters per gram (mL/g) was initially assumed as an average K_d value for the composite soil in the base case scenario.

HSPF requires K_d values for sand, silt, and clay fractions; this was approximated as follows. The range of K_d values for various soil types listed in Table 6-5 for uranium by Thibault, Sheppard, and Smith (1990) were used as a guideline in this investigation. The sand, silt, and clay fractions constituting sub-basins soils were 0.205, 0.49, and 0.305, respectively. It was assumed that K_d for silt and clay fractions was 5 and 250 times, respectively, that of the sand fraction. The K_d values of sand, silt, and clay fractions calculated (to render a composite value of 7,421 mL/g) were 94, 472, and 23,587 mL/g, (or 0.000094, 0.000472, and 0.023587 liters per milligram [L/mg]) respectively.

Table 6-5. Uranium K_d Values (Thibault, Sheppard, and Smith 1990) for Various Size Fractions Jefferson Proving Ground, Madison, Indiana

Soil Type	Geometric Mean K_d (mL/g)	Observed Range of K_d (mL/g)
Sand (>70% sand-sized particles)	35	0.03-2,200
Loam (even distribution of sand, silt and clay-sized particles or >80% silt-sized particles)	15	0.2-4,500
Clay (>35% clay-sized particles)	1,600	46-395,100

Calibration was completed by adjusting the mass released per penetrator within each sub-basin until the average concentration in the surface water and sediment was achieved. K_d was adjusted to achieve a match between the predicted surface water concentration and sediment concentration. The calibrated rates of uranium released (corrosion and dissolution) in Big Creek sub-basins were reduced by a factor of 9 and by a factor of 100 in Middle Fork Creek sub-basins. For Big Creek sub-basins, the rate of uranium released per penetrator began at 4.84 g/y, peaked at 5.95 g/y, and ended at 4.29 g/y. For Middle Fork Creek sub-basins, the rate of uranium released per penetrator began at 0.44 g/y, peaked at 0.49 g/y, and ended at 0.49 g/y. The lower rates compared to those illustrated in Figure 6-2 may result from periodic reducing conditions. Differences in rates between Big Creek and Middle Fork Creek may be due to site topography. The flow divide separating Big Creek from Middle Fork Creek basins occurs within the DU Impact Area. Penetrators impacting within the Middle Fork Creek sub-basin are impacting on an upslope (think of firing into a hillside). Penetrators impacting in the Big Creek sub-basin (south of Big Creek) are impacting on the downslope (on the other side of the topographic divide). As a result, penetrators in Middle Fork Creek may be more deeply buried and as a result experience more reducing conditions (slower corrosion and dissolution rates) than penetrators within Big Creek sub-basins. The calibrated composite K_d value is 2,200 mL/g.

Results from a series of column tests with penetrators and soils from JPG have recently become available (see discussion in Appendix F). These tests simulated an accelerated cycle of soil conditions from flooded to dry, which likely would have resulted in a range of corrosion and dissolution rates similar to what might be experienced by penetrators at JPG. At the conclusion of 1.3 years of testing, the soils were analyzed to determine uranium content. The mass of uranium in the soil was then combined with the measured mass of uranium leached from the soil during the testing period to determine the total mass dissolved from the penetrator. The resulting mass release rate from the penetrator was approximately one-eighth the value calculated based on dissolution rate in Table 6-4 and very close to the calibration value used for the Big Creek sub-basin.

6.4 CALIBRATION RESULTS

Model calibration results presented in this section characterize modeled concentrations that are representative of current observed average concentrations. As such, the predicted concentrations represent model results at timeframes equal to 18 to 29 years since model initiation. Model initiation can also be thought of as time zero (T0). To achieve calibration, model predictions (dissolved and sediment concentrations) must match observed concentrations 18 to 29 years after T0. Model output is presented in terms of dissolved uranium concentrations in surface water and uranium concentrations in suspended silt fraction. Recall that HSPF provides output by size fraction. Silt fraction was selected for output since concentrations for this fraction occur between the sand and clay size fractions.

Figure 6-3 illustrates the dissolved uranium concentration in Big Creek sub-basin 114 (western boundary of the DU Impact Area). Note that the scale of Figure 6.3 is in mg/L. The maximum concentration in surface water between 18 to 29 years after T0 is 5 µg/L, which is slightly higher than the observed average of 3 µg/L in Big Creek surface water. Observed data also show that dissolved uranium concentrations at the western boundary of the DU Impact Area are on average 1 µg/L. Therefore, the calibrated model results are somewhat conservative (above) compared to observed results. Within the DU Impact Area, observed average concentrations are 3 µg/L compared to the 5 µg/L simulated concentrations. Figure 6-3 also shows dissolved levels fluctuating seasonally with modeled runoff ranging from just under 1 to nearly 5 µg/L. Observed data did show some seasonal fluctuations with higher dissolved levels observed during periods of low flow in summer, especially where runoff from the DU impact trench is expected to enter Big Creek (note the surface water model as currently configured does not have the resolution to reproduce this site feature).

Predicted uranium concentrations in sediment at Big Creek sub-basin 114 is 3.2 mg/kg. Figure 6-4 illustrates the uranium concentration in suspended silt, which ranges from about 0.1 to 0.8 mg/kg (note that units shown on the figures for suspended sediment concentrations are in mg/mg and were converted to mg/kg).

One word of caution is necessary when reviewing and interpreting figures depicting predicted uranium concentrations in surface water or sediment. At very low-flow conditions, HSPF produces unrealistically high concentrations. As simulated flow approaches zero, very small amounts of mass result in the unrealistic concentrations. Further, during very low flow conditions, small changes in flow result in large fluctuations in predicted concentrations, even though the mass in the system remains very small. This is a limitation of the model itself and is acknowledged by the code authors.

Figure 6-5 illustrates the dissolved uranium concentration in Middle Fork Creek sub-basin 5 (just south of the DU Impact Area). This sub-basin contains the most DU mass (see Figure 6-1) and also receives contributions from sub-basin 2 located upstream. Dissolved concentration ranges from 0.4 to 0.6 µg/L 18 to 29 years after T0. Predicted uranium concentrations in suspended silt is <0.1 mg/kg (Figure 6-6) at this location on Middle Fork Creek.

Calibration Results for Dissolved Uranium Concentration Big Creek, Sub-Basin #114

Note: Model simulation start date is Jan 1, 2013. Predictions at years 2031 to 2042 represent results 18-29 years after model start time and represent calibration period.

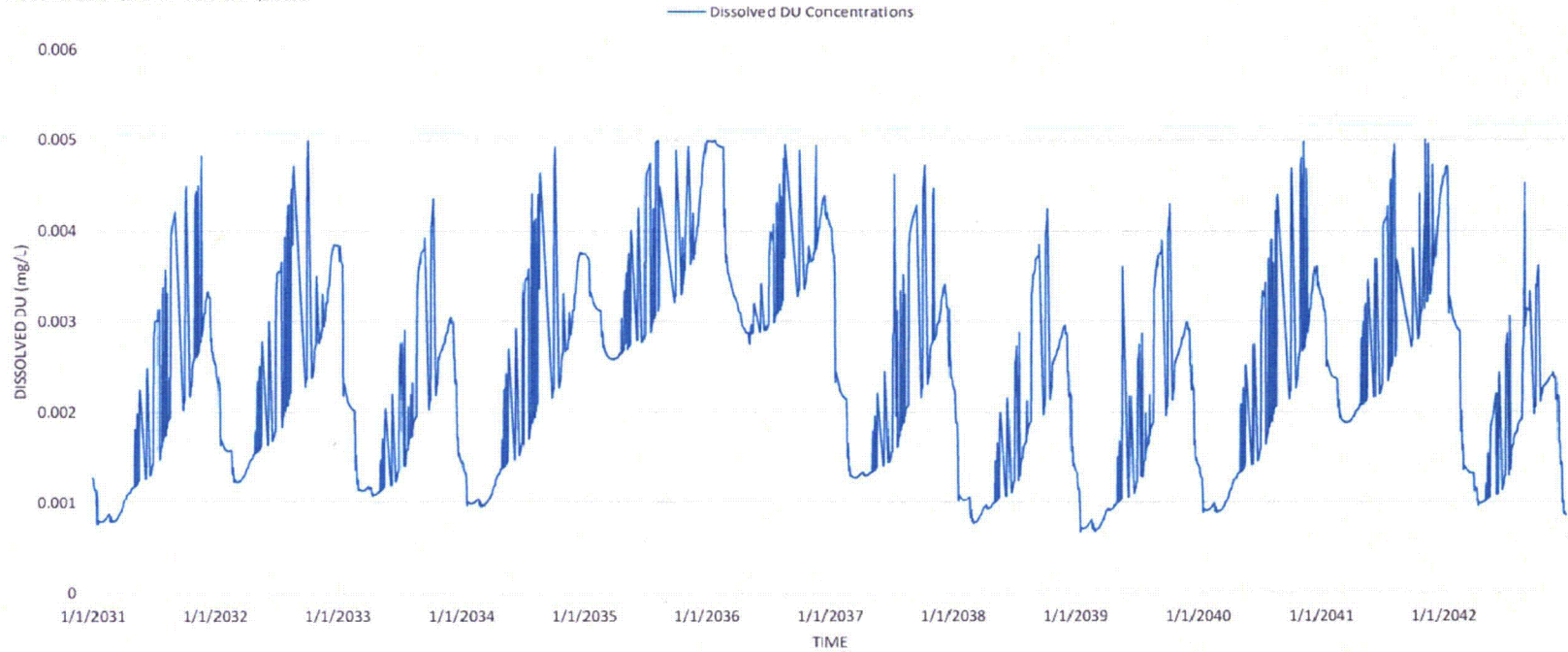


Figure 6-3. Calibration Results for Dissolved Uranium Concentration in Big Creek at Sub-Basin 114

Calibration Results for Uranium Concentration in Suspended Silt Big Creek Sub-Basin #114

Note: Model simulation start date is Jan 1, 2013.
Predictions at years 2031-2042 represent results
18-29 years after model start time and represent
calibration period.



Figure 6-4. Calibration Results for Uranium Concentration in Suspended Silt, Big Creek Sub-Basin 114

Calibration Results for Dissolved Uranium Concentration Middle Fork Creek, Sub-Basin #5

Note: Model simulation start date is Jan 1, 2013.
Predictions at years 2031 to 2042 represent
results 18-29 years after model start time and
represent calibration period.

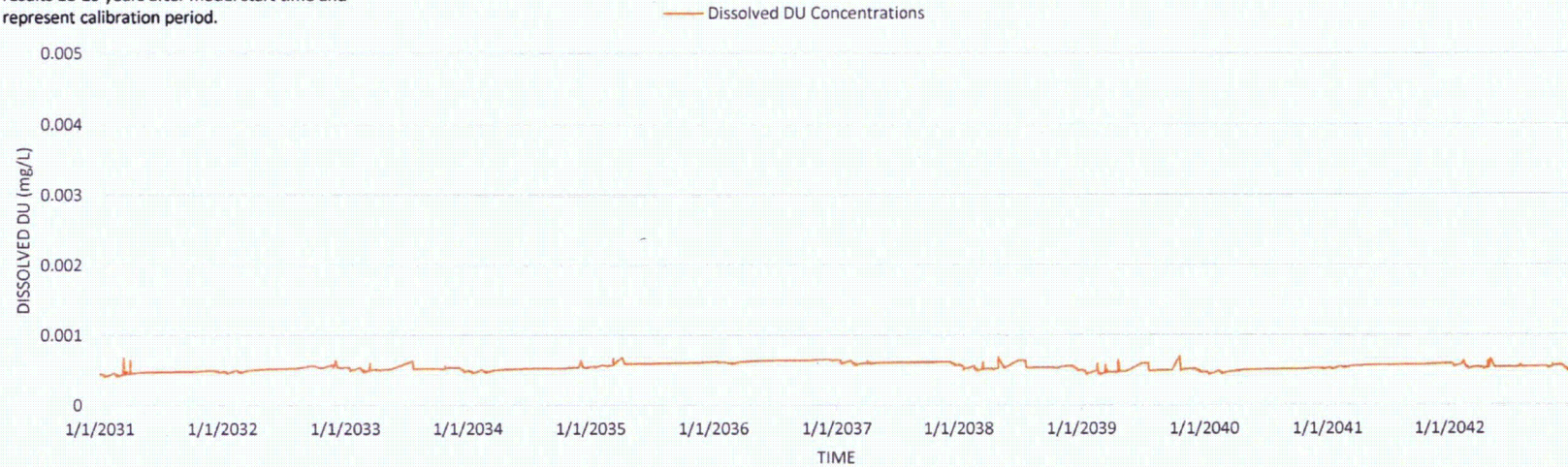


Figure 6-5. Calibration Results for Dissolved Uranium Concentration in Middle Fork Creek Sub-Basin 5

Calibration Results for Uranium Concentration in Suspended Silt Middle Fork Creek, Sub-Basin #5

Note: Model simulation start date is Jan 1, 2013.
Predictions at years 2031-2042 represent results 18-
29 years after model start time and represent
calibration period.

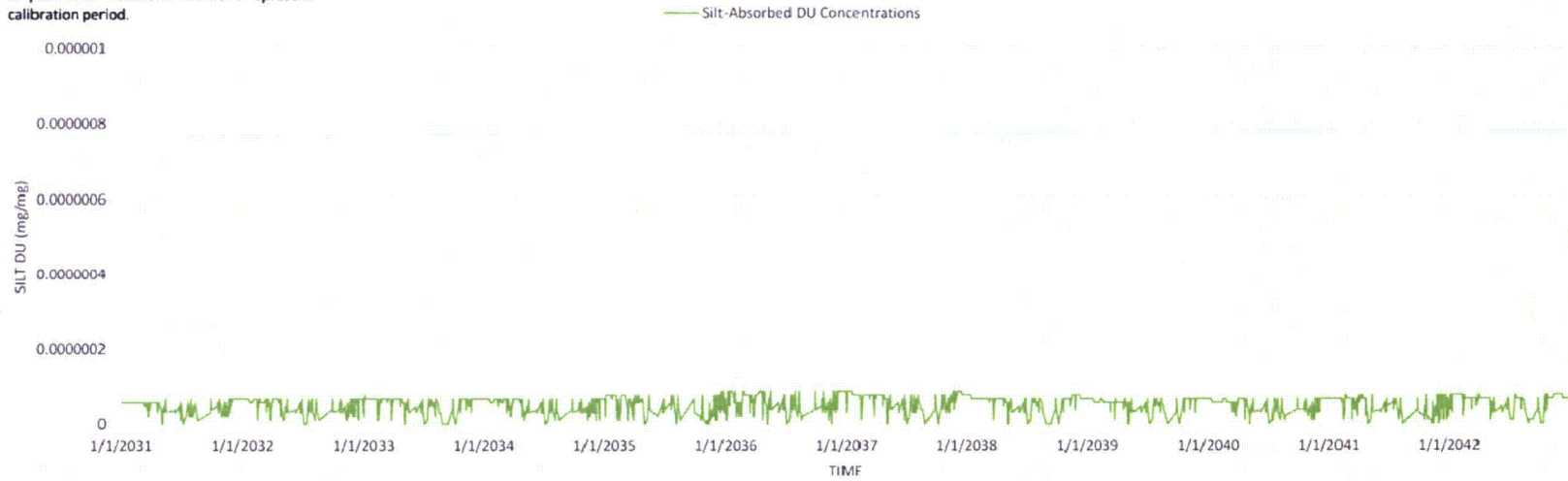


Figure 6-6. Calibration Results for Uranium Concentration in Suspended Silt, Middle Fork Creek Sub-Basin 5

Predicted surface water and sediment concentrations in Big Creek and Middle Fork Creek are in agreement with observed average concentrations. Therefore, the transport model is considered calibrated.

6.5 SENSITIVITY ANALYSIS

Simulations were performed to assess sensitivity of results to variations in K_d and dissolution rates. One parameter was changed at a time and its impact on the predicted DU fate and transport was assessed.

6.5.1 K_d

K_d was varied between the average sorption and desorption laboratory-derived values for JPG soils. Composite values of 429 mL/g for desorption test results and 7,004 mL/g for sorption test results were simulated. Predicted uranium concentrations in surface water and suspended silt in Big Creek sub-basin 114 (western boundary of DU Impact Area) are shown in Figures 6-7 and 6-8, respectively. Base case calibration results are included on the figures for comparison.

At the lower composite K_d of 429 mL/g, predicted surface water concentrations are higher while concentrations in sediments are lower, as expected when compared to base case calibration results. Dissolved uranium in surface water increases to 12 to 14 $\mu\text{g/L}$, while suspended sediment concentrations show a corresponding drop in predicted uranium levels. Decreasing K_d by a factor of about 5 increases predicted surface water concentrations by just over 3.5 times the calibration results and decreases the adsorbed sediment concentration by a factor of 2 to 3 times when compared to calibration results.

The opposite is true when using a composite K_d of 7,004 mL/g. Predicted surface water concentrations range from about 1 to 2.5 $\mu\text{g/L}$; suspended sediment concentrations range from 0.4 to 0.9 mg/kg. Increasing K_d by factor of about 3 results in predicted surface water concentrations roughly one half of calibration results and increases adsorbed sediment concentrations by a factor of 2 to 3 times when compared to calibration results.

6.5.2 DU Dissolution Rates

Penetrator corrosion and dissolution rates (the rate at which uranium mass is released to the model for transport) were reduced by a factor of 2; all other input parameters remained the same as those used in the calibrated base case model. Results from this simulation at Big Creek sub-basin 114 showed dissolved and suspended sediment concentrations (Figures 6-9 and 6-10, respectively) were reduced by a factor of 2, indicating a linear or near linear correlation between predicted concentrations and the penetrator corrosion and dissolution rates. Decrease in the corrosion and dissolution rates also results in a longer period of time before the penetrators completely corrode and dissolve, meaning mass will be released for a longer period of time, albeit at lower levels.

During model development and calibration efforts, another CSM for penetrator distribution was evaluated. In this case, the number of penetrators (and DU mass distribution) was roughly the opposite of that described in Section 6.1.1 with the number of penetrators in Middle Fork Creek sub-basins roughly twice that found in Big Creek sub-basins. To match the observed uranium levels in both creeks, dissolution rates in Big Creek sub-basins were near the maximum estimated dissolution rates (Section 6.1.3), resulting in the corrosion and dissolution of all penetrators within about 85 to 90 years. In Middle Fork Creek, dissolution rates were substantially less (by a factor of 90X) to match observed levels. In short, results from this second CSM for penetrator distribution show increased dissolution rates result in higher predicted concentrations and shorter duration of uranium mass released for flow and transport.

Note: Model simulation start date is Jan 1, 2013. Predictions at years 2030 to 2035 represent results 17-22 years after model start time.

Dissolved Uranium Concentration K_d Sensitivity Results

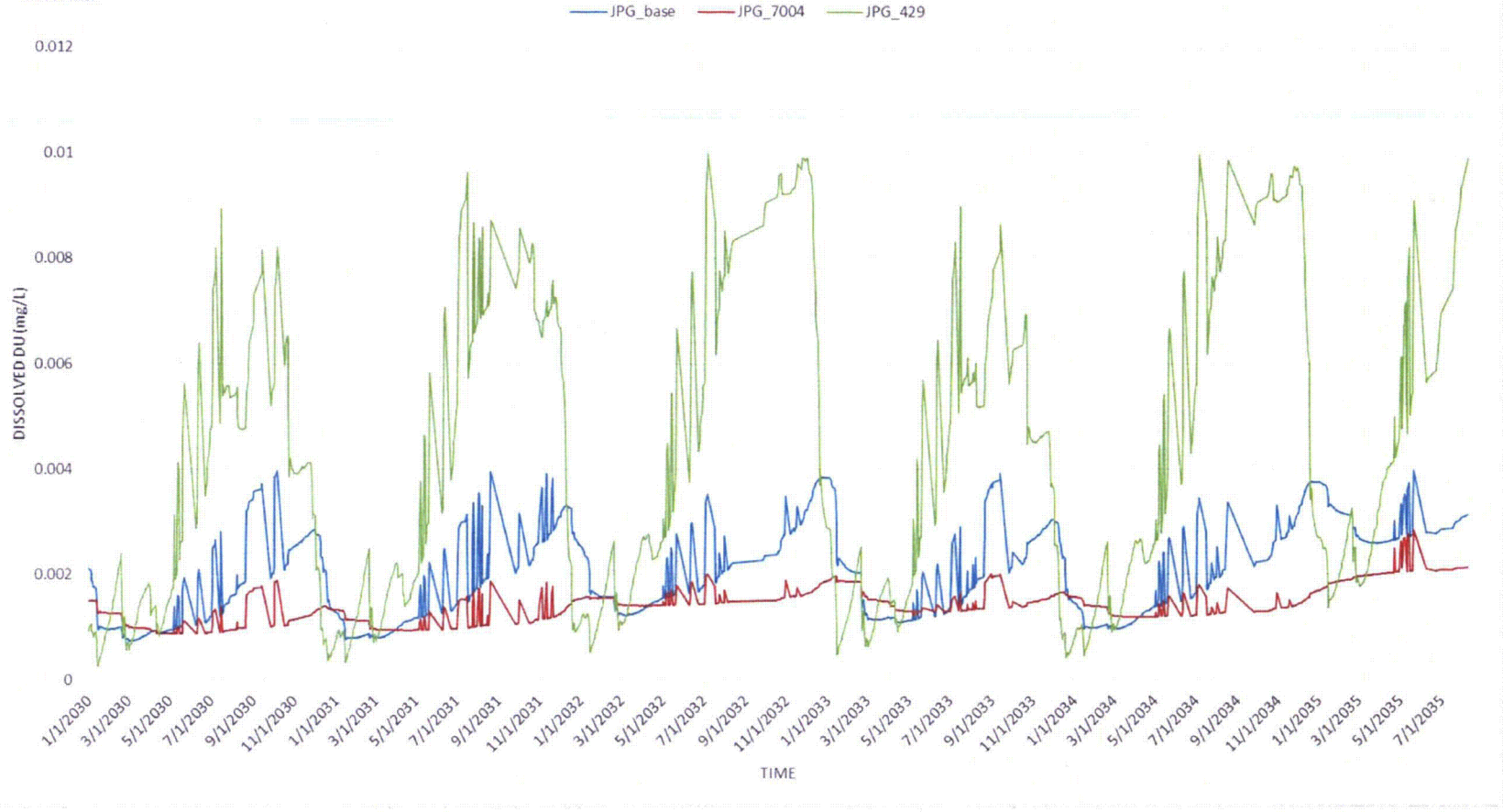


Figure 6-7. Dissolved Uranium Concentration K_d Sensitivity Results

Uranium Concentration in Suspended Silt K_d Sensitivity Results

Note: Model simulation start date is Jan 1, 2013.
Predictions at years 2030 to 2035 represent
results 17-22 years after model start time.

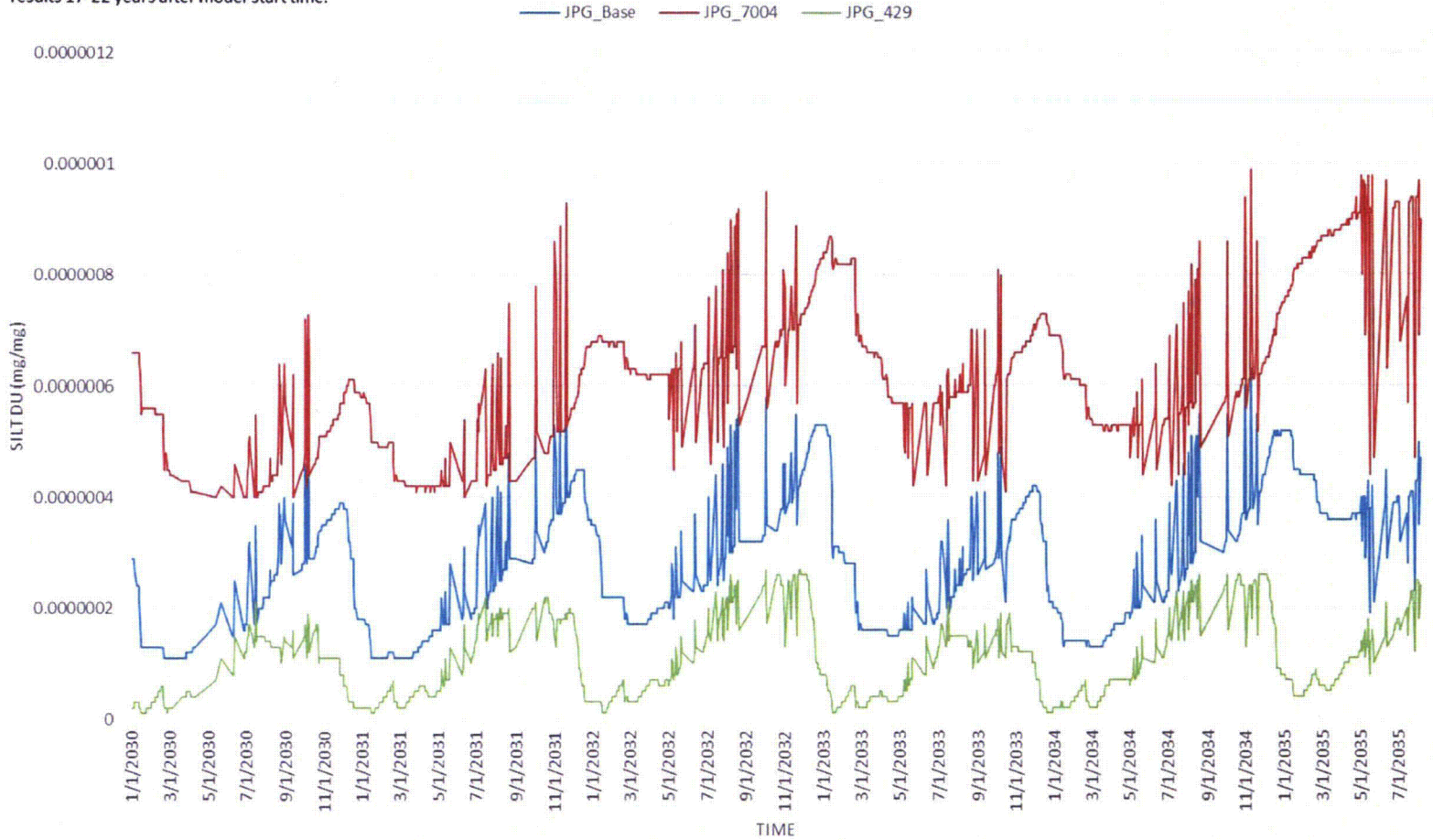


Figure 6-8. Uranium Concentration in Suspended Silt K_d Sensitivity Results

Sensitivity of Dissolved Uranium Concentration to Dissolution Rate Sub-Basin #114

Note: Model simulation start date is Jan 1, 2013. Predictions at years 2031-2042 represent results 18-29 years after model

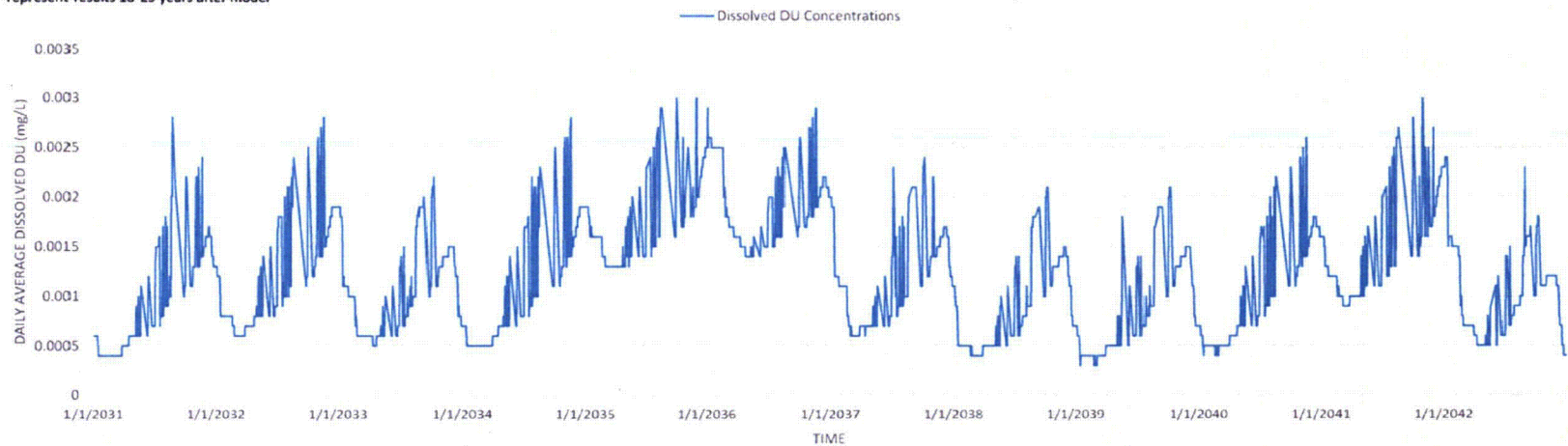


Figure 6-9. Sensitivity of Dissolved Uranium Concentration to Dissolution Rate at Sub-Basin 114

Sensitivity of Uranium Concentration in Suspended Silt to Dissolution Rate Sub-Basin #114

Note: Model simulation start date is Jan 1, 2013. Predictions at years 2031-2042 represent results 18-29 years after model start time.

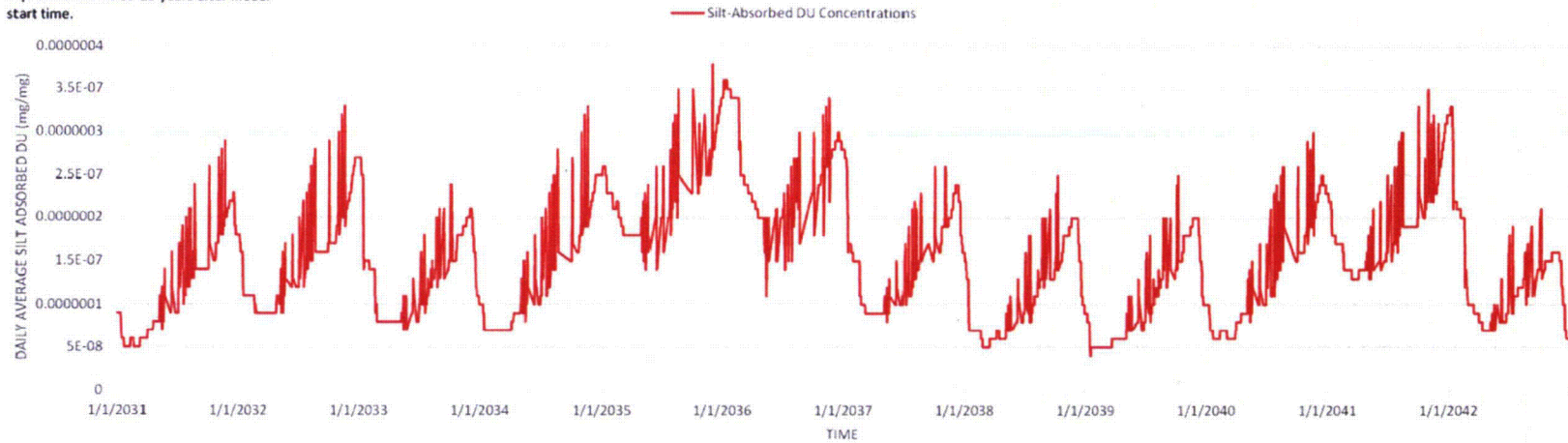


Figure 6-10. Sensitivity of Uranium Concentration in Suspended Silt to Dissolution Rate at Sub-Basin 114

THIS PAGE WAS INTENTIONALLY LEFT BLANK

7. PREDICTED FUTURE DU FATE AND TRANSPORT

Predicted future DU fate and transport modeling was performed to assess DU in Big Creek and Middle Fork Creek via surface water pathway over a period of 500 years. A second simulation examining the potential effects of climate change (increase in temperature) over the next 100 years also was completed.

7.1 DEVELOPING LONG-TERM BASE CASE SCENARIO

Base case is defined here as the set of input parameters used to develop the calibrated surface water flow and DU transport model. This base case set of parameters is used to perform long-term predictive DU transport modeling to assess potential long-term impacts from DU at the former JPG.

The first step in developing long-term base case simulation was to create the hourly input time series data (e.g., precipitation, potential evapotranspiration, and ambient temperature). Since meteorological data for the JPG site was available for a fairly short duration (2002 to 2011), annual precipitation data from the nearby Versailles weather station for 57 years (1949 to 2005) was used to generate long-term annual precipitation time series. The average annual precipitation for this period is 43.1 in/y (compared to 47 in/y average used to determine the water budget for JPG from 30 years of record at Madison, Indiana). Existing potential evapotranspiration and temperature data were cloned to extend these time series for long-term simulations. Several simplifications have been made to create, efficiently store, and handle these time series within HSPF; the following assumptions have been invoked:

- The precipitation data have relatively small skewness and can be described by normal distribution
- The effect of climate change on the base case scenario is insignificant.

Initially, a 1,000-year annual precipitation time series was created. However, HSPF requires an hourly (interval) precipitation time series for the complete duration of the simulation. The process of converting annual time series to hourly data was simplified to facilitate disaggregation (refer to WDMUtil documentation), storage, and handling during HSPF run execution. A 1,000-year hourly time series for precipitation, temperature, potential evapotranspiration, and DU source terms are large, difficult to store and handle within HSPF, and are subject to uncertainty due to limited historical data available to generate the time series for JPG. The methodology implemented to overcome these issues includes the following:

1. The 1,000-year annual precipitation values were compiled; 500 values were randomly selected from the 1,000 values.
2. Data from 2007 was assumed as a representative year of the temporal (hourly) precipitation distribution (hourly precipitation as percentage of the annual value).
3. The ratio for each of the 500 annual values in the array developed in (1) to the 2007 annual precipitation was computed.
4. The 2007 hourly precipitation values were multiplied by the ratio computed in (3) above and corresponding hourly precipitations for each of the 500 years were computed.

The limitation of the frequency analysis for meteorological data (proposed above) must be emphasized as a rule; in general, estimating frequencies (or probabilities of occurrence) of events (such as precipitation) for greater than twice the available record length should be avoided.

The conditions simulated using the time series developed above should provide a fairly reasonable representation of the likely conditions at JPG over the next 100 years. DU mass release rates (DU mass

per year released into the model) time series from corrosion and dissolution were the same as used in the calibrated transport simulation discussed in Section 6. Of note is that the mass release rates parallel the information shown in Figure 6-2, in Big Creek starting out with an initially lower rate (4.84 g/y), rising to a maximum rate (5.95 g/y) between 18 to 21 years, then dropping back down to a slightly lower rate (declining to 4.29 g/y after 500 years) over the remaining period. Mass release rates in Middle Fork Creek are much lower. Both represent long-term, nearly constant mass release for transport in both Big Creek and Middle Fork Creek. Results for the first 100 years are presented.

Predicted future DU concentrations in surface water and sediment were examined down Big Creek and Middle Fork Creek, starting with the western boundary of the DU Impact Area and continuing downstream to the former JPG property boundary and offsite to the west-southwest.

In Big Creek, results are shown at sub-basin 114 (western boundary of DU Impact Area), sub-basin 117 (last sub-basin on former JPG property), and sub-basin 128 (last sub-basin prior to confluence with Middle Fork Creek) offsite and southwest of the former JPG. The long-term and nearly constant mass release results in similar surface water DU concentration levels (ranging from ~1 to 5 µg/L over the 100 years presented in Figures 7-1 and 7-2) at both sub-basins 114 and 117. There are no clear or apparent trends in the dissolved DU concentrations in either sub-basin, which is consistent with a long-term, nearly constant source. Highest predicted concentrations occur near the time of highest mass release rate into the model (~18 to 21 years after simulation start or model time 2033 to 2036). Concentrations in bed sediment are in equilibrium with surface water levels based upon a composite K_d of 2,200 mL/g. Therefore, predicted bed sediments are on the order of 1 to 4 mg/kg over the period.

Farther downstream on Big Creek at sub-basin 128 (Figure 7-3), maximum predicted DU concentrations in surface water are below 2 µg/L; predicted bed sediment concentrations are also less at sub-basin 128, generally 1 mg/kg or less. The decrease observed at sub-basin 128 compared to results at sub-basins 114 and 117 reflects mixing with continually larger flow and sediment volumes associated with increased drainage areas and more agricultural lands west of the former JPG.

Figures 7-4 and 7-5 illustrate predicted DU concentrations in Middle Fork Creek surface water at sub-basins 5 (just south of the DU Impact Area) and sub-basin 15 (at the western boundary of the former JPG), respectively. Predicted concentrations at sub-basin 5 range from about 0.2 to 0.6 µg/L. Results at sub-basin 15 are almost all below 0.2 µg/L. Predicted surface water concentrations are in equilibrium with bed sediment concentrations with predicted bed sediment concentrations less than 1 mg/kg (same composite K_d of 2,200 mL/g is used).

7.2 SENSITIVITY ANALYSIS (CLIMATE CHANGE SCENARIO)

A hypothetical scenario was simulated to assess sensitivity of results to changes in climate due to global warming. The effect of rising temperatures and higher potential evapotranspiration due to global warming and their impacts on stream/overland flow; sediment and DU fate and transport were assessed. The following assumptions were made in setting up the input parameters:

- Global temperature over next 100 years increases by 3°C and stabilizes thereafter
- The rainfall distribution was likely to change, but the overall impacts (during adverse and mild periods) are likely to average reasonably well on an annual basis; therefore, the same precipitation time series data are used
- Annual daily average temperatures were linearly increased (total 3°C over the next 100 years) and hourly temperature time series were generated
- Based on daily maximum and minimum temperatures, an algorithm in WDMUtil was used to generate the hourly potential evapotranspiration time series.

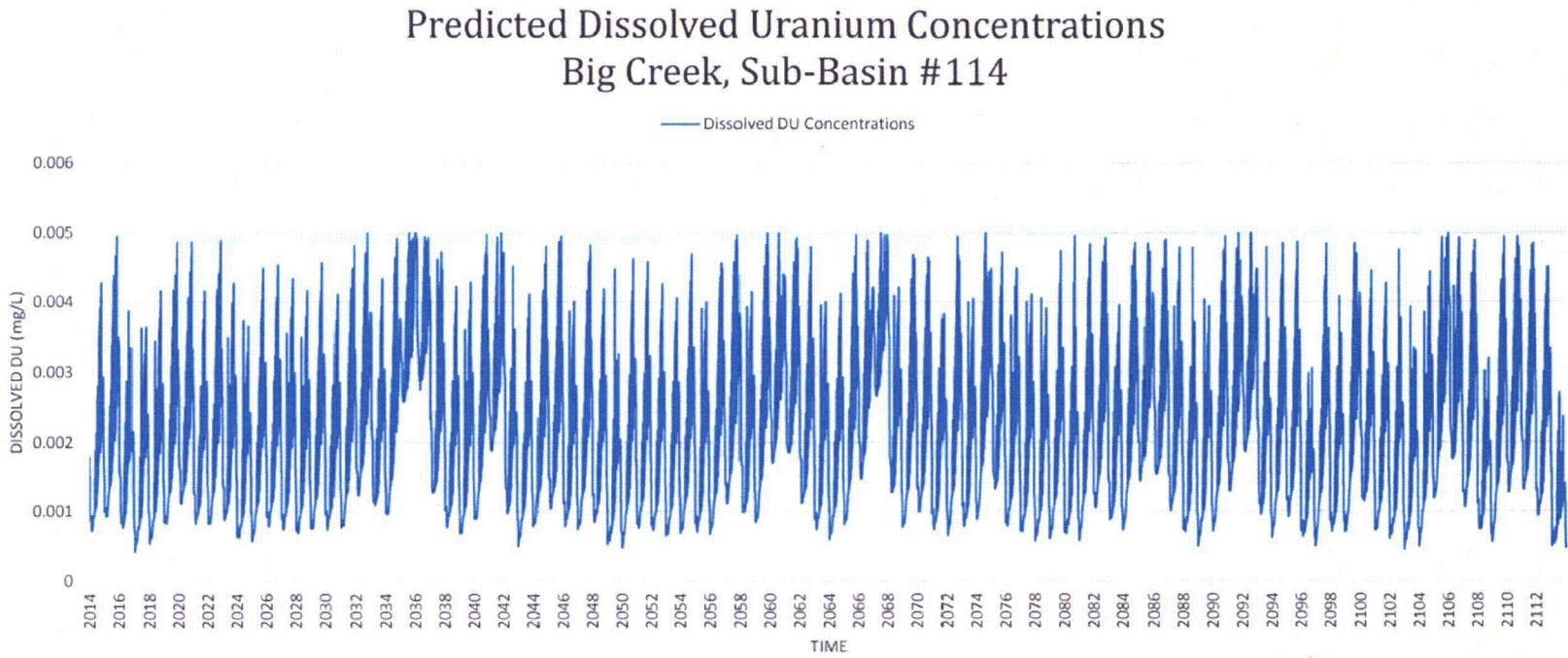


Figure 7-1. Predicted Dissolved Uranium Concentrations in Big Creek at Sub-Basin 114

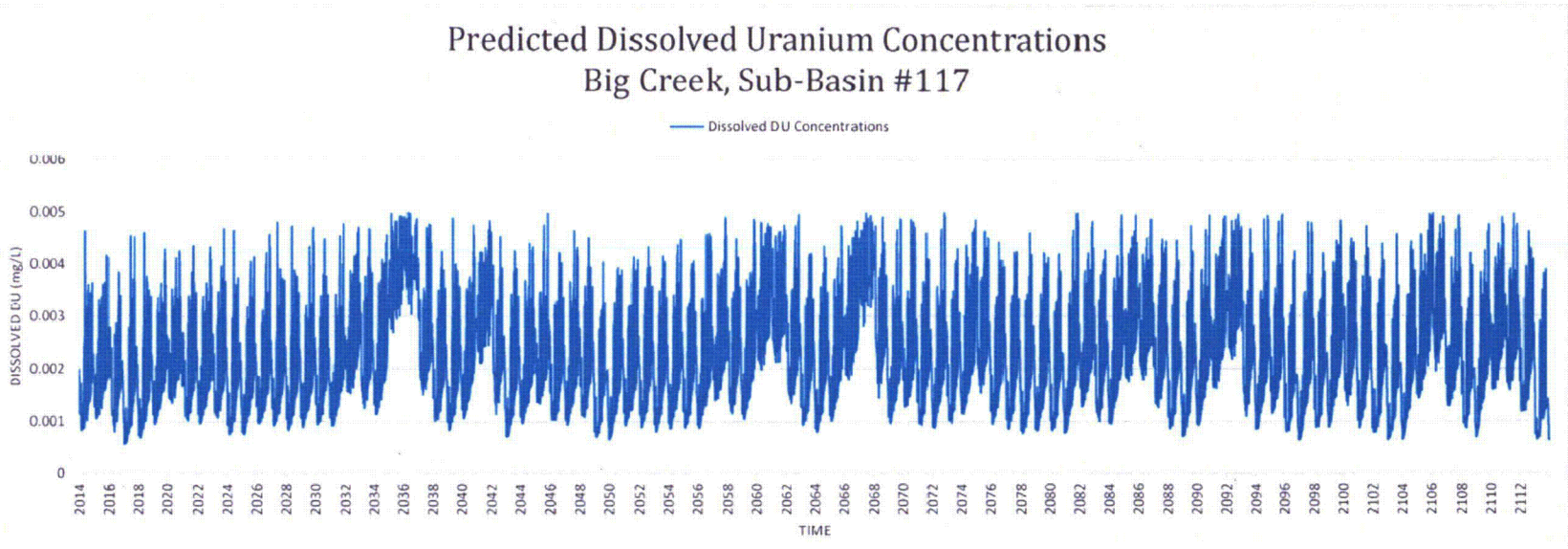


Figure 7-2. Predicted Dissolved Uranium Concentrations in Big Creek at Sub-Basin 117

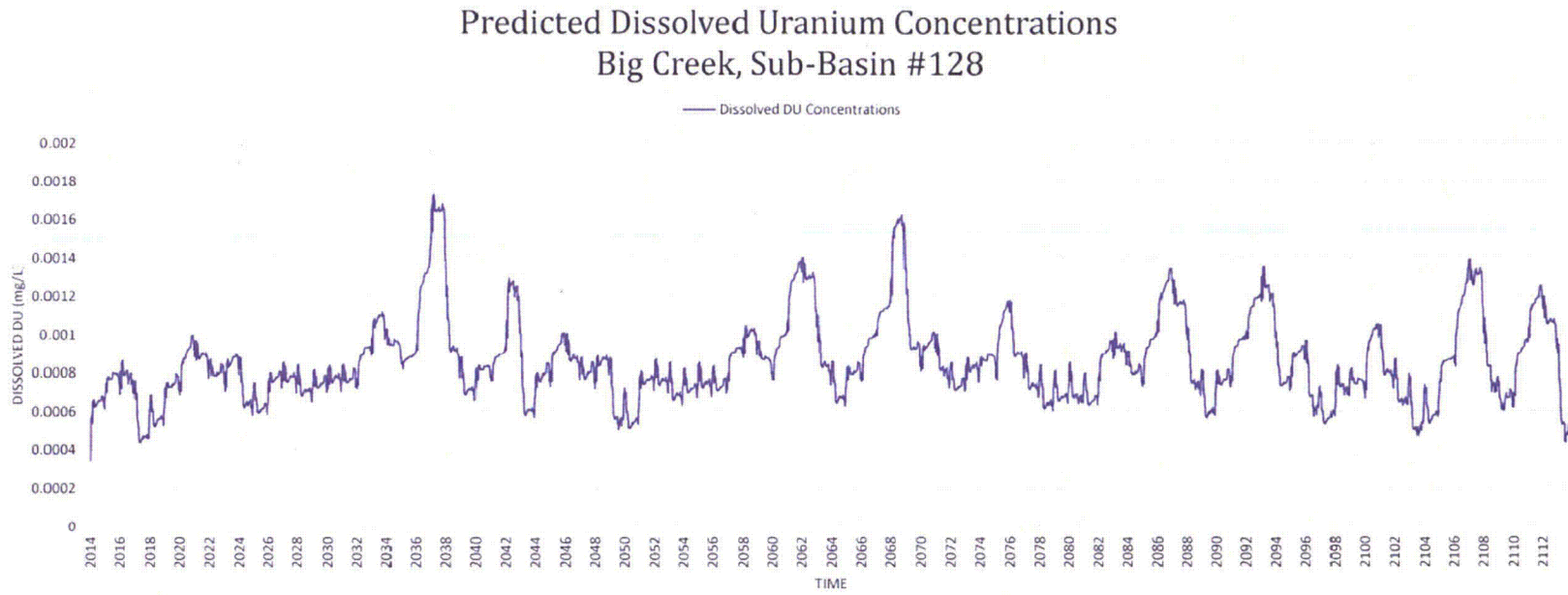


Figure 7-3. Predicted Dissolved Uranium Concentrations in Big Creek at Sub-Basin 128

Predicted Dissolved Uranium Concentrations Middle Fork Creek, Sub-Basin #5

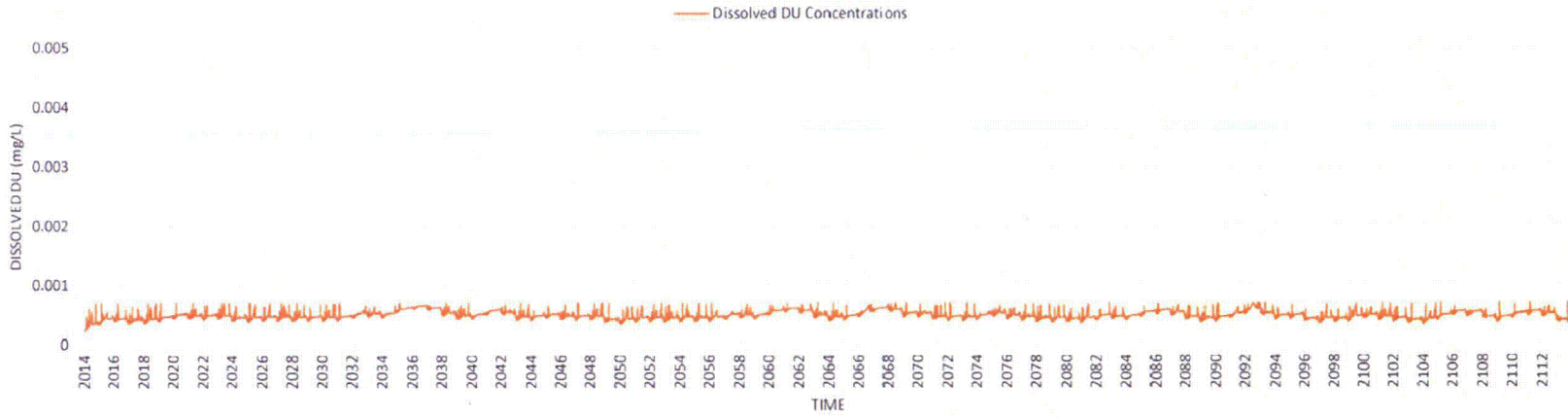


Figure 7-4. Predicted Dissolved Uranium Concentrations in Middle Fork Creek at Sub-Basin 5

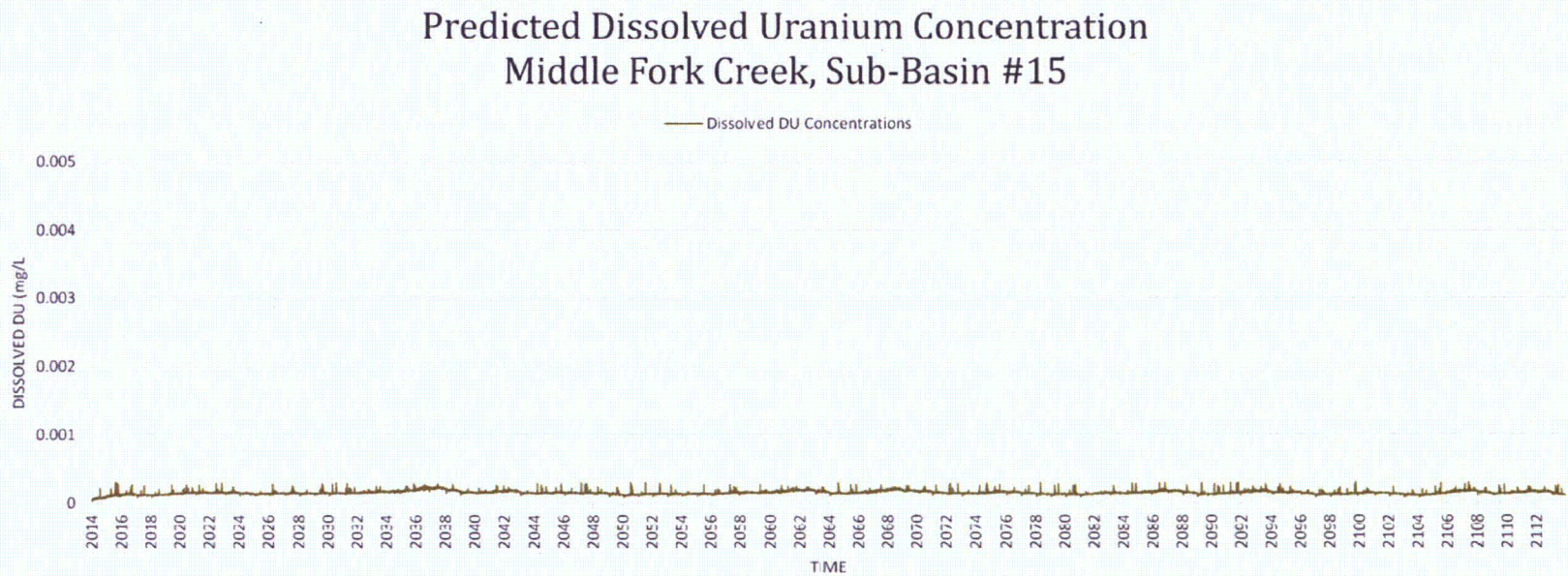


Figure 7-5. Predicted Dissolved Uranium Concentration in Middle Fork Creek at Sub-Basin 15

The biggest difference between this scenario and the long-term DU transport scenario described in Section 7.1 is the increase in evapotranspiration over the 100-year simulation period. As shown in Figure 7-6, evapotranspiration rates increase as the temperature increases, with the relative difference between base case rates increasing over time. Near the end of the simulation, annual high evapotranspiration rates are about 4 in/y greater than base case, while annual low evapotranspiration rates are similar or slightly greater by about 1 inch a year. This increase in evapotranspiration reduces the amount of precipitation available for surface runoff.

Simulated stage at Big Creek sub-basin 114 (western boundary of DU Impact Area) are compared between base case and climate change scenarios (Figure 7-7) near the end of the 100-year simulation period (2108 to 2112). As expected, simulated stage (and therefore simulated flow) in Big Creek are slightly less in the climate change scenario results. Low-flow conditions were similar, with differences in results becoming more substantial at higher-flow conditions.

Predicted DU concentrations in Big Creek surface water at sub-basin 114 for the period 2100 to 2112 are compared against base case results in Figure 7-8. The rate of DU mass released for transport is the same in both simulations. Predicted results in both scenarios are very similar with a slight increase ($<1 \mu\text{g/L}$) in the climate change scenario.

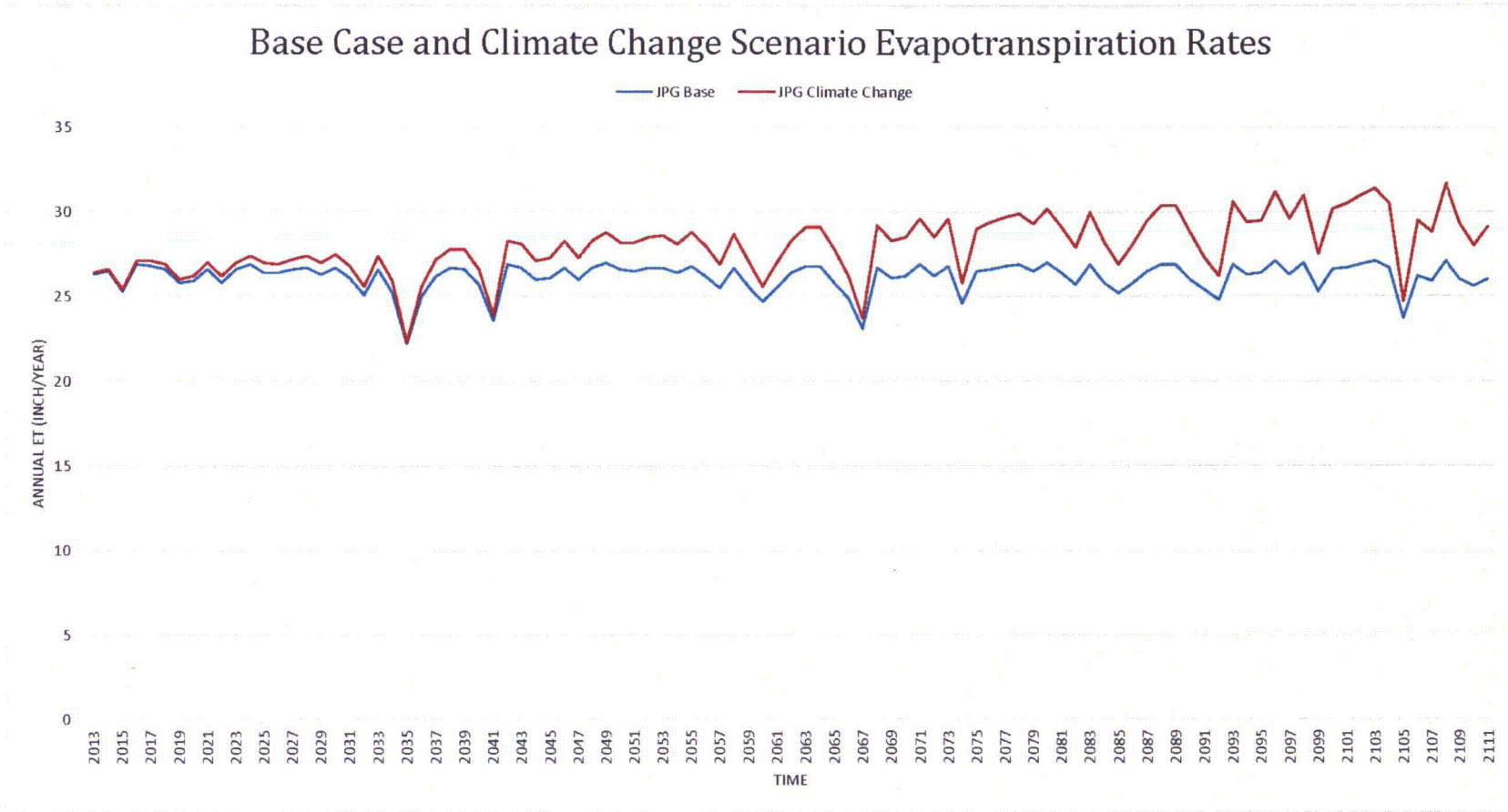


Figure 7-6. Base Case and Climate Change Scenario Evapotranspiration Rates

Base Case and Climate Change Scenario Results for Predicted Stage at Model Years 2108-2112

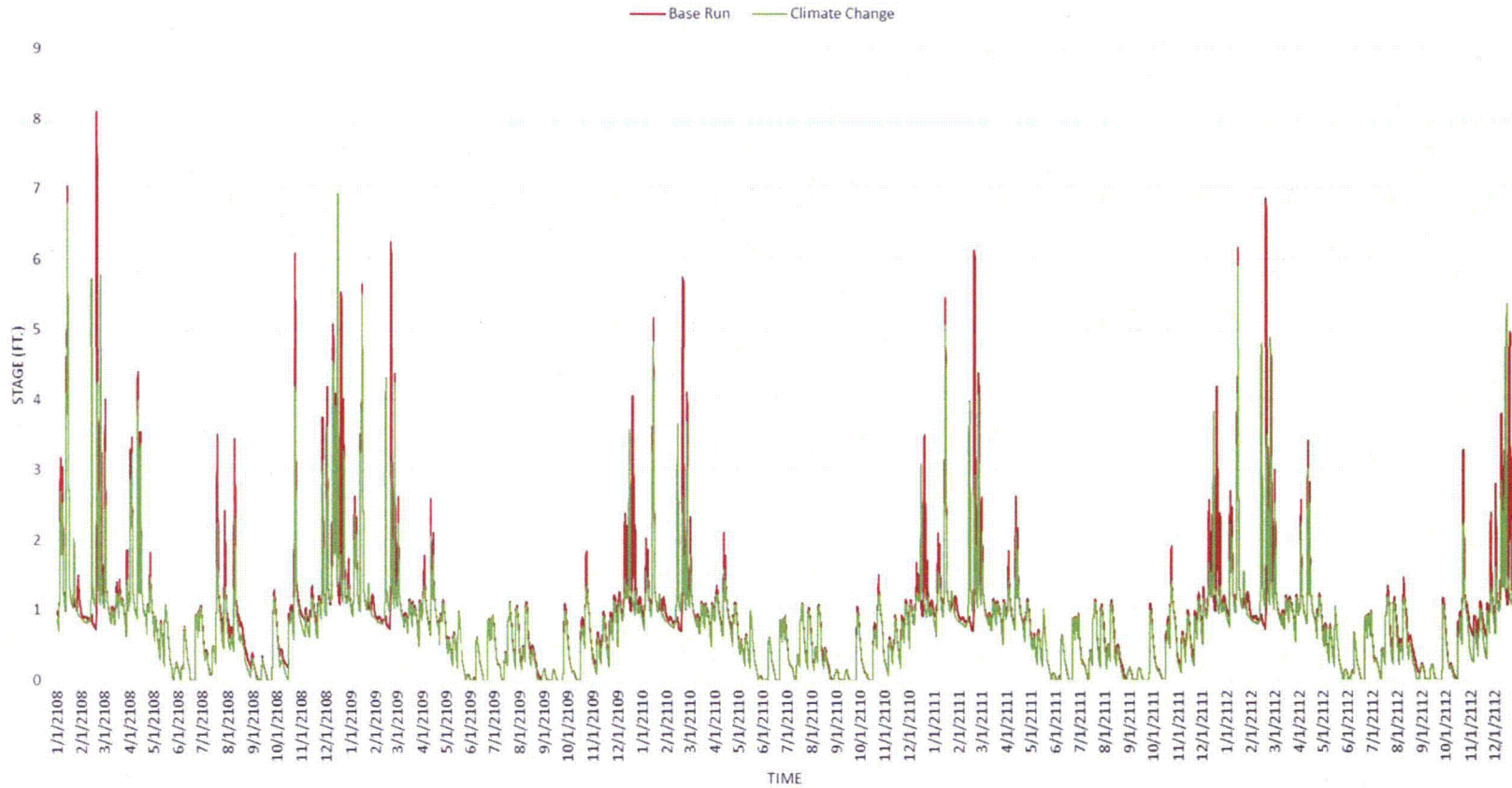


Figure 7-7. Base Case and Climate Change Scenario Results for Predicted Stage at Model Years 2108-2112

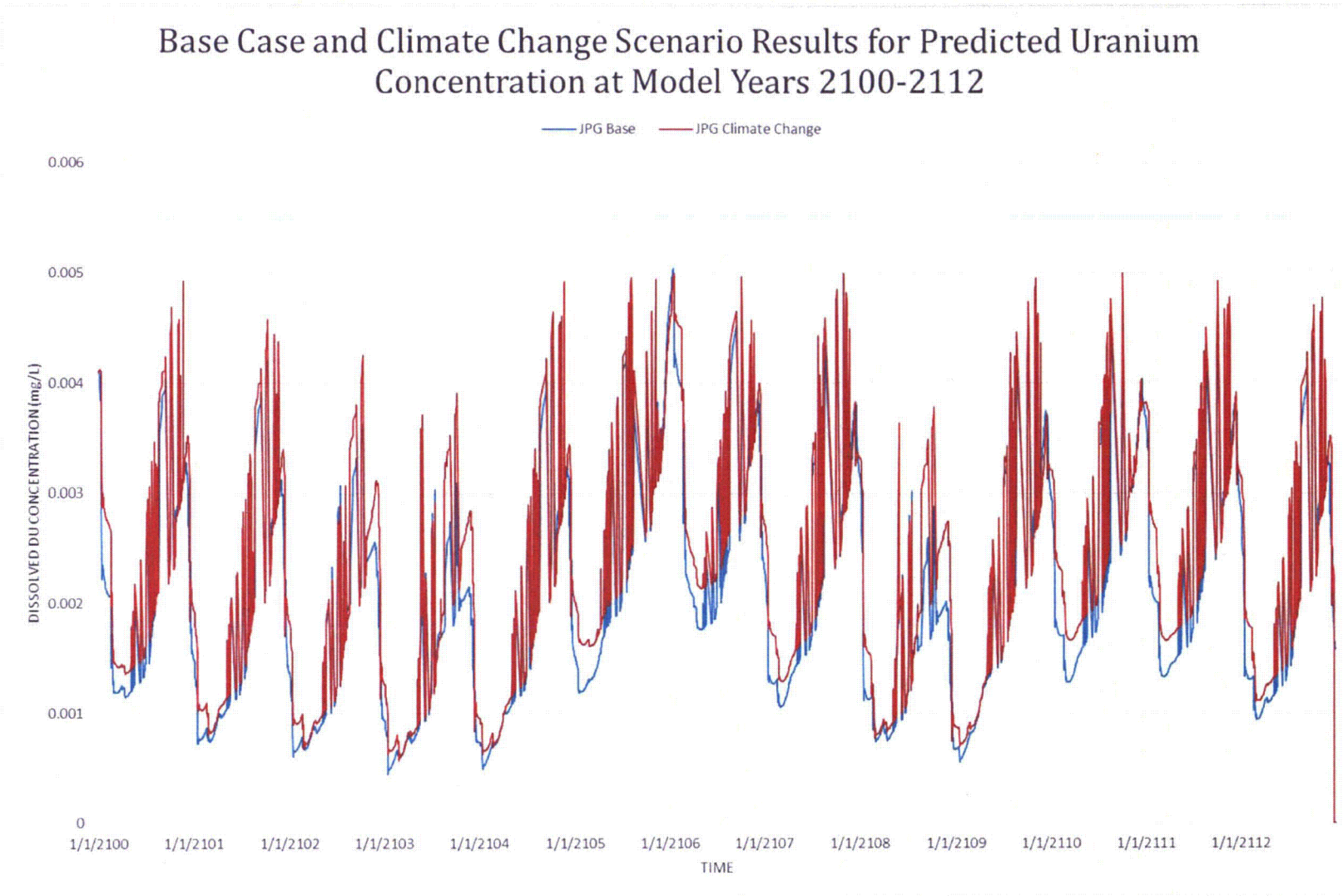


Figure 7-8. Base Case and Climate Change Scenario Results for Predicted Uranium Concentration at Model Years 2100-2112

THIS PAGE WAS INTENTIONALLY LEFT BLANK

8. DISCUSSION AND ANALYSIS OF RESULTS

The calibrated flow and sediment transport model provides the key to understanding predicted DU fate and transport results. Model results are discussed, including assumptions, limitations, and uncertainty.

8.1 FLOW MODEL AND SEDIMENT TRANSPORT

Of the 57 sub-basins, 10 (6 Big Creek sub-basins and 4 Middle Fork Creek sub-basins) of the sub-basins contain penetrators that may weather (corrosion and dissolution) and release DU into the surface water pathway. These 10 sub-basins represent a fraction (11 percent) of the areas drained by Big Creek and Middle Fork Creek. Further, the DU typically is located in only a portion of some of the sub-basins. For example, much of sub-basin 110 extending well to the east of the DU Impact Area contains no DU.

There is substantial mixing of clean water and sediment from the remaining 46 sub-basins; 89 percent of the sub-basins area contains no or negligible DU. Table 8-1 summarizes the area for each of the 10 sub-basins with DU in Big Creek and Middle Fork Creek and the percentage by area for each of the sub-basins.

**Table 8-1. Area Summary of Sub-Basins Having DU
Jefferson Proving Ground, Madison, Indiana**

Sub-Basin #	Area (acres)	% of total
Big Creek		
110	571	1.7%
111	227	0.7%
112	422	1.2%
113	386	1.1%
116	567	1.7%
118	777	2.3%
Big Creek Total	2,950	8.7%
Middle Fork Creek		
1	1,093	10.0%
2	161	1.5%
5	289	2.7%
8	433	4.0%
Middle Fork Creek Total	1,976	18.1%
Combined Big Creek and Middle Fork Creek Sub-Basins with DU Relative to Total Area		
Total Area Sub-Basins with DU	4,926	11%
Total Area	44,949	

Output from the calibrated flow model for the period 2007 to 2010 illustrates the relative contribution of sub-basins to the overall surface water flow and sediment transport in Big Creek and Middle Fork Creek, beginning from the headwaters or upstream reaches, extending through the former Proving Ground and DU Impact Area, to the confluence between the two creeks west of the former Proving Ground.

8.1.1 Big Creek

Big Creek headwaters occur east and northeast of the former Proving Ground. Sub-basins 100 through 109 are east and upstream of sub-basin 110 (the easternmost sub-basin along the main Big Creek channel containing DU). Down the main channel, sub-basins 111 and 112 drain the DU Impact Area and also contain DU. Sub-basin 113 is a small tributary north of the main channel draining a portion of the DU Impact Area; it joins with the main channel just east of the western boundary of the DU Impact Area.

Sub-basin 114 is the last (westernmost) sub-basin along the main channel within the DU Impact Area. Two additional sub-basins drain portions of the DU Impact Area and contain DU. Sub-basin 116 contains a small tributary south of the main Big Creek channel; sub-basin 118 contains a small tributary north of the main channel and north of sub-basin 113. Both join the main Big Creek channel west of the DU Impact Area but still within the former Proving Ground. Downstream from the DU Impact Area, sub-basin 117 represents the last sub-basin on the main channel prior to Big Creek flowing off the former Proving Ground. Sub-basin 122 bisects the western property boundary and includes the contributions of Marble Creek. Sub-basin 128 represents the westernmost segment of the main channel prior to confluence with Middle Fork Creek; it contains the contributions from all upstream Big Creek sub-basins, including contributions from Camp Creek.

Table 8-2 summarizes the surface water flow and sediment flux for Big Creek sub-basins for the period 2007 to 2010. Total flow is provided in acre feet. Sediment flux is presented in tons per year moving out of a sub-basin. Observations from Table 8-2 include:

- Upstream contributions from sub-basins 108 (recall this includes contributions from sub-basins 100 to 107) and sub-basin 109 (40 percent of Big Creek drainage area) consist of 38.7 percent of the total flow leaving Big Creek at sub-basin 128 (in short, roughly 38.7 percent of the flow moving down Big Creek originates upstream from the DU Impact Area watersheds). The upstream sediment flux from sub-basins 108 and 109 is 42.6 percent of the total sediment flux leaving Big Creek at sub-basin 128.
- Sub-basins with DU along the main channel of Big Creek (sub-basins 110, 111, and 112) contribute 3.5 percent of the flow. Total contribution of flow from Big Creek sub-basins with DU (110 to 113) exiting the DU Impact Area at sub-basin 114 is 10.7 percent of the flow.
- Total contribution of flow from all Big Creek sub-basins containing DU is 17.3 percent of the total flow at sub-basin 117 near the western boundary of the former Proving Ground and 8.2 percent of the flow leaving Big Creek at sub-basin 128.
- Camp Creek sub-basins represent 17 percent of the Big Creek drainage area and contribute 17.9 percent of the total flow and 31.5 percent of the sediment flux leaving Big Creek at sub-basin 128.
- The combined flow and sediment flux from upstream (sub-basins 108 and 109) with Camp Creek sub-basins account for 56.5 percent of the flow and 74 percent of the sediment flux leaving Big Creek at sub-basin 128. The relatively higher proportion of sediment flux from these sub-basins is due to a higher percentage of agricultural land use.
- Total flow leaving Big Creek at sub-basin 128 ranges from 38,480 acre feet (ac ft) in 2010 to 89,370 ac ft in 2009 and generally correlates to annual precipitation totals.
- Total sediment flux out ranges from 3,896 tons in 2007 to 17,490 tons in 2009. Sediment flux does not correlate with annual precipitation totals; rather, it is dependent upon the timing and intensity of storm events.

8.1.2 Middle Fork Creek

Middle Fork Creek headwaters (Figure 3-1) occur east and southeast of the DU Impact Area and within the eastern boundary of the former Proving Ground. Sub-basin 1 is the easternmost basin along the main channel, extending from near the former Proving Ground boundary into the western portion of the DU Impact Area. Four sub-basins (3, 6, 10, and 11) occur south of sub-basin 1, each containing a small headwater tributary to the main channel. The main channel flows southwest through sub-basins 2, 5, and 8, each of which drains a portion of the DU Impact Area. From there, the main channel follows a

**Table 8-2. Annual Summary of Surface Water Flow and Sediment Transport, Big Creek 2007-2010
Jefferson Proving Ground, Madison, Indiana**

Basin Name	Sub-Basin	Area (ac)	Cumulative Area (ac)	Total Flow Volume (ac ft)				Sediment Flux (tons per year)			
				2007	2008	2009	2010	2007 Out	2008 Out	2009 Out	2010 Out
Big Creek	108	201.252	12538.66	22460	30600	32730	14050	1671	5128	7300	3876
Big Creek	109	762.6362	13301.30	1250	1758	1893	795	34.8	49.9	69.4	34.5
	108+109			23710	32358	34623	14845	1705.8	5177.9	7369.4	3910.5
	% of 128			38.5	38.7	38.7	38.6	44.1	42.8	42.1	41.8
Big Creek	110	571.7585	13873.06	24790	33750	36100	15440	1684	5124	7265	3818
Big Creek	111	226.803	14099.86	25170	34270	36660	15670	1695	5136	7277	3823
Big Creek	112	421.5432	14521.40	25920	35280	37711	16110	1699	5118	7240	3796
	main channel source area 110, 111, and 112			2210	2922	3088	1265	-6.8	-59.9	-129.4	-114.5
	main channel source area %			3.6	3.5	3.5	3.3	-0.2	-0.5	-0.7	-1.2
Big Creek	113	385.8762	14907.28	634	899	966	404	14.8	19.2	26.8	13.3
Big Creek	114	30.35825	14937.64	25970	35360	37780	16130	1700	5112	7240	3794
	110-113 source area flow at DU boundary			2844	3821	4054	1669	8	-40.7	-102.6	-101.2
	% 110 -113 source area flows at west DU impact area boundary			11.0	10.8	10.7	10.3	0.5	-0.8	-1.4	-2.7
Big Creek	116	567.1097	15504.75	946	1331	1430	603	25.99	38.5	55.1	27.1
Big Creek	117	409.0409	16461.86	29270	39910	42670	18170	1787	5265	7402	3849
Big Creek	118	777.3975	17239.25	1281	1818	1950	811	19.2	15.3	21.2	11
	All source area contributions			5071	6970	7434	3083	53.19	13.1	-26.3	-63.1
	All source area flows %			8.2	8.3	8.3	8.0	1.4	0.1	-0.2	-0.7
	% All source area flows at JPG boundary			17.3	17.5	17.4	17.0	3.0	0.2	-0.4	-1.6
Marble Creek	202	782.898	3053.111	5139	7211	7736	3252	115.3	197.5	287.1	158.3
Big Creek	122	455.5275	22896.97	40290	55280	59140	25070	2041	5793	8084	4156
Camp Creek	302	1425.386	5842.63	10930	14740	15780	7099	1042	3637	5483	3117
	302% of total			17.8	17.6	17.7	18.4	26.9	30.0	31.3	33.3
	302+108+109			34640.0	47098.0	50403.0	21944.0	2747.8	8814.9	12852.4	7027.5
	302+108+109 %			56.3	56.4	56.4	57.0	71.0	72.8	73.5	75.2
Big Creek	128	437.6785	34060.17	61510	83530	89370	38480	3869	12110	17490	9351

more westerly path to the western boundary of the former Proving Ground; sub-basin 15 bisects the western boundary, with most of the sub-basin drainage within the former Proving Ground boundary. From this point, Middle Fork Creek turns to a southwesterly flow direction. Sub-basin 21 represents the westernmost segment of the main channel prior to confluence with Big Creek; it contains contributions from all upstream Middle Fork Creek sub-basins.

Table 8-3 summarizes the surface water flow and sediment flux for Middle Fork Creek sub-basins for the period 2007 to 2010. Total flow is provided in acre feet. Sediment flux is presented in tons per year moving out of a sub-basin. Observations from Table 8-3 include:

- Sub-basins with DU along Middle Fork Creek (sub-basins 1, 2, 5, and 8) contribute 18 percent of the total Middle Fork Creek basin area and 17 percent of the total flow exiting at sub-basin 21.
- Sub-basins with DU along Middle Fork Creek (sub-basins 1, 2, 5, and 8) contributed 10 percent of the sediment flux as predicted at sub-basin 21 in 2007 when the total sediment flux leaving the model from Middle Fork Creek was lowest. In 2008 through 2010, these same sub-basins contributed a smaller fraction (4.5 percent) of the total sediment mass exiting the model.
- Forty-one percent of the flow and 61 to 75 percent of the sediment flux leaving Middle Fork Creek at sub-basin 21 is contributed downstream from sub-basin 15; the majority of this area (with the exception of portions of sub-basins 16, 18, and 20) is west of the western boundary of JPG.
- Total flow leaving Middle Fork Creek at sub-basin 21 is 31 percent of the flow leaving Big Creek sub-basin 128. Total flow ranges from 12,130 ac ft in 2010 to 28,150 ac ft in 2009 and generally correlates to annual precipitation totals.
- Total sediment flux out at sub-basin 21 is 17 to 21 percent of the sediment flux leaving Big Creek sub-basin 128 and ranges from 799 tons in 2007 to 3,041 tons in 2009. Similar to observations in Big Creek, sediment flux does not correlate with annual precipitation totals; rather, it is dependent upon the timing and intensity of storm events. Higher relative sediment flux is observed in 2007 relative to 2010, even though the precipitation in 2007 exceeded the precipitation in 2010. At lower sediment flux, the sediment contribution from sub-basins draining the DU Impact Area increases relative to contributions when sediment flux is greater.

8.2 DU TRANSPORT RESULTS

The surface water flow and transport model provides the framework for DU transport with DU carried by surface water runoff in dissolved form or attached to sediment transported by surface water (as overland flow runoff or within streams).

The DU transport model was calibrated to average observed conditions in Big Creek and Middle Fork Creek surface water and sediment data. No attempt was made to reproduce the spatial and temporal variations with the observed data. Matching the average observed concentrations is deemed appropriate given the uncertainty in penetrator distribution within each sub-basin over time (during test firing, twice per year recovery actions, and remaining penetrators on site).

Weather data from 2007 in conjunction with longer term range in observed precipitation were used in both model calibration and long term predictive transport simulations. Of note here is the frequency and timing of precipitation in 2007, which results in relatively low sediment runoff when compared to predicted runoff based upon precipitation data in 2008 through 2010 (even though rainfall in 2010 was less than rainfall in 2007). The lower sediment yield in 2007 requires lower DU mass released into the

**Table 8-3. Annual Summary of Surface Water Flow and Sediment Transport, Middle Fork Creek 2007-2010
 Jefferson Proving Ground, Madison, Indiana**

Basin Name	Sub-Basin	Cumulative Area (ac)	Total Flow Volume (ac ft)				Sediment Flux (tons)			
			2007	2008	2009	2010	2007	2008	2009	2010
Middle Fork	1	1093	1811	2540	2729	1115	42.8	48.8	72.43	36.2
Middle Fork	2	1254	2083	2923	3139	1322	49.5	57.5	84.8	42.1
Middle Fork	5	1989	3292	4622	4965	2091	80.9	97.8	136.7	67.3
Middle Fork	8	3258	5359	7518	8083	3403	133	156	218.3	107.6
Source area relative contribution			3271	4579	4922	2074	82.08	99.3	141.44	69.52
Source area contribution % of total			17.2	17.5	17.5	17.1	10.3	4.8	4.7	4.2
Middle Fork	15	6656	11190	15590	16740	7099	314.5	520	747.2	391.3
Contribution west of JPG			7860	10621	11410	5031	484.9	1545	2293.8	1271.7
Contribution west of JPG %			41	41	41	41	61	75	75	76
Middle Fork	21	10886	19050	26211	28150	12130	799.4	2065	3041	1663

model for transport to achieve calibration. The higher sediment yields in 2008 through 2010 would require slightly higher mass release rates to achieve the same calibrated results. Observations during model development and calibration indicate the use of weather data from a different year as the basis for transport calibration would result in the similar predicted concentrations in surface water and sediment, but the timeframe for source depletion (complete penetration corrosion and dissolution would be shorter).

DU corrosion and dissolution rates and model transport predictions indicate current observed conditions are close to the timeframe of maximum observed concentrations, if assumptions regarding those rates and their implementation in the surface water model are correct. Predictions for Big Creek indicate generally low levels of DU in surface water and sediment (<5 µg/L and <5 mg/kg, respectively) with concentrations reaching similar levels in Big Creek between the DU Impact Area and the western boundary of the former JPG, dropping to lower levels (<2 µg/L and 2 mg/kg, respectively) downstream of JPG. Predicted results on Middle Fork Creek are less than 1 µg/L and 1 mg/kg in surface water and sediment, respectively.

DU transport predictions are most sensitive to source term (mass of DU released into the model from penetrator corrosion and dissolution) and K_d . Increases in the source term yield increased predicted concentrations in surface water and sediment. Increasing K_d results in lower predicted dissolved concentrations in surface water and higher predicted concentrations in sediments.

8.3 LIMITATIONS, ASSUMPTIONS, AND UNCERTAINTY

All models require simplifying assumptions, contain inherent limitations, and contain uncertainty. A listing of model limitations, assumptions, and uncertainty are included to further understanding of model predictions/results.

Limitations

- **HSPF**—At very low-flow conditions, the model provides unrealistically high predictions of DU levels in surface water; the dissolved DU mass is very low in these instances, but the volume of water is also very low, resulting in the over-prediction of DU in surface water.
- **HSPF**—HSPF does not explicitly simulate removal of contaminants adsorbed to the sediment in overland flow (within sub-basins) and rather assumes that the mass of particular constituent(s) is directly proportional to the mass of sediment removed by using user-input potency factors for sand, silt, and clay fractions. Since source areas are generally limited to a fraction of a sub-basin area, estimating average representative values for potency factors is likely to introduce significant uncertainty. Therefore, this approach was not pursued.
- **Data Gap**—Stream flow measurement data are available only from low-flow conditions (maximum stage at which a flow measurement was recorded is 2.25 ft). These data are used to develop both rating curves and the Ftables used to relate measured stage (or depth) to stream flow. Accuracy of potential evapotranspiration time series could be enhanced externally by using more rigorous procedures/algorithms. This will most likely improve precision and quality of runoff predictions.
- **Data Gap**—Manual measurement of bed slope variation along the stream length where transducers are located could reduce uncertainty in the corresponding Ftable's development.
- **Data Gap**—Very little data on surface water and suspended sediment load (including DU concentrations) exist at higher flow conditions during or immediately following storm events.
- **Data Gap**—Collection of co-located surface water and sediment samples was difficult; in several locations, sediment samples were collected adjacent (on inside bend of creek) to the location of surface water sampling locations.

- **Data Gap**—Resolution of processes within sub-basins (e.g., assessment of transport at points within a sub-basin is not possible without further segmentation of sub-basins) can enhance predictive capabilities and reliability of the modeling results. However, increasing the number of characteristics (such as soil type, overland slope, management practices) to delineate watershed into smaller sub-basins increases model complexities (run time, data storage and handling needs, etc.) and requires sufficient high quality data (spatial and/or temporal) to reduce parameters' uncertainty.

Assumptions

- Collected surface water and sediment data are representative of DU transport at the former Proving Ground and can be used to calibrate the HSPF model for DU transport.
- Current land use remains consistent (invariant) over period of simulation.
- Existing historical precipitation (1949 to 2005 at Versailles, Indiana) can be used to develop future long-term predicted precipitation.
- 2007 precipitation data are representative of typical conditions and are used (along with temperature data) with historical weather data to develop predicted future precipitation time series.
- DU transport from penetrator weathering begins when – penetrators were fired from 1984 through 1994; assumed all penetrators are available for weathering and transport beginning in 1994 despite the fact that many are located in subsurface soil and while susceptible to corrosion and dissolution, not likely available for overland transport since corrosion products are deeper in soil column.
- The same weather data assumed for future transport predictions were assumed valid for DU transport calibration; weather data from 1984 or 1994 were not used to calibrate the DU transport model.
- One average overland slope value (estimated by BASINS/HSPF from DEM data) is used in all sub-basins; this may under-predict the amount of sediment yield and DU transport near streams where slopes are steeper and over-predict sediment yield and DU transport in uplands where the land surface is flatter than the average slope.

Uncertainty

- Spatial and vertical distribution of penetrators within and adjacent to DU Impact Areas is not well-known.
- K_d varies over wide range; using average K_d approach may over-predict or under-predict DU levels relative to actual conditions due to local geochemical variations. Values of K_d for various soil fractions (sand, silt, and clay) were assumed and could be an additional source of uncertainty.
- Future land use could impact short or long-term predictions.
- Future weather patterns, including potential impacts of climate change, could impact short or long-term predictions.
- Penetrator weather rate (corrosion and dissolution), and conditions (such as pH and redox potential).
- Potential for exposure of penetrators due to excessive local gully erosion within sub-basins.

- Measured flow at the gauging stations used to develop rating curves and Ftables. At very low-flow conditions, measurement becomes uncertain as flow rates and/or channel depths are too shallow for accurate measurement of flow conditions; at higher flow conditions (greater than ~2.5-ft stage) safe measurement of flow becomes a concern and field measurement of flow was not performed (this also may be listed as a data gap).
- **Land Use**—Comparison of land uses for the National Land Cover data and land use derived from infrared analysis were similar, with key differences noted in more grass land and bare soil identified in Infrared analysis for 6-m resolution. Bare soil classification may overestimate the amount of sediment flux generated from farm land. There is also a difference in total area – area determined from the infrared analysis is 44,383 ac versus 44,959 ac, a difference of 1.3 percent due to resolution 6-m versus default 30-m grid.

9. CONCLUSIONS

The JPG site in Madison, Indiana, was characterized by low permeable soils and limited groundwater recharge. Surface runoff hydrographs recorded at JPG generally exhibit fairly sharp rising and falling limbs (sometimes indicating flash flood conditions of short duration). During these periods, most of the surface runoff and erosion occurs.

The primary objective of this investigation was to assess the fate and transport of DU at the JPG site. Based on the site hydrogeological conditions and physicochemical properties of uranium, oxidized (corroded) species of uranium are likely to be mobilized primarily as adsorbed to the sediments. Other pathways of DU migration/transport include as dissolved in surface runoff, interflow, and base flow and/or as disintegrated DU particles mobilized (such as during flash floods) and again depositing within the sub-basins or the JPG stream network.

Using HSPF (and BASINS) code as the platform, a surface water flow, sediment, and DU component fate and transport model was developed. The model was used to simulate and investigate the long-term on/offsite migration and impact of DU. The land use pattern within the surface water model domain is fairly diverse. About 55 percent of the model area is forested where sediment yields are lowest (limited erosion). However, precipitation falling in upland areas of the watershed that was either uncultivated or under agriculture simulated higher sediment yields. This sediment and runoff from the DU Impact Area mixed with sediment and surface water from nonimpacted areas and was transported through Middle Fork Creek and Big Creek.

The model was calibrated, verified, and used to simulate long-term (500-year) DU transport scenarios to assess the fate and transport of the estimated 73,500 kg of the DU remaining on the former JPG. Key tasks accomplished and findings from the modeling effort include:

- Flow model calibrated to observed stage at seven continuous recording gauging locations and to overall water balance (total precipitation = infiltration + runoff + evapotranspiration ± storage).
- DU transport calibrated to observed conditions (observed DU in Big Creek and Middle Fork Creek surface water and sediment sampling data)
 - Calibration consisted of adjusting the mass released from penetrators within each sub-basin so that modeled DU in surface water and adsorbed to sediment matched corresponding observed DU concentrations (on average) at current times
 - K_d (2,200 mL/g) adjusted to obtain match between predicted surface water and sediment DU levels and occurs between the desorption (429 mL/g) and sorption (7,004 L/kg) test results.
- Predicted future DU in Big Creek surface water and sediment are low (surface water <5 µg/L; sediment <5 mg/kg) where Big Creek exits the DU Impact Area (at gauging station BC01, sub-basin 114).
- Predicted future DU in Middle Fork Creek surface water and sediment are low (surface water <1 µg/L; sediment <1 mg/kg) where Big Creek exits the DU Impact Area (at gauging station BC01, sub-basin 114).
- The mass released to surface water pathway from penetrator weathering continues for the entire 500-year period, decreasing slowly over the period of simulation. This continuing source results in relatively similar constant DU levels (aside from seasonal variations) at the DU Impact Area that decrease downstream from the DU Impact Area due to mixing (contribution

from larger drainage areas that are unaffected (not contributing DU mass) in both Big Creek and Middle Fork Creek, especially after the creeks exit the former JPG.

- Modeled contribution to surface water flow from each sub-basin is generally proportional to the area of the sub-basin.
- DU mass loading rate from source sub-basins is directly proportional to their cumulative DU penetrator mass (Figure 6-1).
- Timing and intensity of storm events affect sediment load. Calendar year 2007 precipitation was 47 in, near average; however, sediment load was much less than calendar year 2010 where precipitation was only 36 in. Examination of weather data showed precipitation events in 2007 were more spread out than in 2010, and in particular 9.2 in of rain falling in June 2010 generated 76 percent of the sediment flux for the year. When sediment flux is low (as in calendar year 2007), the relative contribution from source area sub-basins increases relative to higher sediment flux (less mixing in low sediment flux periods, more mixing in higher sediment flux years).
- Land use on JPG, and in particular the source area sub-basins, are 96 to 98 percent forest or grass land use, resulting in little sediment runoff from these areas relative to off JPG where land use contains a higher percentage of cultivated land (farmland plus bare soil). East of the former JPG, grass and forested land combined is 63 percent; cultivated land is 36 percent. West of the former JPG, grass and forested land combined is 51 percent (Big Creek) to 53 percent (Middle Fork Creek) and cultivated land is 41 percent (Middle Fork Creek) to 45 percent (Big Creek). The higher percentage of cultivated land (farmland plus bare soil) east and west of the former JPG property generates more sediment runoff per acre than the grass and forest land use comprising most of the area within the former JPG property.

10. REFERENCES

- Anderson E.A., 1973. National Weather Service River Forecast System-Snow Accumulation and Ablation Model. NOAA Technical Memo, NWS HYDRO-17, U.S. Dept. of Commerce, Washington, D.C.
- Bechert, C.H., and J.M. Heckard. 1966. In Lindsey, A.A., ed, Natural features of Indiana: Indianapolis, Indiana Academy on Science, p. 100-115.
- Chen, J.P., and Yiaccoumi, S. 2002. Modeling of Depleted Uranium Transport in Subsurface Systems. *Water, Air, and Soil Pollution* 140: 173–201.
- Franzmeier, D.P., G.C. Steinhardt, and D.G. Schulze. 2004. Indiana soil and landscape evaluation manual. Ay-323. Version 1.0. Purdue Univ. Coop. Extension Service, West Lafayette, IN 47907. 72p.
- Gray, H.H. 2001. Miscellaneous Map 69 modified from Gray, H.H. 2000. Physiographic Divisions of Indiana, Indiana Geological Survey Special Report 61, Plate 1.
- Indiana Geological Survey. 2002. Bedrock Geology of Indiana (Indiana Geological Survey, 1:500,000, Polygon Shapefile), Bloomington, Indiana. This shapefile was derived and modified from a pre-existing published paper map: Gray, H.H., C.H. Ault, and S.J. Keller, 1987, Bedrock Geologic Map of Indiana, Indiana, Geological Survey Miscellaneous Map 48.
- Indianamap.Org. 2005. 6-meter resolution Digital Elevation Model accessed at Indianamap.org.
- Kaiser-Hill. 2002. Actinide Migration Evaluation Pathway Analysis Summary Report, Tech. Report No. ER-108, Kaiser-Hill, Rocky Flats Environmental Technology Site.
- Neitsch, S.L., J.G. Arnold, J.R. Kiniry, J.R. Williams. 2011. Soil and Water Assessment Tool Theoretical Documentation Version 2009. Grassland, Soil and Water Research Laboratory – Agricultural Research Service Blackland Research Center – Texas AgriLife Research; Texas Water Resources Institute Technical Report No. 406, Texas A&M University System, College Station, Texas, September.
- Parkhurst, M.A., K.M. Krupka, K.J. Cantrell, J.A. Glissmeyer, S.P. Shelton, E.W. Morgan, and S. Mattigod. 2012. Final Report Review of Depleted Uranium Soil Contamination and Environmental Migration: Oxide Generation, Characteristics, and Dispersion. Prepared for the U.S. Army Institute of Public Health by Battelle Memorial Institute Pacific Northwest National Laboratory, July.
- Philips, J.R. 1957. The theory of infiltration: the infiltration equation and its solution. *Soil Sci* 83:345–375. Reference for National Land Cover Dataset. USDA/NRCS. 2006. <http://www.mrlc.gov/finddata.php>
- SAIC (Science Applications International Corporation). 2002. Environmental Report, JPG, Madison, Indiana. Prepared for the U.S. Army SBCCOM. June.
- SAIC. 2007. Well Location Selection Report. Prepared for US. Department of Army Contract No. W912QR-04-D-0019.
- SAIC. 2008. Well Construction and Surface Water Data Report. Prepared for US. Department of Army Contract No. DACW62-03-D-0003.

- SAIC. 2010. Slug Testing Report, Depleted Uranium Impact Area Site Characterization: Aquifer Testing for Hydraulic Conductivity, Jefferson Proving Ground, Madison, Indiana. Final. Prepared for U.S. Department of Army, Installation Support Management Activity, 5183 Blackhawk Road, Aberdeen Proving Ground, Maryland 21010-5424 and U.S. Army Corps of Engineers, Louisville District, 600 Dr. Martin Luther King, Jr. Place, Louisville, Kentucky 40202-2230. Submitted by Science Applications International Corporation (SAIC), 12100 Sunset Hills Road, Reston, Virginia 20190 under Contract No. DACW62-03-D-0003, Delivery Order No. CY07. August.
- SAIC. 2013. Radiation Monitoring Report for License Sub-1435 Jefferson Proving Ground Summary of Results for the March-April 2012 Sampling Event, Final. Submitted to: U.S. Department of Army U.S. Army Garrison, Rock Island Arsenal, Rock Island, Illinois. January 2013.
- Thibault, D.H., M.I. Sheppard, and P.A. Smith. 1990. A Critical Compilation and Review of Default Soil Solid/Liquid Partition Coefficients, K_d , for Use in Environmental Assessments. AECL-10125, Whiteshell Nuclear Research Establishment, Atomic Energy of Canada Limited, Pinawa, Canada.
- USDA NRCS (U.S. Department of Agriculture Natural Resources Conservation Service). 1999. Soil Taxonomy: A basic system of soil classification for making and interpreting soil surveys. 2nd edition. USDA NRCS Handbook 436.
- USDA NRCS. 2005. Soil Survey Geographic Database (SSURGO) for Jefferson County, Indiana – Interim Product, SV 2.7.
- USDA NRCS. 2006. National Land Cover Dataset, accessed at <http://www.mrlc.gov/finddata.php>
- USEPA (U.S. Environmental Protection Agency). 1999. Understanding Variation in Partition Coefficient, K_d , Values, Volume II, Office of Air and Radiation, EPA 402-R-99-004B, Washington, DC: USEPA.
- USEPA. 2001a. Better Assessment Science Integrating Point and Nonpoint Sources (BASINS), User's Manual. EPA-823-H-01-001, Washington, DC: USEPA.
- USEPA. 2001b. Hydrological Simulation Program – Fortran, HSPF Version 12, User's Manual. Bicknell, B.R., J.C. Imhoff, J.L. Kittle, Jr., T.H. Jobes, and A.S. Donigian, Jr. Washington, DC: USEPA.
- USEPA. 2001c. winHSPF Version 2.0 User's manual. Duda, P., J. Kittle, Jr., M. Gray, P. Hummel, and R. Dusenbury. Washington, DC: USEPA.
- USEPA. 2004. Wadeable Streams Assessment: Field Operations Manual. EPA841-B-04-004. U.S. Environmental Protection Agency, Office of Water and Office of Research and Development, Washington DC. Final. July.
- USEPA. 2013. <http://www.epa.gov/nrmrl/wswrd/wq/models/swmm/>
- USGS (U.S. Geological Survey). 1987. Roughness Characteristics of Natural Channels by Harry Barnes, Jr., USGS Water Supply Paper 1849.

APPENDIX F

SITE CHARACTERIZATION SUMMARY

**Depleted Uranium Impact Area
Jefferson Proving Ground, Madison, Indiana**

THIS PAGE WAS INTENTIONALLY LEFT BLANK